PELLETIZED SLAG CEMENT : HYDRAULIC POTENTIAL AND AUTOCLAVE REACTIVITY

By

ROBERT DOUGLAS HOOTON, B.A.Sc., M.A.Sc.

A Thesis

Submitted to the School of Graduate Studies

in Partial Fulfilment of the Requirements

for the degree

Doctor of Philosophy

October 1981

PELLETIZED SLAG CEMENT: AUTOCLAVE REACTIVITY

DOCTOR OF PHILOSOPHY (1981)
(Civil Engineering)

McMASTER UNIVERSITY
Hamilton, Ontario

TITLE: Pelletized Slag Cement: Hydraulic Potential and Autoclave Reactivity

AUTHOR: Robert Douglas Hooton, B.A.Sc. (University of Toronto)

M.A.Sc. (University of Toronto)

SUPERVISOR: Dr.John J. Emery

NUMBER OF PAGES: xvi, 251

ABSTRACT

With the current pressures to conserve energy and protect the environment, research to take advantage of the cementitious nature of vitreous pelletized blast furnace slag (a byproduct of the steel industry) should yield both economic and technical advantages to the Canadian construction industry.

Three specific areas were chosen for study.

1. The development of a test method to quantify the degree of vitrification achieved in the quenching of blast furnace slags (a property known to have fundamental influence on its reactivity) and the evaluation of new and existing test methods with regard to simplicity and accuracy for potential use as a basis for commercial quality control.

2. The study of the incorporation of slag cement in autoclaved binders having a wide range of compositions in the ternary system containing slag, portland cement and ground quartz (silica flour).

3. The effects of variations in the physical and chemical properties of slag cement on autoclave reactivity.

Within the previously defined areas, a few of the findings are given.

1. From analysis of glass content determinations, the method adopted is critical to the results obtained. The McMaster Individual Particle Analysis was found to give the most accurate

and reliable glass content values when compared to a QXRD standard procedure and when used to predict strength potential.

2. Optimum strengths were obtained with ternary slag-portland cement-silica flour binders containing 60 to 75 per cent slag. When autoclaved 4h at 185°C, high strengths corresponded to the presence of semi-crystalline C-S-H resulting in fine pore size distributions, and mixtures of C-S-H and αC_2SH. It was also found that slag was activated by silica flour alone resulting in high compressive strengths, high tensile to compressive strength ratios and relatively well crystallized tobermorite.

3. The degree of vitrification of slag was found to have the most significant influence on strength of autoclave cured pastes but the trend was not clear at high glass contents. The CaO and MgO contents were significantly related to strength when combined with the degree of vitrification. However, for evaluating slag hydraulicity, it is suggested that only physical strength testing has the authority for engineering decision making.

ACKNOWLEDGEMENTS

I would like to thank Dr.J.J.Emery for his support and encouragement throughout this work. Also, I would like to thank the members of my committee ; Dr.R.G.Drysdale and Dr.P.S.Nicholson and especially Prof.R.H.Mills for their guidance.

Also I would like to thank the following people for their technical contributions:

Dr.J.J.Beaudoin of National Research Council for the mercury porosimetry analyses,

Ms.J.Bentzen for help in modification of the silica extraction technique,

Mr.W.Berry of Standard Slag Cement Company for slag samples and South African glass content determinations,

Dr.H.Chen and Mr.P.Grindrod of Canada Cement Lafarge for the cement analyses,

Mr.R.P.Cotsworth of National Slag Limited for allowing me to collect slag samples,

Mr.D.Davey formerly of Cooke Concrete Limited for allowing and participating in the industrial block trials,

Mr.R.Doelle of Dofasco for the chemical analyses of the slags,

Mr.J.R.Foster of Dravo Lime Company for the U.V. reflectance glass contents,

Mr.G.Gerrites and Mr.J.Cartwright of Indusmin Limited for the analysis of the silica flour,

Dr.L.P.MacDonald and Mr.L.Zimmerman of St.Lawrence Cement Company for the cement analyses,

Dr.G.Osbourne of Building Research Station for providing some of the slag mineral standards.

I would also like to thank Mr.M.Forget and Mr.W.Sherriff of the Department of Civil Engineering and the technical staff of the various departments forming the Institute for Materials Research who provided information and assistance to this multi-disciplinary study.

I would like to thank Ms.C.Crooks for her typing and lastly I would like to thank Barbara for her typing and for her patience throughout this endeavour.

TABLE OF CONTENTS

PAGE

LIST OF TABLES

LIST OF FIGURES

1. INTRODUCTION

1.1 BACKGROUND

With the current pressures to conserve energy and protect the environment, research to take advantage of the cementitious nature of vitreous pelletized blast furnace slag (a byproduct of the steel industry) should yield both economic and technical advantages to the Canadian construction industry. Pelletizing of liquid slag, initially to produce a light weight aggregate, was developed in Hamilton, and the process is now being adopted at steel works in many countries. Unfortunately, demand for this energy efficient product, particularly in cementitious applications, has been slow to develop since the fundamental hydraulicity aspects and product performance characteristics have not been defined. Further, the slow development in the use of blended cements in North America is also partially due to the attitude and inertia of the building materials and construction industry which, unlike its European counterpart, has had the use of almost unlimited and uninterrupted sources of raw materials and energy for the production of portland cement.

These attitudes are changing since it is clear that substantial energy savings are possible with about 3 to 5 MJ saved for every kg of portland cement replaced by slag cement. Since the cost of energy has risen dramatically over the past decade these large energy reductions can translate into attractive economic savings, and most of the major

portland cement manufacturers have recently taken notice.

This work was concerned with elucidating the hydraulic properties of pelletized slag, factors affecting its quality as cementing material, with emphasis on high pressure steam (autoclave) curing applications. Approximately 90 per cent of the concrete block and brick produced in Ontario is autoclave cured but the costs of plant operation have risen enormously with the increasing cost of producing steam and the largely energy related, increasing costs of cementing materials. Therefore, because of energy considerations coupled with lack of research on slag in autoclave applications, this area of study was thought to be very relevant to the needs of the building products industry.

Within this general context, three specific areas were chosen for study.

1. The development of a test method to quantify the degree of vitrification achieved in the quenching of blast furnace slags (a property known to have a fundamental influence on its reactivity) and the evaluation of new and existing test methods with regard to simplicity and accuracy for potential use as a basis for commercial quality control.
2. The study of the incorporation of slag cement in autoclaved binders having a wide range of compositions in the ternary system containing slag, portland cement and ground quartz (silica flour).
3. The effects of variations in the physical and chemical properties of slag cement on autoclave reactivity.

Unlike Menzel's (1934) study of the complete range of portland cement-quartz binders, the published studies on slag have only concentrated on one or two isolated binder combinations. Therefore, to establish a base for work on the effects of slag properties on reactivity, it was thought to be necessary to establish slag reactivity over the complete range of slag, portland cement and silica flour binders. Also, before the effects of variable slag properties could be studied, a reliable method of determining the degree of vitrification, likely the most important slag property, had to be developed and evaluated.

Therefore, it is thought that the combination of these three areas form a comprehensive study of slag hydraulicity with regard to developing its commercial use in autoclaved products.

1.2 OUTLINE OF STUDY

As a background to the experimental work, the production, processing and properties of blast furnace slag are discussed in Chapter 2. Also given is a background and literature review on the cementitious properties of blast furnace slags, autoclave curing in general and finally the study of autoclaved cements incorporating slag.

It is well known that the degree of vitrification achieved upon quenching of blast furnace slag is fundamental to its reactivity as a cementing material. However, the development and adoption of a simple, yet reliable test for the measurement of this property, with regard to quality control purposes, has been a subject of concern due to the numerous test methods available and the large variations in results obtained. This is evidenced by the lack of test methods offered for its measurement in national standards for slag (e.g. CSA A 363 -M 1977 in Canada; ASTM C595 in the United States; DIN 1164 in West Germany).

In Chapter 3, eleven different glass content determination methods are discussed, with the techniques detailed in the Appendices. Of these, six methods were chosen for study, including three commercially used for quality purposes in Canada, the United States and South Africa. Also included was a previously developed procedure, known as the McMaster individual particle analysis, which was modified to give two values of glass content depending on how a certain particle type was interpreted. A standard method using quantitative X-ray diffraction (QXRD) with synthetically produced mineral standards was developed as a basis for evaluating the accuracy of the five other glass

content methods chosen for study.

Thirty-six slags from both Canadian and foreign sources, and one synthetically produced glass were evaluated by each of the glass content determination methods and compared. The chemical and mineralogical properties of the eighteen slags chosen for study in Chapter 5 were also determined.

The properties of autoclaved pastes and mortars are described in Chapter 4, over a wide range of binder compositions containing mixtures of one sample of slag cement, normal portland cement and silica flour. A single autoclave curing cycle, typical of those used in local commercial practice, was adopted. The properties measured for each of the autoclaved pastes included compressive and tensile strength, solid density, apparent porosity, non-evaporable water content and quantities for most of the unhydrated and hydrated phases.

QXRD was used for most of the phase analysis with a sample of 11.3Å tobermorite being synthesized and used as the basis for the quantification of this component in the autoclaved pastes.

As an applied extension to this work, industrial trials were performed using slag/portland cement/silica flour binders to produce concrete block. Waste cement kiln dust was also tested to replace portland cement in one of these trials. In order to improve the economic viability of using pelletized slag for cementitious purposes, the slag used in these trials was only partially ground. This was accomplished using a concrete mixer with a high speed, intensive rotor which was able to produce a combination binder and fine aggregate material in six minutes.

In Chapter 5, one ternary binder combination, containing 60 weight per cent slag, 20 per cent portland cement and 20 per cent silica flour, was chosen for further study. This composition was thought to be commercially practical as indicated from the previous experimental work and the industrial trials. Seventeen of the slags and the synthetically produced glass evaluated in Chapter 3 were used to produce autoclaved pastes. The slags studied had a range of chemical compositions, glass contents (some of which were altered by heat treatment) and finenesses of grinding. To evaluate the variations in these slag properties, the same properties of the autoclaved pastes were measured as in Chapter 4. Furthermore, in this work, pastes containing each slag were mixed at three water/cement ratios resulting in three values of apparent porosity. This was used to establish the strength-porosity relationship for pastes containing each slag, in order to assess their strength properties at a common value of porosity (by interpolation).

Multiple linear regression analyses were performed in order to develop relationships and assess the significance of the variations in slag on properties of the autoclaved pastes.

In Chapter 6, conclusions are drawn from the experimental findings, and suggestions for future research are given.

A list of the abbreviations and terminology used throughout this work is given in Table 1.1.

TABLE 1.1

LISTS OF ABBREVIATIONS AND TERMINOLOGY

(a) Cement Chemistry Notation for Oxides in Mineralogical Compounds

Abbreviation	C	S	A	M	F	H	$\overline{C}$	$\overline{S}$
Oxide	CaO	SiO_2	Al_2O_3	MgO	Fe_2O_3	H_2O	CO_2	SO_3

(b) Analysis Techniques

Abbreviation	Technique
XRD	X- ray diffraction
QXRD	Quantitative X-ray diffraction
XRF	X-ray fluorescence
DTA	Differential thermal analysis
SEM	Scanning Electron Microscope
EDXRA	Energy dispersive X-ray analyser

(c) Standards and Organizations

Abbreviation	Organization
CSA	Canadian Standards Association
ASTM	American Society for Testing and Materials
DIN	West German standards organization
ACI	American Concrete Institute

(d) Other Cement Terminology

Abbreviation	Meaning
W/C	= water to total cementitious materials ratio
Wn/C	= non-evaporable water content per unit weight of cementitious material
Wn/Wo	= ratio of non-evaporable water to original water content of paste
C-S-H	= notation adopted for calcium silicate hydrates of the tobermorite group but of largely undetermined composition and usually poorly crystallized.

2. BACKGROUND AND LITERATURE REVIEW

2.1 INTRODUCTION

The purpose of this chapter is to provide background information on the areas covered in the experimental work and to evaluate the work done previously in each area. First, the production, processing and utilization of blast furnace slag is discussed in general to introduce the relatively new development of pelletized slag. The next section deals with the cementitious aspects of slag and factors affecting its reactivity. The hydration products and properties of high pressure steam cured cements are then discussed. Finally, the limited work done previously on autoclaved cements incorporating slag is covered.

2.2 IRON BLAST FURNACE SLAG *

2.2.1 Production and Properties

The iron blast furnace operation is a continuous process. The blended raw materials (burden) and coke are introduced at the top and as the materials move down through the furnace, they are heated from below. Air is injected near the bottom of the furnace and the ignited coke eventually supplies enough heat to melt the burden. The slag results from fusion of the fluxing stone (limestone and/or dolomite) together with the gangue (siliceous and aluminous residues from the iron ore) and coke ash in the blast furnace. (It should be noted that steel-making slag is typically recycled as part of the burden). The molten slag floats on top of the molten iron and below the unmelted burden. Both molten materials are drawn off at regular intervals from the continuous process furnace. Slag is tapped from modern blast furnaces using high quality ore burdens at a rate of 280 to 340 kg per tonne of hot metal (Schröder, 1969). A flow sheet for the production of blast furnace slag is given in Figure 2.1. Since the raw material burden is carefully controlled to give consistent iron production, the range of slag chemical compositions is fairly narrow for a specific ore and furnace operation.

The major oxides in the slag are not free but combined, and the equilibrium compositions of Canadian slags are typically mostly

*While there are many types of ferrous and non-ferrous slags, for brevity in this work, iron blast furnace slag will be referred to as slag.

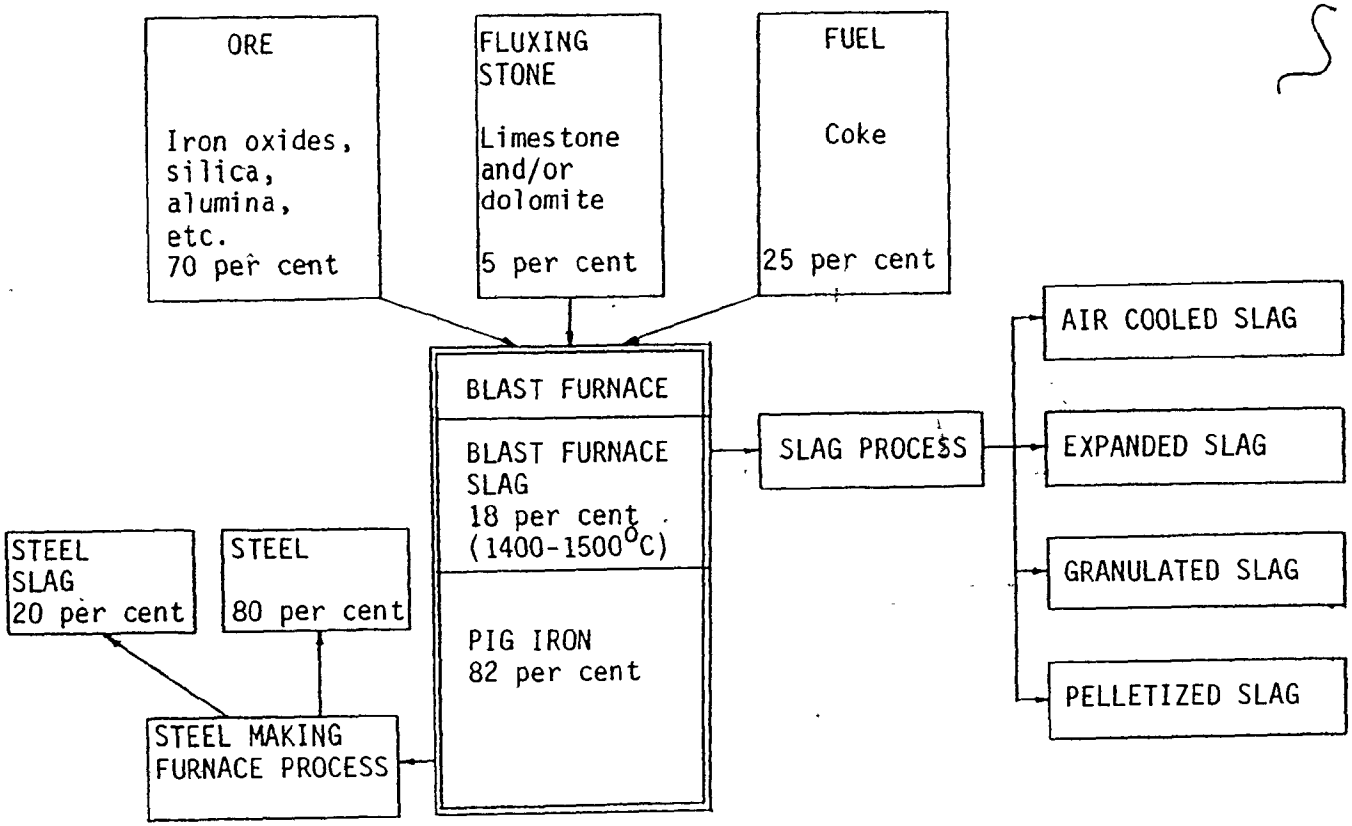

FIGURE 2.1: SCHEMATIC OF IRON PRODUCTION AND BLAST FURNACE SLAG PROCESSES (after Kim, 1975) Weight percentages shown are approximate.

melilite solid solutions (between akermanite and gehlinite) with minor amounts of diopside or monticellite. The range of blast furnace slag compositions containing 10 per cent MgO (typical of North American slags) is shown in Figure 2.2. Detailed studies on the compositions

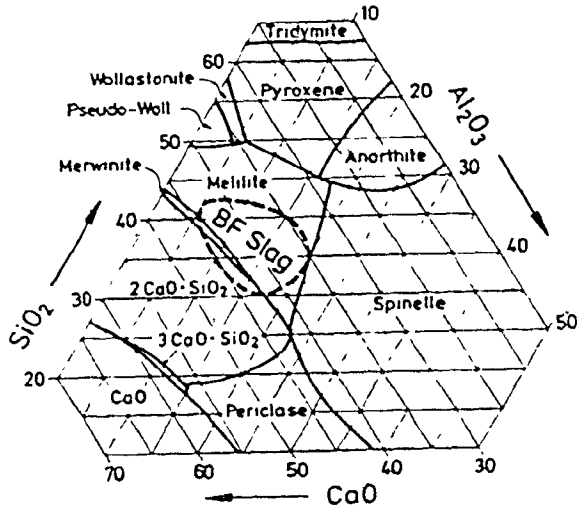

FIGURE 2.2: MAIN FIELD OF COMPOSITION FOR BLAST FURNACE SLAGS CONTAINING 10 WEIGHT PER CENT MgO (Smolczyk, 1980)

of blast furnace slags and the influence of blast furnace operations have been summarized by Osborn and co-workers (1954), Kramer (1962), and Schröder (1969).

The physical state of the slag is fundamental to its cementitious properties. Common North American practice is to cool the slag slowly in pits (referred to as air-cooled slag) which allows sufficient time for the molecules to arrange themselves into crystalline mineral compounds as the slag solidifies. Unfortunately, these crystalline

compounds have little or no cementitious value (Lea, 1971). However, when quenched from its molten state (after discharge from the furnace) the molecules in the slag are not given sufficient time to crystallize due to the high viscosity developed with falling temperatures. As a result, the disorganized liquid structure is retained in a metastable amorphous, vitreous or glassy state.* The glass structure represents energy locked in the slag at a perched Ahhrenius potential (Mills, 1976), and imparts latent hydraulic properties as discussed later.

However, industrial quenching methods are not always effective in producing completely vitreous slags. If the slag temperature just prior to quenching is lower than the liquidus temperature of the slag, some of the slag will already be crystalline. Also the quenching rate may not be high enough to prevent further crystallization before the viscosity of the slag becomes high enough to prevent it. The viscosity of a slag at constant temperature is also a function of its chemical composition, which therefore also influences the effectiveness of a fixed quenching rate.

The methods of processing slag, as shown in Figure 2.1, and uses for each type are described in following sections.

---

* The terms amorphous, vitreous and glassy are used interchangeably throughout this work to describe the disorganized structure of quenched slag. The term commonly used by producers and users is glass.

2.2.2 Air Cooled Slag

As mentioned previously, the bulk of available slag in North America is cooled slowly in pits, then broken up and crushed for use as aggregate or granular base. However, as energy savings become a more important consideration in the manufacture of cements, the production of hydraulically inert air-cooled slag will likely decrease. While perhaps not always used to its optimum "energy" advantage, it should be noted that blast furnace slag is almost fully utilized and therefore must be classified as a by-product rather than a waste material. In 1976, over 90 per cent of the slag produced in Canada was air-cooled (Emery, 1978).

2.2.3 Foamed Slag

Foamed slag (sometimes referred to as expanded slag), which is utilized as a light weight aggregate, is produced by introduction of a limited amount of water to the molten slag. The water is vaporized and the escaping vapour bubbles caught in the solidifying product result in a light weight, porous product. Disadvantages of this process include the high H_2S emissions during foaming and the high water absorption of the product when used as an aggregate. No expanded slag has been produced in Canada since the 1960's.

2.2.4 Water Granulated Slag

The most commonly employed method of quenching slag is by water granulation. The molten slag is usually broken up by water jets, then immediately immersed in water, but several variations are used (Lea, 1971). While an effective method of quenching, water granulation has several disadvantages from environmental and production viewpoints. The quenching water becomes contaminated with sulphur and other compounds leached from the slag, and sulphides combine with the water to form hydrogen sulphide. Besides potential air and water pollution problems the slag has a high residual moisture content and must be dried (energy intensive) prior to grinding for cementitious uses. Currently, no granulated blast furnace slag is produced in Canada and only a small amount is produced in the United States(Emery,1978).However, granulation is being considered in several locations and a large plant is now being installed at Sparrows Point, Maryland. Besides cement replacement, unground granulated slag has been used as a fine aggregate in concrete and in stabilized base for roads.

2.2.5 Pelletized Slag

The slag pelletizer was developed by National Slag Limited in Hamilton (Margesson and England, 1971) as a means of bringing the very high gas emission levels typical of the "pit foaming" process under control. Pelletized slag is produced by expanding molten blast furnace slag under water sprays, and then passing the flow of this pyroplastic material over a spinning drum, on which fins are mounted, breaking the slag up and flinging it in the air for a sufficient time (and distance

of approximately 15 meters) that surface tension forms pellets (Emery, Kim and Cotsworth, 1976). The sulfide gases are trapped inside the pores as the pellets solidify. This concept of using limited water sprays and a finned, rotating drum to quench slag (for cement purposes) had also been used prior to 1909 in England and Germany (Anon, 1909), and since around 1950 in the U.S.S.R. (Kholin and Royak, 1962).

In addition to positive control of gas emission, several other benefits of pelletizing slag have been demonstrated. From the point of view of slag handling, the pelletizer takes the molten material which would normally require several days of air cooling, and turns it into an easily handled product that can be immediately removed from the blast furnace area. This quick-cooling aspect of pelletizing is very important in situations where only limited space is available for slag handling adjacent to the furnace.

Production of a very satisfactory light weight aggregate with low absorption and good thermal conductivity properties generally results in a fairly crystalline slag structure (Emery, Cotsworth and Hooton, 1976). However, by increasing the water spray intensity and the speed of the spinning drum, it was found that a high degree of vitrification could be obtained, making pelletized slag suitable for cementitious applications. The major advantages of using pelletized slag instead of water granulated slag for cement production is the low residual moisture content of the pellets (average 5.5 per cent, Emery, Cotsworth and Hooton, 1976) resulting in less energy required for drying. It has also been shown that pelletized slag requires less

energy when grinding to typical cement finenesses (Osbourne, 1977).

Also, Kramer (1962) reported that the production of a low density porous glass, instead of a dense, compact glass, resulted in higher strengths of cements, especially at early ages and low portland cement additions. Pelletized slag, as previously mentioned, has the advantage of such a porous structure. Another feature of pelletized slag found by Roper (1980) was a much higher variation in chemical composition between slag grains than in granulated slags as detected using an electron microprobe. He postulated that this variability might be due to a state of incipient crystallization of the glass. This may be advantageous since Hawthorn and co-workers (1980) suggested that areas of incipient crystallization may act as nucleation sites for hydration. In Canada, pelletized slag is produced in Hamilton with production exceeding 0.2M tonnes (Emery, 1978). It is currently used as light weight aggregate in concrete slabs and block products, and to produce separately ground slag cement (Molland, 1976). While still a relatively new product, the use of pelletized slag is expanding, with current production in eight countries in at least twenty-two installations (Cotsworth, 1979).

2.3 FACTORS AFFECTING SLAG HYDRAULICITY

2.3.1 General

Major reviews on the hydraulicity of slag were given by Keil (1954), Kramer (1962), Schröder (1969), Satarin (1974), and Smolczyk (1980). The properties of slag which have been generally accepted as influencing its reactivity are:

1. the degree of vitrification (glass content),
2. the chemical composition,
3. the mineralogical composition,
4. the fineness of grinding, and
5. the type of activation provided.

In this section, a summary of the published work is given, in terms of each of the five aforementioned factors.

2.3.2 Degree of Vitrification

As discussed further in Chapter 3, the latent hydraulicity of quenched slag is generally considered to result from the perched Arrhenius energy level of its amorphous structure in comparison to a crystalline structure of the same composition (Mills, 1976). Unlike commercial glasses, the high basicity of slag glass makes its structure only meta-stable, and it can be completely devitrified by heating to less than 1000^{o}C. At ambient temperatures, crystallization is only inhibited by the high viscosity of the solid.

The degree of vitrification achieved in quenched slags is affected by the temperature at the onset of quenching, the applied cooling rate and the chemical composition. Blondiau (1951) found that reduction of granulation temperatures from just 1538°C to 1479°C resulted in strength reductions of the cement of 10 to 40 per cent. Fierens and Poswick (1977) found that the hydration of completely vitrified slags was affected by the quenching rate applied. The higher reactivity of more quickly quenched slags was found to be the result of fewer defects in the glass structure. However, this trend was not as clear when applied to industrial slags (Fierens, 1979).

Schwiete and Dölbor (1963) modified quenching conditions for each of 30 slags and found that the predominant factor affecting strength was glass content, as shown in Figure 2.3. Although increasing crystalline contents reduced hydraulicity , it was thought that slags with glass contents as low as 30 to 40 per cent could still be employed.

Other researchers, as Smolczyk (1980) pointed out, have not found a linear glass content-strength relationship, and in some cases small amounts of crystalline inclusions were advantageous. As shown in Figure 2.4, Demoulian and co-workers (1980) found that the strengths of slags with glass contents in excess of 95 per cent were reduced. Figure 2.4 also shows that the influence of over 30 per cent merwinite crystal content on strength development was very small. They concluded that the composition of the glass fraction was enhanced with regard to reactivity by the C_3MS_2 crystallization, and that this counteracted the effect of reduced glass content.

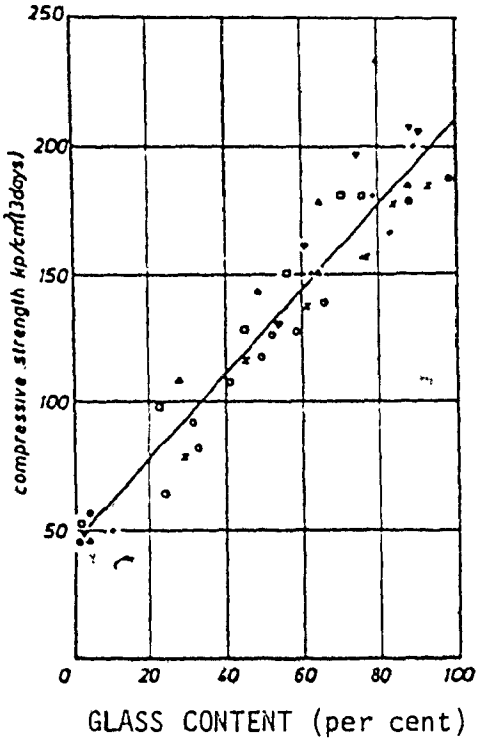

FIGURE 2.3: RELATIONSHIP BETWEEN GLASS CONTENT AND 3 DAY STRENGTH DEVELOPMENT (after Schwiete and Dölbor, 1963)

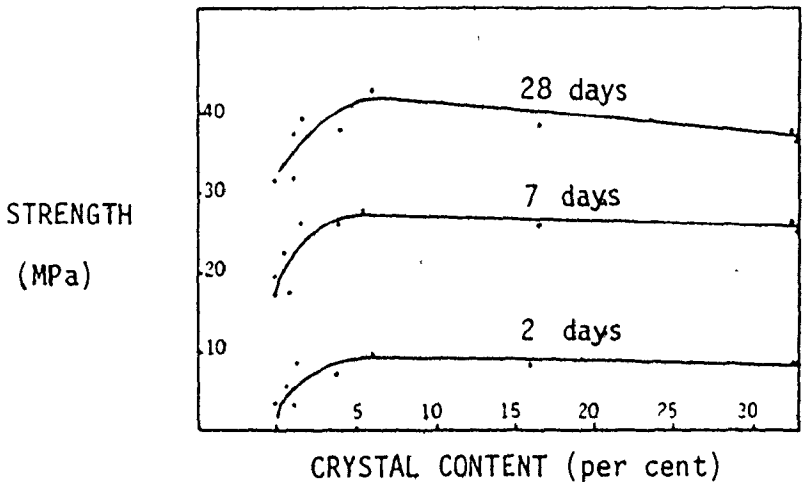

FIGURE 2.4: RELATIONSHIP BETWEEN CRYSTAL CONTENT AND STRENGTH DEVELOPMENT OF STANDARD ISO MORTARS (76 per cent slag, 19 per cent clinker, 5 per cent gypsum) (after Demoulian et al, 1980)

Smolczyk (1980) mentioned that unlike concentrations of large crystals, the presence of a finely distributed crystal content would have little detrimental effect on strength. The reason for this may be that small, finely distributed crystals could remain partially or totally encapsulated in reactive glass when ground to cement finenesses.

Inspite of the fact that a mainly amorphous structure is essential to slag hydraulicity, the inclusion of minimum glass content criteria in standard specifications is rare. One of the reasons for this is that there are many methods used to determine glass contents and the results are not always in agreement. However, even if a standard method was adopted, another problem would be establishing a minimum acceptable glass content. Minimum levels such as 90 per cent have been quoted in commercial data sheets, but as previously discussed, Schwiete and Dölbor (1963) suggested 30 to 40 per cent glass was acceptable, and the results of Demoulian and co-workers (1980) implied that less than 70 per cent glass was still acceptable. Coale and co-workers (1973) on the other hand suggested a minimum glass content of 85 per cent, not only to avoid low reactivity but to reduce the possibility of unsoundness due to the crystallization of periclase. However, with the possible exception of some high magnesia (up to 20 per cent) South African slags (Krüger, 1976), this latter consideration is not a problem.

2.3.3 Chemical Composition

While the vitreous state is essential to slag hydraulicity, the chemical composition of slag is also an influencing factor. Not only does the composition affect the degree of vitrification achieved upon quenching (for a given quenching process, via effects on liquidus temperature and viscosity) but it affects the solubility and hence the reactivity of the glass during hydration. For example, at ambient temperatures commercial glasses of high silica content are not readily attacked by water or alkaline solutions, but as the C/S ratio increases they become more soluble (Krüger, 1976). However, as the C/S ratio increases, the slag also becomes more difficult to vitrify for a given quenching process (Parker and Nurse, 1949).

It is generally accepted that the hydraulic activity of slags increase with increasing CaO and Al_2O_3 contents and decreasing contents of SiO_2 and MnO contents (Schröder, 1969; Yang, 1969). However, Smolczyk (1980) stated that the so called acid slags (C/S<1.0), which were previously considered of poor quality (Keil, 1954; Kramer,1962), were reactive when the low CaO contents were compensated by increases in MgO and Al_2O_3 contents. This was of interest since slags produced in Hamilton often have C/S ratios less than unity (shown later in Table 3.1) yet are still very reactive. Furthermore, as Kondo(1962) mentioned, slag glasses with increasing Al_2O_3 contents may develop higher strengths, but a factor often overlooked is that these glasses also require higher levels of calcium hydroxide activation in order to develop strength. He suggested that this increased CH demand at high

Al_2O_3 contents may be the result of pozzolanic rather than hydraulic reactions and the CH is no longer just an activator. From the literature, the influence of MgO on hydraulicity is conflicting (Kramer, 1962; Schröder, 1969) but most recent studies have shown it to be beneficial (Smolczyk, 1980). The early concerns about the formation of periclase, which could result in unsoundness, have been diminished by the successful use of South African slags containing up to 20 per cent MgO (Stutterheim, 1960; Steyn, 1965; Krüger, 1976).

The effect of minor elements on reactivity is unclear. Keil and Gille (1949) found that synthetic glasses composed of only the major oxides, C-M-A-S, did not exhibit the same reactivity trends as industrial slags. However, according to Nurse (1964), Tanaka and co-workers found that the reactivity of C-A-S glasses was similar to that of industrial slags. Smolczyk (1978) found that the inclusion of minor elements in a complex equation improved predictions of strength but the effects of these oxides changed with the properties of the portland cement activator and with the different curing ages evaluated.

In spite of the fact that the chemical composition of slag is an area over which a slag cement producer has no control (except for the rejection of slags with unusual composition), many of the studies on slag hydraulicity have concentrated on compositional effects (De Langavant, 1949; Sopora, 1959; Coale et al, 1973; Teoreanu and Georgescu, 1974). From these and other studies, at least thirteen compositional moduli have been developed to predict optimum slag compositions, as summarized by Keil (1954), Schröder (1969), Lea (1971),

Terrier (1973), Gupta (1976) and Krüger (1976).

Many of the moduli are derived from the basicity ratios used in blast furnace operations to judge the melting conditions in the blast furnace, as given in Equations 2.1 to 2.3 (Keil, 1954).

$$M1^* = C/S \quad (2.1)$$

$$M2 = (C + M) / S \quad (2.2)$$

$$M3 = (C + M) / (S + A) \quad (2.3)$$

The modulus M3 is also used in the Soviet Union in combination with M4 to evaluate slags for cements (Komar, 1974).

$$M4 = A/S \quad (2.4)$$

Before 1942, the German DIN1164 cement standard required that Equation 2.5 be at least unity for slags used in cements.

$$M5 = (C + M + 0.33\,A) / (S + 0.67A) \geq 1.0 \quad (2.5)$$

But this was replaced by Equation 2.6 which is still contained in DIN1164 (1967) and was adopted in the Canadian CSA A363-M77 preliminary standard.

$$M6 = (C + M + A) / S \geq 1.0 \quad (2.6)$$

In Japan, the modulus M6 is required to be greater than 1.4 (Satarin, 1974).

Another modulus, M7, was given by Keil (1954) which included terms for calcium sulphide and manganese contents in slags.

$$M7 = (C + C\bar{S} + 0.5M + A) / (S + MnO) \geq 1.5 \quad (2.7)$$

---

* The compositional ratios or moduli listed here are labelled M1 to M12 in order to distinguish them in Chapter 5.

De Langavant (1949) proposed an index of quality,

$$M8 = 20 + C + A + 0.5M - 2S \quad (2.8)$$

where the slag quality was judged medium if M8 < 12, good if 12< M8 <16, and very good if M8 >16. However, if this index is applied to typical, modern North American slags where dolomite is used as the blast furnace flux (see Table 3.1), almost all would only be of medium quality.

Sopora (1959) considered iron and manganese to have adverse affects on reactivity and proposed the ratio given in Equation 2.9.

$$M9 = (C + \tfrac{1}{2} M + A) / (S + F + (MnO)^2) \quad (2.9)$$

Schwiete and Dölbor (1963) did not consider the effects of magnesia in the development of their modulus, which was rearranged by Krüger (1976), as shown in Equation 2.10.

$$M10 = (C + 0.9A) / (S + 0.1A) \quad (2.10)$$

Cheron and Lardinois (1969) found a linear relation between Equation 2.11 and compressive strength.

$$M11 = (C + 1.4M + 0.56A) / S \quad (2.11)$$

Coale and co-workers (1973), using synthetically prepared glasses over a wide range of major oxides, found a relation between compressive strength and Equation 2.12 for calcium hydroxide activation.

$$M12 = (6C + 3A) / (7S + 4M) \quad (2.12)$$

But at the same time, it was found that neither this modulus nor the previously mentioned moduli were entirely satisfactory even when applied to an individual phase field. It was concluded that no linear relationship exists between strength and oxide composition over a large range

of compositions. Gupta (1976) and Regourd and co-workers (1980) also found that the prediction of strength development by chemical composition or by many of the previously given moduli was unsatisfactory.

Parker and Nurse (1949) recognized that the glass content was important to any quality calculation and incorporated it (determined microscopically) into their formula along with the product of glass content and the ratio, M5;

$$M13 = 0.38 \text{ (Glass content) } (M5 - 0.72) + 75.0 \qquad (2.13)$$

where M13 is the percentage compressive strength developed in comparison to concrete made from portland cement. Kramer (1962) also found a relationship between strength and glass content as measured by ultra-violet light multiplied by the ratio M1. In these two relationships, the assumption of perfect vitrification (which is made in ratios M1-M12) is not made and these indices, combining glass contents and chemical compositions, appear to be more applicable to evaluation of industrially quenched slags. However, Parker (1954) subsequently reported that inspite of their index, M13, strength testing was still the most satisfactory method of evaluating slag quality.

In conclusion, while chemical composition undoubtedly affects slag reactivity, the effects of compositional changes on hydraulicity are unclear. Also, as the composition of slag is determined by the iron producer to optimize the quality of the iron, the work in this area seems disproportionate to its practical use. In practise, blending of unground slag stockpiles is used to ensure relatively uniform slag properties and hydraulic performance (Warren, 1977).

2.3.4 Mineralogy

Small changes in chemical composition can have large effects on the mineralogical composition of portland cement (Neville, 1972), and the mineralogical composition rather than the chemical composition, determines its hydraulic properties. Therefore, it would follow that the potential mineralogical composition of slag glass might be a more significant influence than its chemical composition on its reactivity. The crystalline compounds found in devitrified slag are mainly the melilite solid solutions series with end members akermanite (C_2MS_2) and gehlinite (C_2AS) with lesser amounts of monticellite (CMS), diopside (CMS_2), merwinite (C_3MS_2) and others. However, the crystalline minerals are generally considered inert towards water (Schröder, 1969; Lea, 1971), likely due to the regular coordination of the atoms in their crystal structures (Pai and Hattiangadi, 1969).

Keil and Gille (1949) concluded that the hydraulic properties of glass could not be evaluated by calculation of the minerals present at equilibrium. Nurse (1964) agreed that this technique could be misleading and that it offered no advantages over the more common relations with oxide composition. However, Regourd and co-workers (1980) recently concluded that the melilite composition, based on measurement of the lattice parameters of devitrified slags, was an important factor affecting reactivity. Solacolu (1958) and Teoreanu and Georgescu (1974) found that variations of strength development with chemical composition were not continuous at phase field boundaries defining different potential equilibrium mineral formations. Therefore,

from the literature, the relevance of equilibrium mineralogical composition to hydraulic activity is unclear.

Akatsu and co-workers (1978) found that in the gehlinite-akermanite system, the most reactive glasses had a composition of 30 to 50 per cent akermanite at 3 and 7 days. However, at 28 days high strengths were obtained from glasses with compositions of 20 to 70 per cent akermanite.

Kondo and Ueda (1969), based on a study of the pH of suspended glasses, considered C_2MS_2 more than just latently hydraulic, while C_2AS and a solid solution mixture were just considered latently hydraulic. Crystalline inclusions contained in quenched slags, such as C_3MS_2 which are not present after equilibrium crystallization (Krüger, 1976) may affect slag reactivity by altering the composition of the glass phase. Schröder (1969) mentioned work done to enhance hydraulicity by thermal treatments to promote favourable, unstable crystallizations of merwinite with respect to gehlinite.

2.3.5 Fineness of Grinding

While the ease with which slag can be ground does not affect its hydraulicity, it does affect the optimum fineness of grinding from both strength development and economic viewpoints. Water granulated slag has been reported to be less easily ground than portland cement (Stutterheim, 1969), thus intergrinding, the traditional method of producing blended cements, would tend to preferentially grind the portland cement component. However, recent work by Osbourne (1977) has shown that pelletized slag, due to its porous structure, requires less energy to grind than granulated slags.

Because of its advantages, as summarized by Schröder (1969), Stutterheim (1969), Lea (1971) and Mills (1976), the practise of separately ground slag has developed in South Africa, England and Canada. In this study, separately ground slags were used and the discussion is focussed on the effects of the fineness of separately ground slag. A Blaine fineness of 400 m^2/kg has been adopted as a standard for comparison since this was found to be optimum for Canadian pelletized slags in commercial operations (Emery, Cotsworth, and Hooton, 1976; Warren, 1977).

Lea (1971) reported the influence of fineness on the 28 day strengths of concrete containing 30 per cent slag cement. Strengths were decreased by 22 per cent when the slag fineness (Blaine) was reduced from 393 m^2/kg to 310 m^2/kg, but only increased by 13 per cent when the slag fineness was increased from 393 m^2/kg to 485 m^2/kg. However, at 75 per cent slag contents, Schröder (1969) reported

approximately equivalent increases in strengths for slag finenesses increased from 350 m^2/kg to 400 m^2/kg and 400 m^2/kg to 450 m^2/kg as shown in Figure 2.5. For the same slag content, Schröder (1969) also found that the effects of fineness on strength were also influenced by the chemical composition of the slag. Depending on the composition, the increases in 28 day strengths varied from 20 to 60 per cent when the fineness was increased from about 280 m^2/kg to 400 m^2/kg.

In general, as with all cementing materials, the reactivity of slag is proportional to its surface area, with the fineness being limited by economic considerations as well as performance considerations such as shrinkage and setting times.

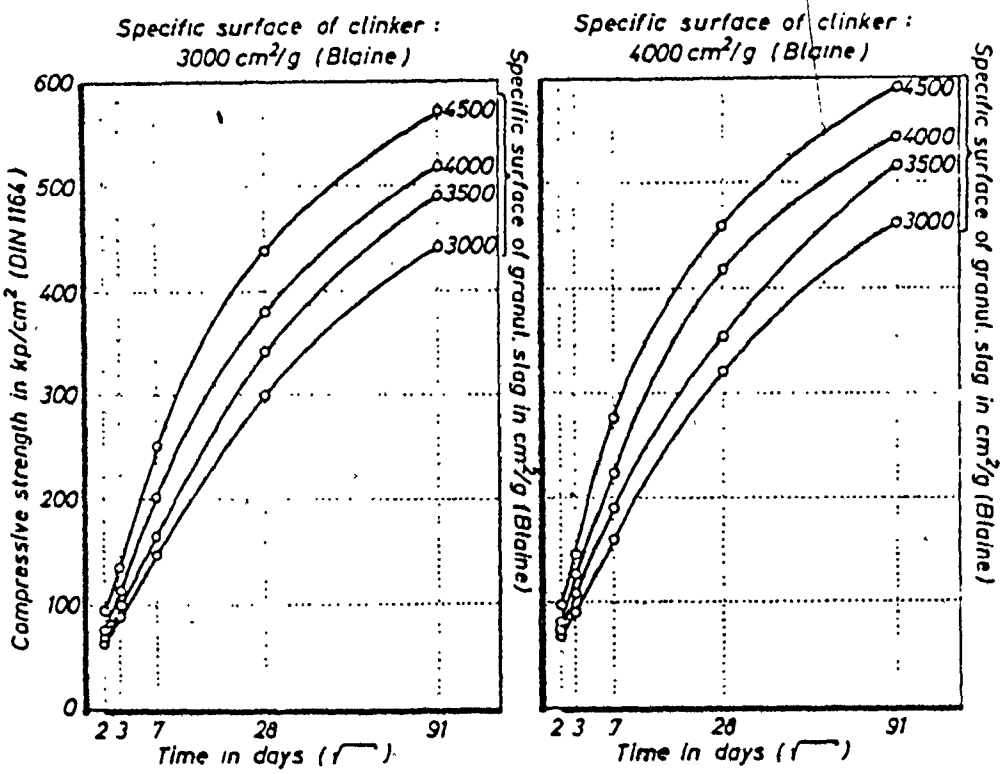

FIGURE 2.5: EFFECT OF FINENESS ON STRENGTHS OF DIN 1164 MORTAR PRISMS CONTAINING 75 PER CENT SLAG (Schröder, 1969)

2.3.6 Activation of Slag Glasses

The reaction mechanism by which the latent hydraulicity of slag glasses is released was proposed by D'Ans and Eick (1954). In water, CaO was initially released from the surface of the slag grains, but the reaction of water with the remaining Al_2O_3 and SiO_2 formed impermeable acidic gels on the surfaces of the slag grains. These coatings acted to inhibit further hydration until sufficient, externally supplied lime was added to dissolve them. This mechanism was confirmed by Kondo and Ueda (1969) for C_2AS glasses where 0.2μm thick coatings of composition ASH_6 were found to form on the glass surfaces.

While slags are generally regarded to be only hydraulic when externally activated by alkaline or sulphate solutions (Gutt, 1971), there are some slags which will set and develop strength in pure water. Keil and Gille (1949) found that C_2MS_2 glasses were reactive in water but that C_2AS was not. Ludwig (1964) found that C_2MS_2 formed a tobermorite-like C-M-S-H phase, but C_2AS also hydrated to form C_2ASH_8. Teorneau and Georgescu (1974) found that some synthetic slag glasses developed strength in water depending on their potential equilibrium minerals. In conflict with previously mentioned references, akermanitic systems were found to be practically inert. Good strengths were developed for C/S between 0.8 and 1.1, and less than 10 per cent alumina contents. Glasses with alumina contents between 12 and 17 per cent, more typical of European slags, were non-reactive.

According to Eitel (1966), D'Ans, Eick and Kaempfe, found that slags high in calcium sulphide were self-activating since in

water, CaS dissolved to form $Ca(OH)_2$ and H_2S. Because of the desulphurization processes used at Dofasco in Hamilton, slags with sulphide contents as high as three per cent are found (see Table 3.1) and this may account for some of the non-activated reactivity found for these slags (Kim, 1975; Emery, Kim and Cotsworth, 1976; Gupta, 1976). However, Teorneau and Georgescu (1974) and Krüger (1976) found that there was no relationship between the strength potential of unactivated and activated slags and therefore there appears to be little value in evaluating the hydraulic potential of an unactivated slag.

The most commonly used activators have been calcium hydroxide, portland cement and gypsum. Other chemical activators, such as Na_2CO_3 (Dron and Petit, 1975) , NaOH, Na_2SiO_3 (Yang, 1969) and $CaCl_2$ (Teorneau and Georgescu, 1974), have also been used. From the practical point of view, portland cement is the most important activator since it is present in almost all concrete.

It is often assumed that when portland cement is used, the activation is actually by the calcium hydroxide liberated as the portland cement hydrates. However, Nurse (1964) mentioned that these are differences between lime and portland cement activation and the type and amount of activation required for optimum strength depends on the slag composition. Keil and Gille (1949) found that when using lime, C_2AS glass developed high strengths while C_2MS_2 did not, but the reverse was true when portland cement was used. In contrast, Krüger (1976) suggests that the hydration reactions of slag activated with hydrated lime and portland cement are similar. In fact, he suggests that lime should be used instead of portland cement for evaluation of a slag's strength

potential.

The activation of slag by portland cement also depends to a large extent on the mineralogical composition of the portland cement (Smolczyk,1980). Larger amounts of C_3S have been found to be beneficial (Maiko et al, 1976). The hydration temperature is also a factor when evaluating hydraulic potential. Maiko and co-workers (1976) using 50 per cent portland cement-50 per cent slag glass blends found that the composition of glasses developing high strengths at 20°C (CAS_2, CMS and melilite solid solutions) were not necessarily the same as those at 90°C (αCS, CAS_2 and C_2MS_2).

Ludwig (1964) found that the hydration products of portland-slag cements were the same as for portland cement, except that, at higher slag contents, smaller quantities of calcium hydroxide and $C_4(A,F)H_{13}$ hydrogarnets were found.

Smolczyk and Romberg (1976) mentioned that the inclusion of slag affected both the porosity and the pore size distribution of pastes at ambient temperatures. Increasing the slag content of pastes from 0 to 76 per cent had the effect of reducing the volume of large pores (greater than 300µm diameter) by about one third. This is important since the presence of large "capillary" pores both increases the permeability and decreases the strength of cement pastes (Kayyali et al, 1980).

2.4 AUTOCLAVE CURING AND REACTIONS

2.4.1 Background

2.4.1.1 Autoclave Curing Cycles

Autoclave curing is the name usually used when referring to curing at temperatures in excess of 100°C in saturated steam. The terms hydrothermal curing and high temperature and pressure curing can also refer to autoclave curing but also include curing at other than saturated steam pressures.

Autoclaving is most often employed to cure concrete brick and block and calcium silicate brick (sand-lime brick). In a typical commercial process the binder and aggregate components are mixed in the same manner as normal concrete but with much lower water contents. Specific amounts of the mix are vibrated in molds until a constant specimen height is achieved. The formed blocks or bricks are then immediately de-molded and loaded on to racks. The racks mounted on wheeled carts, are usually placed in "kilns" and moist cured at 60°C to 70°C for several hours to develop the "green" strength needed to resist damage from both handling and thermal stresses. The carts are then loaded into long, cylindrical, pressure vessels where steam is admitted until the maximum temperature (and dependent steam pressure) are reached in one to two hours. Commonly used maximum temperatures range from 160°C to 190°C (0.55 MPa to 1.17 MPa steam pressure) (Davey, 1979) and these are maintained for two to eight hours, depending on the working schedule of the plant. At the end of the curing cycle the steam is usually released and used to heat a second pressure vessel

with atmospheric pressure obtained in 0.3h to 0.5h. The carts are unloaded, and upon cooling the blocks are ready for use.

2.4.1.2 Use and Advantages of Autoclaving

Autoclaving was first used in the United States in 1868, (ACI Committee 516, 1965) but did not develop until Menzel's (1934) extensive research on autoclaving and the use of silica to replace part of the portland cement.

Due to the capital costs involved with building such a plant, and more recently the energy costs of producing steam, autoclave curing is not used extensively to produce concrete block in North America. However Southern Ontario is an exception with about 90 per cent of the blocks being autoclaved (Davey, 1979).

Besides producing products that have strengths equivalent to 28 day moist cured concrete in only a few hours, other advantages to autoclaving were summarized by Nurse (1949) and the American Concrete Institute (ACI, Committee 516, 1965). These included; reduction in the portland cement or lime required, by partial replacement with ground quartz (which only becomes reactive at temperatures greater than 100^{o}C as shown in Figure 2.6), increased strength by reaction of the aggregates with the binder (and stabilization of some unsound aggregates), reduction in drying shrinkage by about 50 per cent, increased resistance to sulphate attack and the elimination of efflorescence.The final products also have a very low residual moisture content, which coupled with reduced drying shrinkage, allows their immediate use.

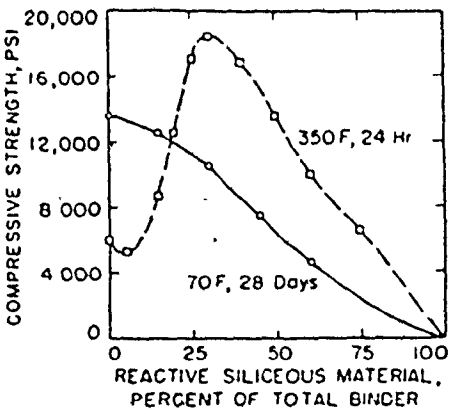

FIGURE 2.6: COMPRESSIVE STRENGTH OF AUTOCLAVED AND MOIST CURED CEMENT PASTE WITH VARIOUS AMOUNTS OF SILICA FLOUR (GROUND QUARTZ)(ACI Committee 516, 1965, after Menzel,1934)
Note: 1MPa = 145.04 psi

2.4.1.3 Autoclave Reactions

The nature of autoclave hydration products is similar to those found in concrete cured at ambient temperatures with the following exceptions.

1. The calcium /silica (C/S) ratios of autoclave hydrates which result in maximum strengths are much lower, ranging from 0.81 to 1.5.

2. Silica flour (ground quartz), which is practically inert at ambient temperatures, reacts with the lime liberated by the hydration of portland cement at temperatures greater than 100^{o}C to form more calcium silicate hydrates. This elimination of free lime is the major reason for increased sulphate resistance. Silica flour is usually blended with portland cement

to provide a C/S ratio consistent with high strengths.

3. The degree of crystallinity of the C-S-H* found in autoclaved hydration products is much higher than the nearly amorphous C-S-H formed at ambient temperatures.

4. Autoclaved portland cement was found (Powers and Brownyard, 1948) to have a very low surface area resulting from a collapsed structure with high volume stability.

2.4.2 Calcium Silicate Hydrates formed from Autoclaving

Calcium silicate hydrates have been extensively studied under autoclave curing since they comprise most of the hydration products formed in portland cement-quartz reactions and account for most of the strength developed. Comprehensive reviews on the composition of autoclaved calcium silicates were given by Heller and Taylor (1956), Taylor (1962, 1964, 1967), Kalousek (1969) and Taylor and Roy (1980). Their physical and mechanical properties were studied in many works including those by Kalousek (1954-1,2), Aitken and Taylor (1960,1962), Dyczek and Petri (1974), Beaudoin and Feldman (1975), and Crennan and co-workers (1977).

Since the autoclave curing cycle of 185°C for 4h was chosen for study in this work, the discussion of previous studies has been limited to temperatures close to 185°C. However most studies have been either interested in equilibrium reaction products or have adopted

---

* C-S-H is the term adopted by Taylor (1962) to represent poorly crystalline calcium silicate hydrates of the tobermorite group and covering a range of compositions.

older, long autoclave periods and as a result, very little information is available for shorter autoclave periods. This lack of knowledge about reactions and properties of cements at short autoclave cycles was also noted by Taylor and Roy (1980).

For lime-quartz pastes autoclaved for at least 25h in most cases, the hydration products detected are given in Table 2.1. Some of these phases, particularily xonotlite (C_6S_6H), would not likely be present at shorter autoclave periods (Kamel, 1973-1). The range of formation for poorly crystallized C-S-H would likely be wider for shorter periods of autoclaving since it has been found to be an intermediate or meta-stable phase in some cases (Chan and co-workers, 1978; Taylor and Roy, 1980), converting to other phases after longer autoclave periods.

The ranges of phases formed from portland cement-quartz pastes autoclaved for 25h, are shown in Figure 2.7. The range of commonly used C/S ratios and temperatures shown by the shaded region in Figure 2.7 indicates the predominance of 11.Å tobermorite ($C_5S_6H_5$) in commercial products.

Studying the reaction of lime-quartz mixtures after 5h at 180°C, Chan et al (1978) found crystalline tobermorite and xonotlite for C/S equal to 1.0, and poorly crystalline tobermorite when C/S equalled 0.8. The crystallinity of the tobermorite was also found to depend on the quartz particle size, in agreement with Crennan and co-workers (1972). In a similar study, El-Hemaly and co-workers (1977) found that the addition of 5.6 per cent Al_2O_3, at C / (S+A) equal to 0.8 resulted

TABLE 2.1

COMPOUNDS DETECTED IN LIME - QUARTZ PASTES (Aitken and Taylor,1960)

Compound	Overall CaO/SiO_2 ratios of pastes in which detected	Range of temperatures in which compound was formed (°C)
Gyrolite	0·33–0·67	165–200
C-S-H (ill-crystallized)	0·33–3·00	90–175
Tobermorite (crystalline 11 Å form)	0·33–1·08	125–200
Xonotlite	0·67–3·00	165–200
"Phase F"	1·00–3·00	155–200
α-C_2S-hydrate	1·50–3·00	125–175
Hillebrandite	1·67–2·00	165–200

Note: Phase F is a compound of possible composition $C_5S_3H_2$

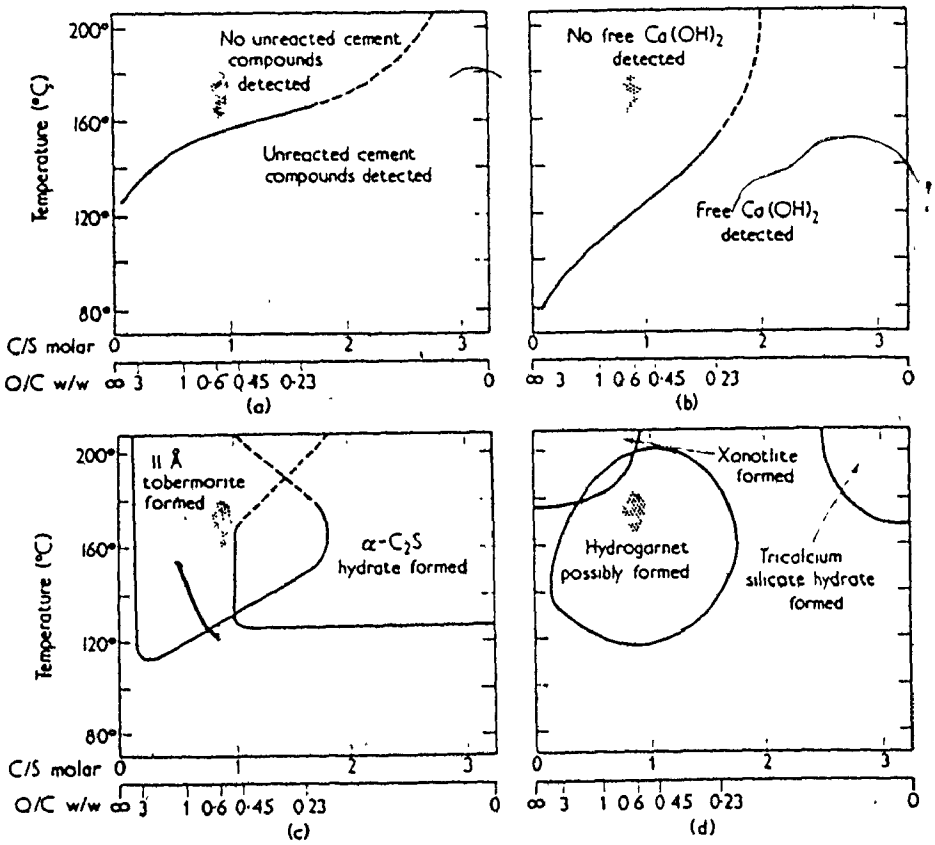

FIGURE 2.7: PHASES DETECTED BY XRD IN CEMENT AND CEMENT - QUARTZ PASTES CURED FOR 25h (Aitken and Taylor,1962)

Note: Q/C = quartz / portland cement ratio by weight

in the formation of more crystalline tobermorite.

Comparing the reaction of hydrated lime-quartz and portland cement-quartz pastes, Aitken and Taylor (1962) found that portland cement was slower to react. While with lime, the quartz was often completely reacted, unreacted quartz was detected in all portland cement containing pastes. They attributed the formation of hydrates with higher C/S ratios than the bulk C/S ratio of the mixture, to this slow reaction.

Maximum αC_2SH contents resulted from low quartz contents of around 5 to 10 per cent (Kalousek, 1954-2; Sanders and Smothers, 1957). It is readily formed in short autoclave periods when the C/S of the cementing mixture is greater than 1.5(Taylor, 1964).

Other phases, sometimes identified in autoclaved portland cement and portland cement-quartz pastes have been tricalcium silicate hydrate ($C_3SH_{1.5}$) and possibly hydrogarnet ($C_3AS_zH_{6-2z}$ solid solution) (Aitken and Taylor, 1962), hillebrandite (βC_2SH) and xonotlite (C_6S_6H). Other minor or irregularily occurring phases were discussed by Kalousek (1969) and by Taylor and Roy (1980). Tricalcium silicate hydrate is usually only found in portland cement pastes since a small quantity of added quartz suppresses its formation (Aitken and Taylor, 1962). Below 165°C, αC_2SH and CH are more likely to form (Taylor, 1964). Xonotlite readily forms at temperatures greater than 200°C and more slowly at lower temperatures. However, the presence of only a few tenths of a per cent of Al_2O_3 retarded the formation of xonotlite and stabilized the initially formed tobermorite phases at 175°C (Kalousek, 1957).

The addition of 5 per cent Al_2O_3 in the tobermorite lattice was found to reduce shrinkage by about 50 per cent (Noorlander, 1967). When the Al_2O_3 content of the lime-quartz-kaolin cementing mixtures exceeded five per cent, the hydrogarnet C_3ASH_4 was also detected after 24h at 175°C (Kalousek, 1957). For the same autoclave cycles, Diamond and co-workers (1966) found that up to 10 per cent aluminum could be accommodated in the tobermorite structure without appearance of hydrogarnet. However Aitken and Taylor (1962) only found small quantities of hydrogarnet sporodically in portland cement-quartz mixtures. Kalousek (1969) concluded that hydrogarnets would be rarely found in commercial autoclave products except when large quantities of high alumina fly ash or slag were incorporated in the cement.

Therefore at temperatures around 185°C, and for short autoclave periods, the most likely hydration products depending on the cement composition are tobermorite-like C-S-H of varying degrees of crystallinity, αC_2SH and $C_3SH_{1.5}$.

2.4.3 Physical Properties of Autoclaved Hydrates

Several studies have associated the presence of tobermorite phases with high strengths, and αC_2SH with low strengths (Sanders and Smothers, 1957; Aitken and Taylor, 1962). The crystallinity of the tobermorite - C-S-H is an important factor as well. Maximum crystallinity did not correspond to maximum strength (Crennan et al, 1972; Alexanderson,1979-1),and an optimum degree of crystallinity or mixture of crystalline and amorphous C-S-H may result in optimum

strengths (Taylor, 1964).Alexanderson(1979-1) found a linear relationship between the crystallinity of C-S-H (up to 60 per cent) and the inverse of its BET specific surface. In the same study it was also found that shrinkage decreased with increasing crystallinity.

Work by Butt and co-workers in the Soviet Union was summarized by Taylor (1967). They tested strengths of blocks made from several autoclave hydration products as shown in Table 2.2. Less crystalline C-S-H (I) (C-S-H with C/S<1.5) gave higher compressive strengths than 11Å tobermorite, while αC_2SH had practically no strength. It can be observed that high tensile to compressive strength ratios were obtained with 11Å tobermorite, xonotlite and $C_3SH_{1.5}$. This was attributed to the needle shaped morphology of the crystals in the latter two cases. High compressive strengths were associated with high surface areas which were thought to result in good bonding with many points of contact between crystals. The low strength of αC_2SH was attributed to a coarse, but well crystallized hydrate with few points of contact.

The importance of fine, less crystalline hydration products, (having many points of contact) to high strengths was also discussed by Beaudoin and Feldman (1975) and Feldman and Beaudoin (1976). They concluded that porosity, crystal bonding and hydration product density and morphology were all important factors to strength development. They found that the ratio of poorly crystalline C-S-H to well crystallized, dense material (αC_2SH and/or well crystallized tobermorite) required to give optimum strengths was dependant on the porosity of the solid. Taylor (1977) thought that this was a very important concept and it was used to explain the results of his co-workers (Crennan et al,

TABLE 2.2

COMPRESSIVE AND TRANSVERSE STRENGTHS OF BLOCKS CONSISTING OF VARIOUS CALCIUM SILICATE HYDRATES - FOUND BY BUTT AND CO-WORKERS (Taylor, 1967)

Compound	Autoclaving Conditions		Strength, kg/cm²		Bulk density, g cm³	Strength* / Density	
	T°, C	Time, days	Compressive	Transverse		Compressive	Transverse
C-S-H(I)	175	1	230	32	1·13	203	28
11Å-tobermorite	200	5	75	30	1·12	67	27
Nonotlite	250	7	122	74	1 04	117	71
α-C_2S Hydrate	200	4	2 5	1 5	0 87	3	0 5
~-C_2S Hydrate	300	10	14	4	0 98	14	4
TSH	300	20	142	100	1 45	98	69

* Recalculated from original data

Note: TSH = Tricalcium silicate hydrate 1 MPa = 10.2 kg/cm^2

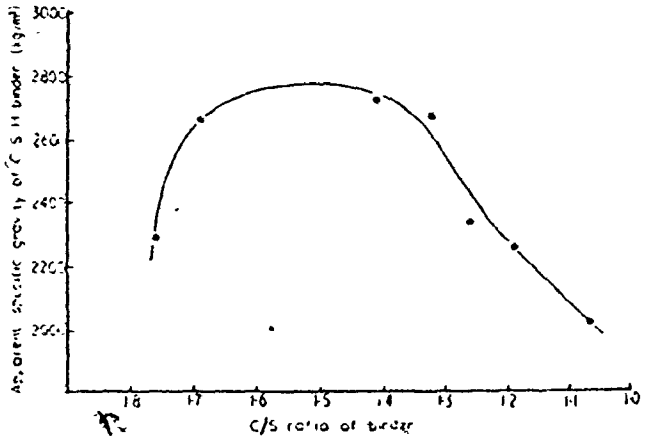

FIGURE 2.8: APPARENT SPECIFIC GRAVITY OF C-S-H BINDER AS A FUNCTION OF ITS C/S RATIO (Smith, 1979)

1977).

Beaudoin and Feldman (1975) used the solid densities of fully hydrated autoclaved pastes to characterize the type and bonding of hydration products present. Low densities corresponded with poorly crystallized C-S-H and higher strengths. Smith (1979) found that the C/S ratio of the C-S-H was also dependant on its density as shown in Figure 2.8. The low density, low C/S materials had the highest strengths.

In an earlier study, Mindess (1970) concluded that the strengths of autoclaved calcium silicate hydrates were influenced mainly by total porosity and pore size distribution, and that phase composition was only of secondary importance.

2.5 STUDIES OF AUTOCLAVED SLAG

2.5.1 Background

While the use of slag in pastes, mortars and concrete has been the subject of many studies, very little work has been directed to its use in autoclave applications. Because of this, a fairly complete summary of these studies are presented in this section. Many of these studies have used slags or synthetic glasses containing mainly CaO, Al_2O_3, and SiO_2, without dealing with the MgO contained in slags typical of North American production. Also many of the studies on autoclaving slag (and portland cement, Taylor and Roy, 1980) concentrate on equilibrium products of hydration at higher temperatures and longer autoclaving periods than those used commercially. Therefore the results obtained in many of the studies have to be viewed with caution when trying to apply them to commercial products.

2.5.2 Synthetic Glasses and Slags without Activation

Negro (1969) mentioned that he had studied the autoclave reactions of melilite glasses with various proportions of vitreous C_2AS and C_2MS_2. Hydration products detected were αC_2SH and C-S-H with xonotlite and plazolite at higher temperatures. Since no $Mg(OH)_2$ was detected, it was assumed that the magnesium ions substituted for calcium ions in the calcium silicate hydrates detected. This agreed with the results of Schwiete and co-workers (1969) who found that increasing MgO contents in the melilite glasses resulted in expansion of the lattice of C_2ASH_8 for hydration at about 22°C.

However, Krüger and Visser (1971), Visser and co-workers (1975) and Krüger (1976) found no evidence to support the formation of a C-M-S-H phase in pastes autoclaved at 215°C for up to 7 days. In these studies, it was found that a glass of composition C_2MS_2 hydrated to serpentine ($M_6S_4H_4$) and an unidentified phase (either C-S-H or calcite) with an XRD peak at 3.027Å . Amorphous gehlinite (C_2AS) hydrated to the hydrogarnet plazolite ($C_3AS_2H_2$), boehmite (γAH) and possibly αC_2SH. A glass of 50 per cent C_2AS, 50 per cent C_2MS_2 proportions and a South African slag (MgO = 15.1 per cent) both hydrated to form plazolite ($C_3AS_2H_2$), aluminum serpentine ($M_5AS_3H_4$) and possibly αC_2SH. Therefore it was concluded that the magnesium in slag glasses did not combine in a C-M-S-H phase but only in MSH phases. Krüger (1976) stated that the possibility existed that water selectively attacked certain cations, leaching them out of the vitreous slag to form hydrated phases. The cations not accounted for in the hydration products might then remain in the unhydrated glass network.

Mascolo and co-workers (1977) autoclaved synthetic glasses at 175°C and found the serpentine $M_5AS_3H_4$ together with C_2AH_6 and plazolite. The amount of C_2AH_6 increased with increasing MgO contents while the plazolite content diminished. For glasses with a constant $(C+M)/S$ ratio, strengths generally increased with increasing MgO content, up to 17.4 per cent.

Govorov (1974) autoclaved synthetic C-M-A-S glasses containing 5 per cent MgO at 150°C, 200°C and 250°C for up to 48h. For 150°C and

200°C autoclaving the main phase found was CSH(B) (C-S-H with C/S $\geq$1.5), with hydrogarnets of the solid solution series $C_3AS_zH_{6-2z}$ (where z=0 to 3) forming at some compositions. The highest strengths were found to correspond to maximum hydrogarnet compositions, however those glass compositions were much different than those typical of blast furnace slags.

2.5.3 Slags Activated With Gypsum

Massidda and Sanna(1979) autoclaved compacts of Italian slag (MgO =5.5 per cent) activated with five per cent gypsum at 180°C for 15 and 72h. The only hydrated phase detected was plazolite, with larger quantities present at 72h but with little difference in strengths. They attributed the high strengths obtained at 180°C (compared to 50°C, 70°C, 120°C and 150°C) to the lower porosities and finer pore size distributions found.

2.5.4 Slags Activated with Lime and Quartz

Midgley and Chopra (1960) autoclaved ground, foamed and granulated slags with various proportions of hydrated lime at 160°C for various periods. Unlike fly ash, quartz and other siliceous materials which consumed large quantities of lime, the slags only fully reacted with ten per cent lime after at least 6h at 160°C. The optimum amount of lime activator was found to be five per cent, resulting in very high strengths as shown in Figure 2.9. Hydrated phases included a hydrogarnet (C_3ASH_2), tobermorite-like C-S-H, and αC_2SH. When higher contents of lime were added, strengths decreased

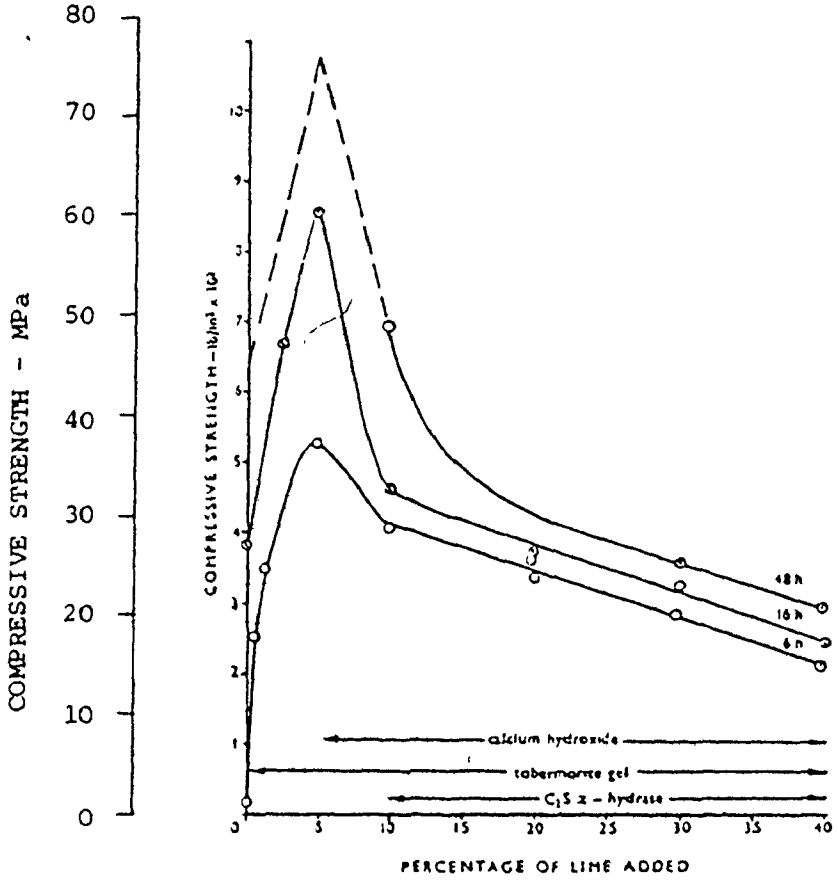

FIGURE 2.9: RELATIONSHIP BETWEEN COMPRESSIVE STRENGTH AND PERCENTAGE OF LIME ADDED TO GRANULATED SLAG FOR VARIOUS PERIODS OF AUTOCLAVING AT 160°C (Midgley and Chopra, 1960)

as the amount of αC_2SH increased at the expense of the C-S-H. The poor strength qualities of αC_2SH were also found by Kalousek (1954-2) for portland cement-quartz pastes. The slags, without lime, hydrated to poorly crystalline C-S-H and a hydrogarnet after 16h autoclaving.

Kondo and co-workers (1975) studied the reaction of pastes containing 80 per cent slag (MgO =3.4 per cent) with 20 per cent lime autoclaved for various periods at 181°C and 213°C. After 0.5, 2 and 6h autoclaving at 181°C, only poorly crystalline C-S-H (composition $C_{1.45}S_{0.8}H_{1.6}$ at 6h) was detected and strengths increased. At 12h, a hydrogarnet (C_3ASH_4) was just detected and further autoclaving resulted in reduced strengths which were thought to be due to increased quantities of hydrogarnet. This is in disagreement with the higher strengths of pastes containing hydrogarnet found by Govorov (1974). It was also found that there was high reactivity up to 0.5h autoclaving, then an almost dormant period occurred until 2h with the reaction rate increasing at later ages.

The dormant period was attributed to an impervious coating forming on the slag grains and temporarily inhibiting further reaction, which was similar to the coatings described by D'Ans and Eick (1954). A slag-lime paste of the same composition was also autoclaved by Abo-El-Enein (1977) with similar hydration products forming, but with slightly different strength development.

In the same study, Kondo and co-workers (1975) autoclaved a paste composition 50 per cent slag, 20 per cent lime and 30 per cent ground quartz. For the first 2h of autoclaving a high lime, poorly crystalline C-S-H was formed and very little quartz was reacted. For

up to 12h autoclaving increased quantities of C-S-H with lower C/S ratios were detected as strengths increased (composition $=C_{1.5}A_{0.1}S_{0.9}H_{1.0}$ at 6h). Lower strengths occurring after longer autoclave periods were attributed to a change in morphology of the C-S-H. It was concluded that the high reactivity of the slag after short periods of autoclaving initially inhibited the reaction of the quartz.

Abo-El-Enein and co-workers (1977, 1978) studied a 25 per cent slag, 25 per cent lime, 50 per cent quartz paste autoclaved at 181°C. After 2h autoclaving only poorly crystalline C-S-H was detected with more crystalline fibrous C-S-H forming after 6h, corresponding to optimum strength. Strengths deteriorated after 12h autoclaving but started to improve after 24h and a very dense C-S-H with a mix of fibrous and platy morphologies was observed in the SEM.

2.5.5 Slag Activated with Portland Cement and Quartz

The study of slag in conjunction with portland cement and quartz was thought to be the most relevant to commercial practice due to the frequent use of portland cement and quartz in autoclave binders.

Menzel (1934) substituted ground, air-cooled slag for quartz in portland cement-quartz mixtures of varying proportions. Due to the crystalline nature of the slag, the strengths were found to decrease almost linearly with increasing slag content after 24h autoclaving at 177°C. In a similar study by Kalousek (1954-2), replacing quartz with ground, expanded slag resulted in lower strengths. Akaiwa and Sudoh

(1966) found that replacing 45 per cent of portland cement by granulated slag lowered strengths after 5h autoclaving at 200°C. Yang (1969) autoclaved suspensions of 75 per cent slag and 25 per cent portland cement, with and without silica flour, for 16h at 183°C. Without silica flour, tobermorite-like C-S-H, a hydrogarnet and possibly xonotlite were detected. With increasing contents of silica flour, the amount of C-S-H increased and the hydrogarnet decreased until it was not detected at 30 per cent silica flour.

An autoclaved slag-portland cement paste was studied by Kamel (1973-1). It consisted of 80 per cent slag, 15 per cent portland cement clinker and 5 per cent gypsum and was autoclaved at 193°C for 5h and 6h. Another paste consisting of one part of the above mixture with 0.5 parts of quartz was also made. After 5h autoclaving, the paste with quartz was found to contain mainly tobermorite (C-S-H) while the paste without quartz also contained a little hillebrandite (βC_2SH). After 6h autoclaving, xonotlite (C_6S_6H) was also detected and this was thought to be responsible for the lower strengths encountered (Kamel, 1973-2).

In a later study, Kamel (1975) found that increasing the temperature from 193°C to 204°C and 213°C reduced the autoclave time required for maximum strength from 5h to 4h and 3h respectively.

Autoclaving portland cement-slag glass mortars at 175°C, Mascolo and co-workers (1977) found that optimum strengths occurred for glasses with 10 per cent MgO and that the optimum strengths were not sensitive to the amount of portland cement used (30, 50 or 70 per cent). When only 30 per cent slag was used, the influence of slag composition on strength

was minimal.

2.5.6 Slag Activated with Quartz

Kamel (1973-1) studied a paste composed of 67 per cent slag and 33 per cent quartz with W/C = 0.25. After 5h autoclaving at 193°C, mostly tobermorite (C-S-H) and a small amount of xonotlite were detected. After 6h, more xonotlite formed at the expense of tobermorite resulting in a lower value of combined water.

2.6 SUMMARY

The production of slag and the types of processing used were discussed with emphasis on granulation and pelletizing quenching processes which make slag suitable for cementitious end uses.

Next, the factors affecting slag hydraulicity were detailed with the main points summarized as follows.

From the literature, a high degree of vitrification is desirable but, due to other influences, partially vitrified slags may possess similar reactivities to completely vitrified slags. From the number of methods used for determination of the degree of vitrification, and the lack of minimum glass content provisions or methods of measurement in standard specifications, there appears to be a need for further work in this area. Also, while several studies have shown that hydraulic potential generally increases with increased glass content, there is disagreement as to the sensitivity of glass content to strength. Very few researchers have gone so far as to recommend a specific minimum glass content, but the suitability of slags with between 30 and 65 per cent contents has been mentioned or implied (Schwiete and Dölbor, 1963; Demoulian et al, 1980).

In spite of the existence of many chemical indices for the prediction of optimum hydraulicity, the effects of chemical composition are not clear but it appears that slags over a wide range of compositions can be utilized for cementitious purposes. From the production viewpoint, consistency of chemical composition would be more important than the actual composition in order to produce a cement with uniform properties.

The usefulness of evaluating a slag in terms of its mineralogical composition is a point of contraversy. However, knowledge of the types of crystalline minerals co-existing with the glass in quenched slags could be important in view of their effect on the chemical composition of the glass component.

Increasing the fineness of grinding will improve the kinetics of slag reaction but energy considerations limit the practical range of grinding.

To develop strengths within a practical time frame, slags require external activation and are most often blended with portland cement. The hydration products of slags activated with portland cement are similar to those of portland cement alone, but the pore size distribution of the hardened paste may be finer.

A typical autoclave product production cycle was described and then the types and properties of autoclaved calcium silicate hydrates were discussed. From the literature, there appears to have been little work done using the short autoclave cycles typical of modern commercial practise. Also, it has been found that variables such as quartz particle size can affect both the kinetics of hydraulic reactions and the crystallinity of the hydration products formed. Therefore, there is also a need to use typical, commercially available materials in the study of autoclave reactions in order to make the work more relevant to the local commercial sector.

From the limited work on the autoclave curing of slag, it appears that when activated by lime or portland cement without quartz,

slag hydrates to tobermorite-like C-S-H and αC_2SH. Hydrogarnets, such as plazolite, have been found, but the shortest autoclave period where this was noted was 12h. With slags having a high MgO content, the aluminium serpentine $M_5AS_3H_4$ was found in several instances but again only at long curing cycles. Other studies have conlcuded that the MgO content of slags substituted into tne C-S-H phase in a similar fashion to Al_2O_3.

When quartz was used as well as lime or portland cement to activate slag, poorly crystalline C-S-H has been found after short autoclave periods with the degree of crystallinity improving after longer autoclaving.

Therefore, for short autoclave periods, the introduction of slag appears to give similar hydration products to those found using typical portland cement-quartz binders.

3. DETERMINATION OF GLASS CONTENT AND ITS IMPORTANCE TO HYDRAULICITY

3.1 INTRODUCTION

3.1.1 General

As with portland cement, the hydraulic reactivity of slag is dependent on its chemical and physical properties. With slag, the presence of glass is the most significant variable, and certainly the most critical to hydraulic performance, since a non-quenched, crystalline slag possesses little reactive potential. The amount of amorphous material obtained can be controlled by the producer, yet due to its nature (i.e. lack of range order, thus not exhibiting XRD patterns), the degree of vitrification is the most difficult slag parameter to quantify. This is born out by the multitude of methods of glass content measurement available, and the widely differing results obtained from each.

3.1.2 Background

Quenching of molten slag was originally introduced to expedite quick removal from the limited space surrounding the furnace. Such quenching by water jets or semi-dry mechanical devices (pelletizers for instance, Margesson and England, 1971), generally forms a glassy or non-crystalline slag structure. The importance of this glassy structure to the utilization of the latent cementitious properties of slag has been known since at least 1863, when Langen first produced cements from granulated (water quenched) slag in Germany (Schröder,

1969).

While other factors, notably chemical and mineralogical composition and the fineness of grinding, affect the hydraulic potential of slag, understanding the structure and trying to estimate the quantity of slag glass has been the subject of numerous studies since 1863. Major contributions and summaries on glass structure and determining glass content are available in the literature (Parker and Nurse, 1949; Keil,1954 ; Kramer, 1962; Schröder, 1969; Nurse, 1964; Lea,1971).

One explanation for the hydraulic activity of glasses has been based on free energy considerations. While not working with slags, Nassau and co-workers (1979) found that certain glasses hydrated in moist air while crystals of the same composition did not. Their explanation of this phenomenon was based on the Gibbs free energy equation and assumed equilibrium conditions and no kinetic barriers. For the transformations:

glass → crystal $G_{g,c}$ is negative

crystal + H_2O → hydrate $G_{c,h}$ is positive,

where G is the Gibbs free energy, g=glass, c=crystal, and h=hydrate.* Therefore for the direct hydration of glass:

glass + H_2O → hydrate $G_{g,h} = G_{g,c} + G_{c,h}$

As long as the magnitude of $G_{g,c}$ is larger than $G_{c,h}$, then $G_{g,h}$ is negative and the glass will hydrate even if the crystal would not. These reactions are illustrated in Figure 3.1. Of course, slags hydrate only very slowly with water, since there are kinetic barriers

* For convenience, the simplified notation of Nassau et al is adopted.

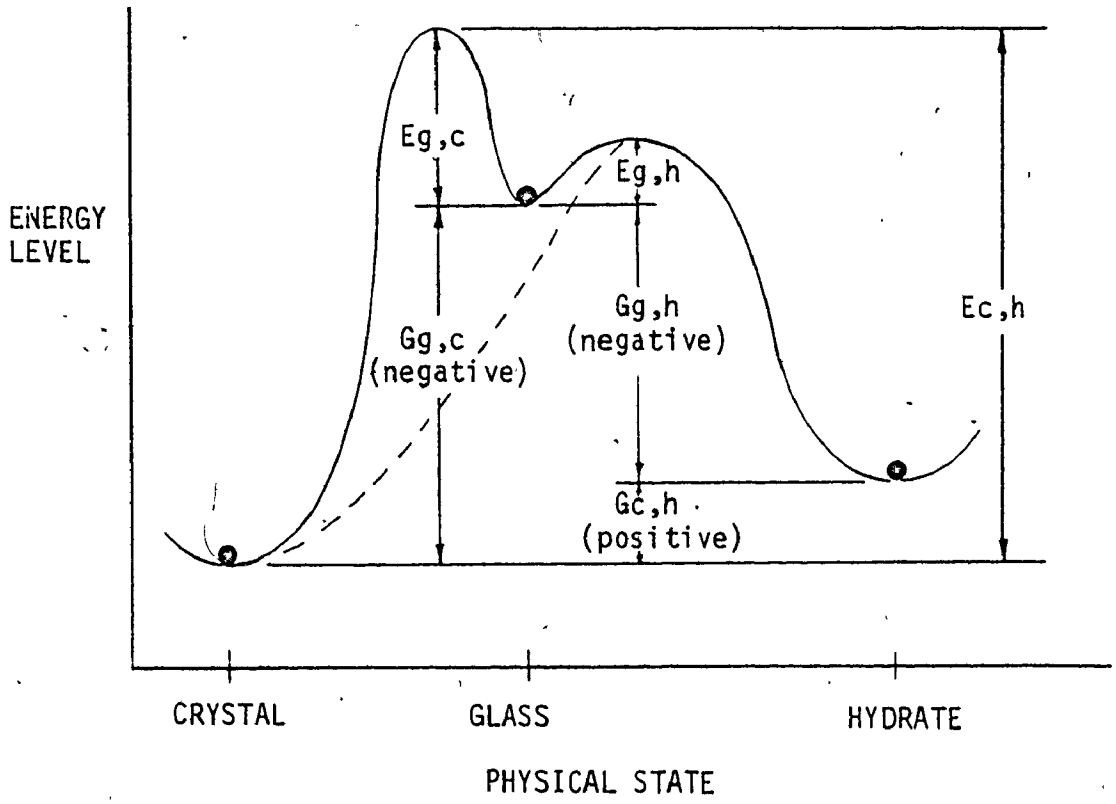

LEGEND:

E = activation energy required to overcome the energy barrier to reaction
G = Gibbs free energy
g = glass, c = crystal, h = hydrate

COMMENTS:

Eg,h can be obtained by chemical means, such as alkaline activation, or by high temperature and pressure curing.
Eg,c is obtained by heating to the devitrification temperature around 850°C.
Ec,h can only be overcome directly by very long periods of hydrothermal curing (35 days at 180°C, Speakman, 1970), or indirectly by first remelting and quenching to a glass, then hydrating.

FIGURE 3.1: CONCEPTUALIZATION OF ARRHENIUS TYPE REACTIONS (using the notation of Nassau et al, 1979)

to hydration, represented by $E_{g,h}$, which can be overcome by alkaline, sulfate, or temperature activation.

The degree of vitrification achieved during quenching depends on several factors: furnace tapping temperature; slag chemistry; slag viscosity; and rate of cooling achieved by the quenching method. The first three factors are interdependent, and determine whether the applied cooling rate will be sufficient to prevent extensive crystal formation. The temperature, chemistry and viscosity of a slag are optimized for blast furnace operations, the primary function being to produce iron with consistent properties. As a result of modern furnace practice coupled with uniform sources of iron ore and limestone flux, slags have become very consistent in chemistry (i.e. slag viscosity becomes mainly dependent on temperature for a specific furnace and burden). As long as the tapping temperature is high enough and a standard quenching process (granulation or pelletization) is used, the resulting glass contents should be fairly constant.

Schröder (1969) has given a detailed account of how changes in blast furnace processes can influence the resulting slags. From experience in collecting individual slag samples from a number of casts for this study, the most variable process aspect influencing the slag is the furnace tapping temperature. In spite of modern controls, the furnace can experience "upsets" and hot metal temperatures recorded over a 3 month period for one furnace varied from 1390°C to 1590°C (Table 3.1), noting that 75 per cent of the hot metal temperatures were between 1490°C and 1550°C for 46 individual samples. Since the liquidus temperature of typical slags varies from 1320°C to 1450°C (Schröder,

TABLE 3.1

RANGE OF CHEMICAL COMPOSITIONS FOR SLAGS PRODUCED FROM ONE BLAST FURNACE OVER A THREE MONTH PERIOD IN 1976 (WEIGHT PER CENT)

ELEMENT	MINIMUM	MAXIMUM	TYPICAL
CaO	34.17	43.16	39.98
SiO_2	33.33	43.68	37.53
Al_2O_3	7.57	10.50	8.33
MgO	8.27	13.51	10.06
K_2O	0.14	1.68	0.44
S	1.23	2.98	2.02
Fe_{Total}	0.31	1.91	0.44
Mn_{Total}	0.28	2.04	0.54
Hot Metal Temperature	1390°C	1590°C	1510°C

1969), the reduction of furnace temperature can result in some crystallization before the slag is quenched. The molten slag was also found by this writer (using an optical pyrometer) to lose approximately 100°C to 150°C between the furnace tap hole and pelletizing drums, passing along a 15m slag runner.

There may be some confusion due to the interchangeable use of the terms glassy, amorphous, non-crystalline and vitrified. All are intended to have the same meaning although it might be argued that iron blast furnace slags cannot form stable glasses due to their high CaO content. While this is true, with a fast enough quenching rate, almost any material can be made into a meta-stable, non-crystalline solid as long as the final temperature of the quenched material is below that for glass crystallization (Nassau, et al., 1979). The glass found in most blast furnace slags is only meta-stable, but at temperatures below 800°C to 900°C (the devitrification temperature range) the glasses are too viscous to rearrange themselves into crystals within a practical time frame.

3.1.3 Problems in Estimation of Glass Content

Realizing the general importance of glass content to slag reactivity, slag cement producers closely monitor glass content as a quality control measure. Unfortunately, there is no common procedure used by these producers for determining the glass content. One of the reasons for this is the inherent difficulty in identifying glass. For example, until recently, it was thought that the interstitial material in portland cement was glass, but as Lea (1971) mentioned, much or

all of this material may be a fine-textured devitrification product. Also, the method of glass content determination adopted by some producers, while not necessarily accurate, gives consistently favourable glass contents for their material.

The reasons that producers seem to, without exception, document glass content as a measure of quality control probably include:

1. The producer knows his source of supply and should be confident that any consistent quenching procedure will likely result in an acceptable glass content.
2. While a glassy structure is essential to reactivity, a high glass content by any procedure does not guarantee a highly reactive slag. There is no exact correlation of glass content to hydraulicity, as discussed in 3.3.4. The producer would probably not be able to reject any unground slag of low glass content, the slag likely being well blended in the stockpile by then. The only feasible method of rejecting incoming material would be by simple observation, since air cooled slag is much different in colour and physical structure than either water granulated or pelletized slags.

Glass contents, from the writer's experience are usually taken on the final product, which if the incoming slag stockpile is properly blended, is very consistent in glass content and hydraulic activity. In some ways glass contents appear to be a placebo to customers, rather than a significant quality assurance parameter - strength testing

being the only real assurance of quality.

While not convinced of the importance of a high glass content (i.e. greater than 95 per cent) to hydraulicity to the exclusion of other influencing factors, the importance of proper quenching as the basis for slag reactivity is recognized. For instance small amounts of crystals may actually act as nucleation sites for hydration (Fierens, 1979; Demoulian et al, 1980). Also due to its widespread use by producers and in specifications, it was thought that some of the various methods of determining glass contents should be compared to see if each gives valid results.

The ASTM Committee revising the blended cements specification C595 has considered the inclusion of a minimum glass content criteria, the problem being that it was proposed that glass content be measured by any acceptable means. Unfortunately, as shown herein, it appears that some methods are insensitive to low glass contents and that by using these methods even air cooled slag might meet the glass content by "any acceptable means" criteria.

Available methods for glass content determination are detailed in the appendices. While not all of these were evaluated, they have been included for the sake of completeness.

3.2 EXPERIMENTAL

3.2.1 Properties of the Slags

Eighteen slags, used in the autoclave reactivity studies in Chapters 4 and 5, formed the basis of an inter-laboratory glass content determination evaluation. The chemical compositions, physical properties and sources of these ground slags are given in Table 3.2, and numbered one to eighteen in the order of their use in Chapter 5. All of these slags were originally quenched by the pelletizing process (Margesson and England, 1971) with the exception of slag eighteen which was a synthetically melted and quenched glass of akermanite composition. The details of its manufacture are given in Appendix A.

The different sources of the slags obtained in Hamilton are the following. DOFASCO is the iron and steel company where the pelletizing process is operated. National Slag Limited is a slag processing company operating the pelletizers and removing the slag from DOFASCO's plant. Standard Slag Cement Company is a separately ground slag cement producer utilizing pelletized slag.

Slags 9, 12, 13, 14 and 15 originated from the same sample of pelletized slag. This sample was not as well quenched as normal pelletized slag intended for cement purposes, since the pelletizing process had been changed (slower drum speed and less water used) for the production of light weight aggregate. This slag sample was also used by Emery and Hooton (1978) in a partial grinding process, which is described later in Section 4.5. Slag 12 was taken from the sieved, minus 75μm portion of the partially ground material and had a Blaine

TABLE 3.2

PROPERTIES OF THE BLAST FURNACE SLAGS

SLAG * NUMBER	XRF CHEMICAL COMPOSITION (weight per cent) CaO	SiO_2	Al_2O_3	MgO	K_2O	Na_2O	S (total)	Fe (total)	Mn (total)	TiO_2	$\frac{C+M+A}{S}$ **	SPECIFIC GRAVITY	BLAINE FINENESS (m^2/kg)	DATE OBTAINED	SOURCE (pelletized unless noted)
1	38.99	37.43	8.57	11.18	0.51	0.35	1.91	1.04	0.61	0.32	1.57	2.90	466	1/77	Standard Slag Cement, Hamilton
2	39.17	36.12	8.72	10.78	0.26	0.09	1.77	2.68	0.60	0.43	1.62	2.94	406	6/76	DOFASCO, Furnace 4, Hamilton
3	37.44	37.75	8.86	10.84	0.72	0.33	1.80	1.52	0.94	0.42	1.51	2.93	407	6/76	DOFASCO, Furnace 4, Hamilton
4	37.68	39.20	8.53	11.24	0.65	0.23	1.62	0.64	0.88	0.34	1.47	2.90	403	5/76	DOFASCO, Furnace 4, Hamilton
5	40.87	31.65	9.47	10.01	0.25	0.06	2.24	2.13	0.38	0.30	1.91	2.97	410	7/76	DOFASCO, Furnace 4, Hamilton
6	42.44	34.91	11.39	7.80	0.49	0.36	0.90	0.49	0.46	0.54	1.77	2.92	398	8/78	Fos-Sur-Mer, France
7	39.44	35.02	9.79	10.94	0.20	0.00	2.37	1.58	0.51	0.33	1.72	2.90	409	7/76	DOFASCO, Furnace 4, Hamilton
8	39.29	33.54	14.21	6.02	0.40	0.73	0.73	1.99	0.88	0.60	1.78	2.93	396	5/77	Port Kembla, NSW, Australia
9	39.43	36.71	8.65	10.95	0.42	0.35	1.83	1.22	0.66	0.36	1.61	2.92	401	6/76	National Slag stockpile, Hamilton
10	40.75	37.10	9.00	9.26	0.65	1.61	1.13	0.64	0.60	0.93	1.59	2.93	401	1/75	OYAKO Ltd., Koverhar, Finland
11	36.21	37.18	8.46	13.55	0.54	0.30	1.64	0.62	0.82	0.30	1.57	2.92	400	5/76	DOFASCO, Furnace 3, Hamilton
12	38.59	35.49	8.43	10.45	0.42	0.25	1.69	1.21	0.66	0.35	1.62	2.82	285	5/77	Slag 9: minus 75μm fines
13	38.7	35.7	8.6	8.83	0.46	nd	1.82	0.85	0.65	0.38	1.57	2.94	396	5/77	Slag 9: devitrified at 1050°C
14	40.8	36.6	8.50	10.7	0.46	nd	0.53	1.00	0.67	0.36	1.64	2.96	393	5/77	Slag 9: remelted, water quenched
15	39.34	36.52	8.60	10.92	0.42	0.43	1.79	1.26	0.67	0.36	1.61	2.89	493	5/77	Slag 9: more finely ground
16	39.22	38.28	8.52	10.89	0.55	0.24	1.82	0.78	0.72	0.34	1.50	2.90	399	6/76	DOFASCO Furnace 4, Hamilton
17	39.75	36.95	8.87	11.37	0.44	nd	2.06	0.58	0.51	nd	1.62	2.91	409	3/76	Standard Slag Cement, Hamilton
18	40.0	42.7	1.22	14.0	0.05	nd	0.26	0.07	0.01	0.05	1.29	2.95	487	4/79	Synthetic melilite, quenched

SLAG NUMBER	SOURCE*** (from the United States, 1978 to 1980, chemical and physical properties not available)
19 to 28, 30, 31	Shenango Corporation, Neville Island, Pennsylvania, water granulated
29	reclaimed from old slag heaps, Pennsylvania, air-cooled and granulated mix
32	Bethlehem Steel Corporation, Sparrows Point, Maryland, water granulated
33 to 37	Waylite Corporation, Bethlehem, Pennsylvania, mechanical foaming process

NOTES:

* The slags are numbered in order of testing

** Oxide ratio must exceed 1.0, CSA A363-M 77

*** These slags were provided by Dravo Lime Company, Pittsburgh, Pennsylvania

fineness of 285 m^2/kg. Slag 9 was ground to 401 m^2/kg in a ball mill, and slag 15 was ground finer to 493 m^2/kg. Slag 13 was devitrified by heating to 1000°C for 24h and then slowly cooling over 8h. Slag 14 was from the same slag sample, but was re-melted and water quenched from 1420°C using the same method described for slag 18 (Appendix A).

For the glass contents determination study, these eighteen slags were augmented by nineteen other slags from the United States, as supplied by Dravo Lime Company. The small samples available only allowed evaluation of these slags for glass content. Chemical analyses were not obtained but the sources are listed in Table 3.2. It must be emphasized that the main purpose of this work was to compare various glass content determination methods rather than to relate glass content to chemical or hydraulic properties, which are subject to many other variables.

All slags numbered 19 to 33 were water granulated, while slags numbered 34 to 37 were produced by a different process intended mainly for light weight aggregate production.

3.2.2 Methods Used For Glass Content Determination

In order to evaluate each method of glass content determination, it was necessary to develop a standard procedure, which could realistically and accurately describe the glass contents of slags for comparison purposes. For this purpose, quantitative X-ray diffraction (QXRD) was used to measure the content of each crystalline component and obtain the glass content by difference. This method, and the

others used are briefly described as follows:

1. QXRD Standard Method (GLX)

Characteristic peak intensities of each crystalline mineral encountered were measured as ratios to the peak intensity of an added internal standard. The weight fraction of each mineral was obtained by comparison of the intensity ratio in the slag to the intensity ratio for pure, synthetically produced minerals. Further details are given in Appendix B.

2. XRD Amorphous Hump (GAH)

In a XRD pattern, the presence of glass was only detected by an amorphous halo or hump between 26° and 35° 2θ (CuKα radiation). This hump is located around the nearest neighbour atomic distance in glass since its structure lacks any long range atomic order. The area of each hump was determined, and expressed as a ratio to the area of the internal standard characteristic peak, as detailed in Appendix C. However, due to lack of a pure glass standard of similar composition, this ratio was not converted into a percentage. This method was used by Millet and co-workers (1977) to determine the glass content of pozzolans.

3. McMaster Individual Particle Analysis

The optical procedure previously developed at McMaster University (Kim, 1975) was modified to distinguish between clear, glassy particles, birefringent crystalline particles and opaque, milky particles, as detailed in Appendix D. To test whether

the milky particles were glassy or microcrystalline in nature, the glassy plus milky particles (GMAC + M) were totalled as well as the glassy particles alone (GMAC). A recent improvement of this method has been made by insertion of a gypsum plate in the microscope. This made identification of the crystal and milky particles easier for the operator, and is detailed at the end of Appendix D.

4. South African Optical Procedure (GSA)

This cross-polarized light procedure was developed to assess the quality of Slagment, a separately ground slag cement produced in South Africa. This method was adopted in Canada by the Standard Slag Cement Company who provided this analysis, and is normally used to assess their Cementitious Hydraulic Slag product. The method, detailed in Appendix E, can only distinguish birefringent, crystalline particles and glass is obtained by difference from the total number of particles observed.

5. Automated Ultra-Violet Reflectance (GUV)

This method employs an ultra-violet spectrophotometer fitted with a solid sample chamber and is described in Appendix F. These readings were provided by the Dravo Lime Company in the United States, which uses this method to assess the slag cement used in its Calcilox sludge stabilization process.

3.2.2 Glass Content Methods not used in this Study

1. The Parker and Nurse Optical Method

This was published in 1949 and is currently employed in a modified form to evaluate Cemsave, a separately ground slag cement marketed by the Frodingham Cement Company in Britain. Using plane light, this method was adopted in part to help in distinguishing the "milky" particles in the McMaster Individual Particle Analysis. Unfortunately, the Frodingham Cement Company has modified this method resulting in it being less accurate, and biased toward higher glass values. Instead of counting the total number of particles in the graticule area as originally used (Appendix G), in the modified method (Appendix H) it is assumed that the whole graticule area, including 10 to 15 per cent blank space (even when a tightly packed single layer of powder is obtained), is glass.

2. Rheinhausen Optical Method

Cross-polarized light is used to examine polished and etched particles. The disadvantage of this method, developed in Germany, is the time and skill involved in sample preparation compared to other optical methods (Appendix I).

3. Optical Mineralogical Composition

This method was developed by Steyn (1965) in South Africa to identify and quantify each crystalline phase in slags, with the glass content obtained by difference. The technique is similar to the Rheinhausen optical method but more involved. While this method likely gives accurate results, the procedure is very tedious and time consuming. The samples, after mounting,

are subjected to ten successive grinding and polishing stages. Then the composition of each sample is determined using linear traverses in seven stages, with six different etchants being used. This procedure is not detailed in the appendices since it is very long and is fully detailed by Steyn (1965).

4. Rheinhausen Ultra-Violet Method

This method was described by Schröder (1969) but a preliminary study of this method, using a portable UV light source, showed this procedure to be more qualitative in nature and also posed a hazard to the eyes of the operator. The accuracy of this method was doubted by Schrämli (1963), who mentioned the anomolous results obtained due to minor oxide staining.

5. Differential Thermal Analysis

This has been used in Germany and South Africa in relationship to hydraulic properties, but with little success (Schrämli, 1963; Terrier, 1973). The method is based on measuring the area of the slag devitrification exotherm(s)(800^{o}C to 900^{o}C) for a known weight of sample. Unfortunately, each mineral has its own exotherm (Krüger, 1976) and the results change with chemical composition of the slag. However, some success has resulted from use of this technique to determine the quantity of slag in blended portland-blast furnace cements (Krüger,1962).

3.3 RESULTS

3.3.1 Glass Contents

The glass contents of the 37 slags, determined by the different methods are summarized in Table 3.3. The glass contents obtained from each method are individually compared to the standard QXRD (GLX) values in Figures 3.2 to 3.6 (with the exception of GSA).

3.3.2 Discussion of Results

1. QXRD Standard Method (GLX)

As mentioned in Section 3.2.2, the GLX method was developed for use as a standard since the values obtained were thought to accurately describe the mineralogical composition of each slag due to the use of calibration standards for each mineral present. The mineralogical compositions obtained are detailed in Table 3.4. However, XRD intensities are affected by many factors, including particle fineness and crystal grain size, and the values obtained may be subject to this type of error. Also more exact calibration curves could have been developed using mixtures of the standard minerals if enough had been available.

While thought to be the most accurate, drawbacks to the use of the QXRD procedure are the availability of a machine and the need for mineral standards. However, most iron producers would have an XRD diffractometer and arrangements could likely be made by the slag cement producer to have XRD patterns done on a regular basis to ensure consistancy of their product.

TABLE 3.3
GLASS CONTENT DETERMINATIONS BY VARIOUS METHODS

SLAG	QXRD - McMASTER		McMASTER - OPTICAL		SOUTH AFRICAN	U.V. REFLECTANCE	
NUMBER	GLX (per cent)	GAH (area ratio)	GMAC (per cent)	GMAC + M (per cent)	GSA (per cent)	GUV* (per cent)	GUV-N (per cent)
1	84	4.7	63	94	97	49	45
2	67	4.8	78	86	99	49	46
3	69	3.2	83	98	98	26	24
4	98	6.4	94	98	99	52	49
5	54	4.8	47	67	97	56	52
6	91	6.4	74	79	98	88	82
7	85	5.7	83	98	98	54	51
8	94	6.1	94	97	97	34	32
9	76	4.9	89	95	97	54	51
TO	69	4.7	58	69	88	46	43
11	93	6.5	87	96	99	45	42
12	72	3.9	64	77	89	35	33
13	10	0.4	6	35	97	10	9
14	93	5.1	89	93	97	16	15
15	77	5.5	74	89	95	57	53
16	95	6.9	93	95	98	65	61
17	89	5.3	67	88	91	128	96
18	89	5.2	88	93	95	10	9
19	82	4.6	76	81	98	87	81
20	77	3.7	74	86	96	120	95
21	88	4.8	79	87	98	101	94
22	89	4.4	95	96	94	123	96
23	89	5.1	85	92	88	80	75
24	86	4.0	87	92	89	100	94
25	82	3.9	80	87	88	105	94
26	92	5.5	73	88	94	140	98
27	83	4.9	79	82	98	138	97
28	85	7.0	85	89	97	135	97
29	36	1.2	38	77	87	44	41
30	93	8.1	84	89	96	131	97
31	91	5.6	71	89	95	116	95
32	95	4.1	78	99	99	89	83
33	45	1.4	56	87	81	38	36
34	71	4.7	69	87	97	86	80
35	84	5.7	86	97	98	72	67
36	42	1.3	47	89	95	50	47
37	46	1.2	41	87	95	64	60

*GUV values obtained by comparison to a standard glass assigned 100 per cent.
Maximum value obtained to date equalled 165 per cent.

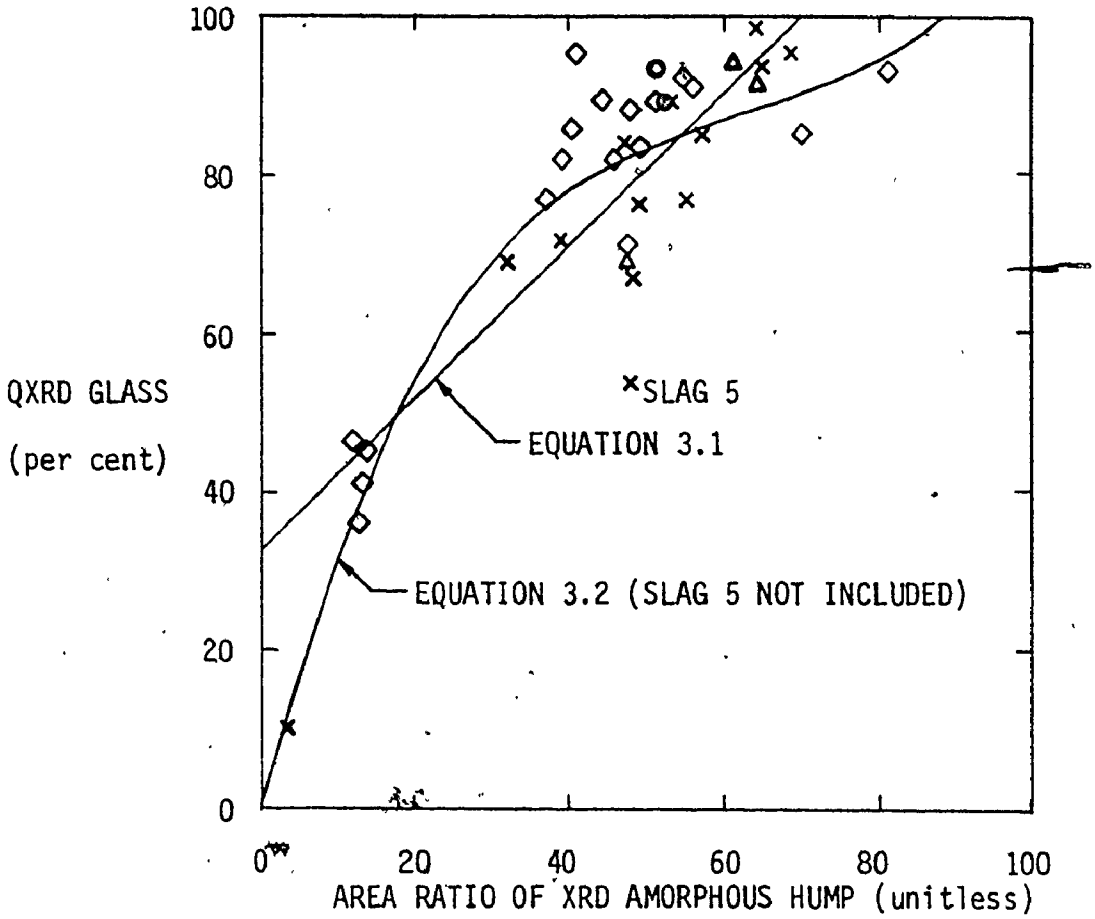

SYMBOL	SLAG SOURCE
×	CANADIAN SLAGS
△	FOREIGN SLAGS (NON USA)
◇	AMERICAN SLAGS
○	ARTIFICIALLY QUENCHED SLAGS

FIGURE 3.2: COMPARISON OF GLASS CONTENT DETERMINATIONS:
AREA RATIO OF XRD AMORPHOUS HUMP (GAH) WITH QXRD (GLX)

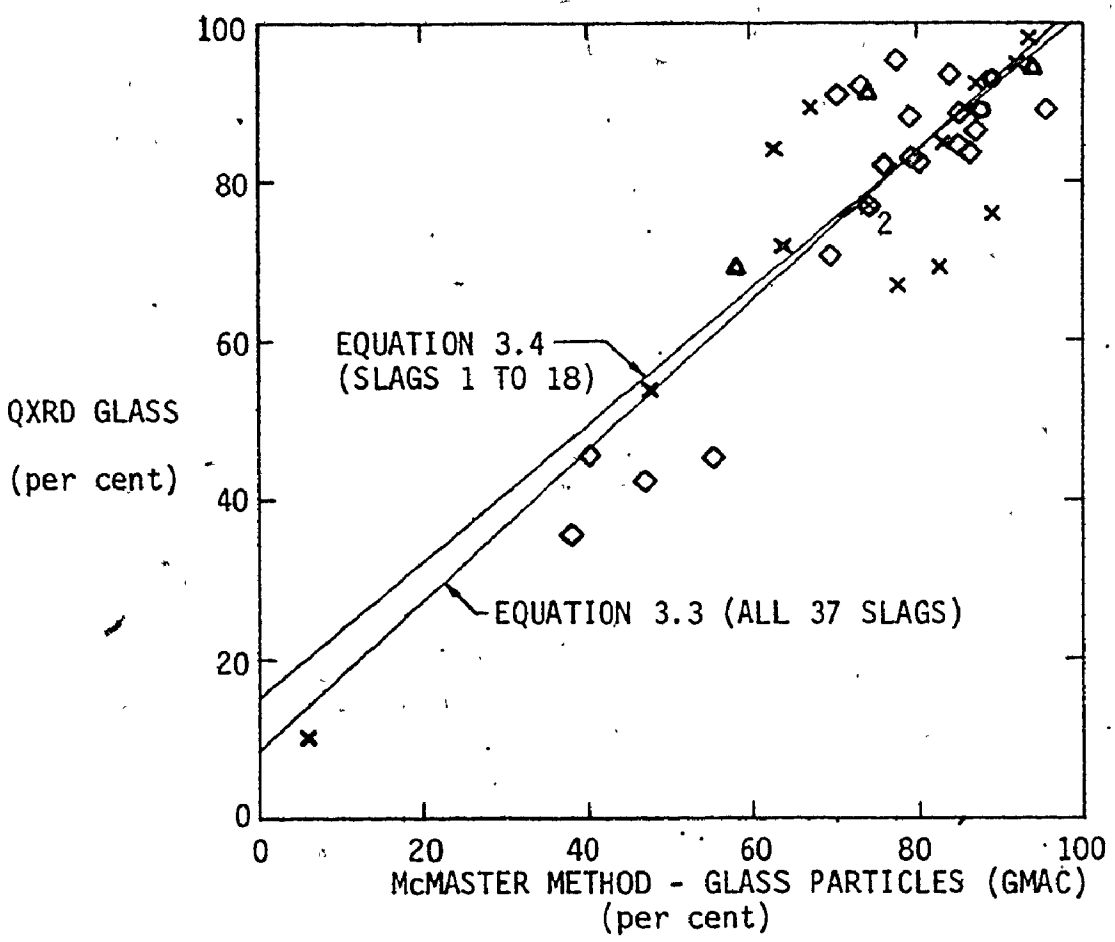

SYMBOL	SLAG SOURCE
×	CANADIAN SLAGS
△	FOREIGN SLAGS (NON USA)
◇	AMERICAN SLAGS
○	ARTIFICIALLY QUENCHED SLAGS
2	COINCIDENT POINTS

FIGURE 3.3: COMPARISON OF GLASS CONTENT DETERMINATIONS: McMASTER METHOD - GLASS PARTICLES (GMAC) WITH QXRD (GLX)

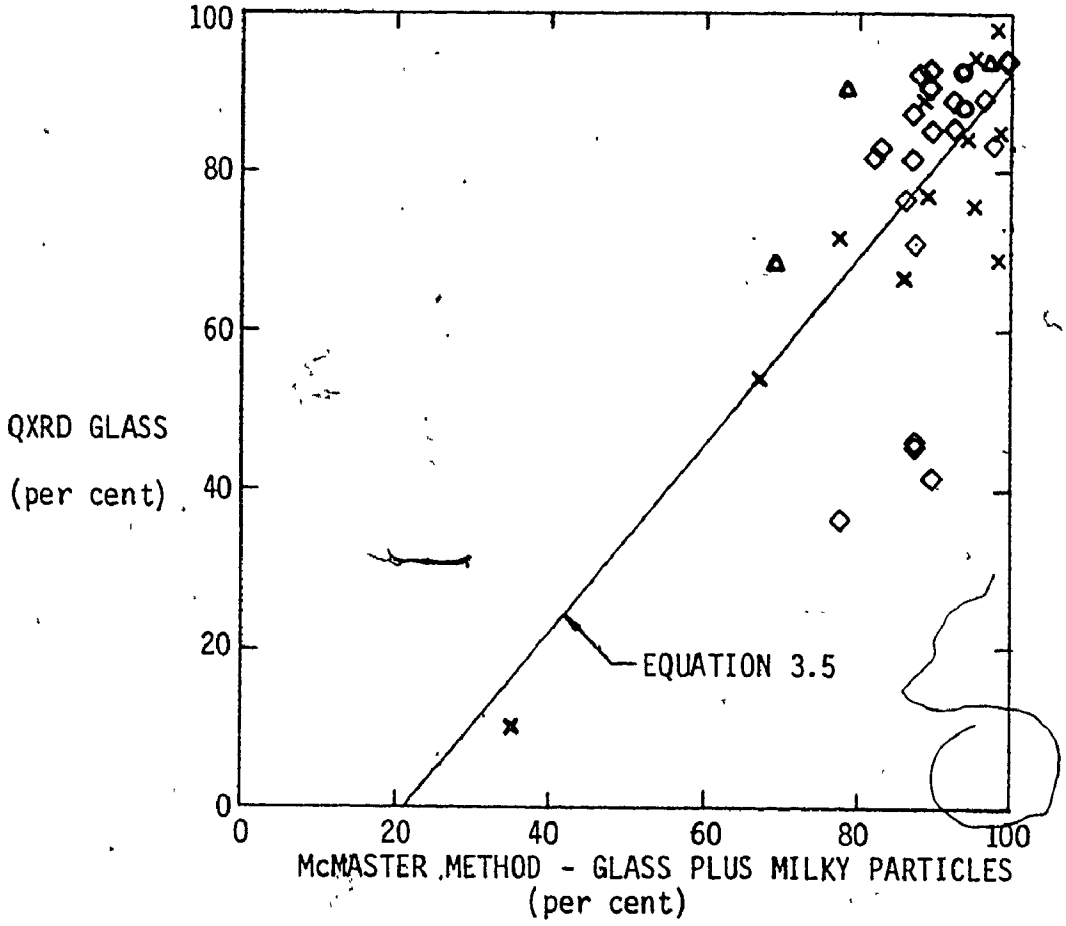

SYMBOL	SLAG SOURCE
×	CANADIAN SLAGS
△	FOREIGN SLAGS (NON USA)
◇	AMERICAN SLAGS
○	ARTIFICIALLY QUENCHED SLAGS

FIGURE 3.4: COMPARISON OF GLASS CONTENT DETERMINATIONS:
McMASTER METHOD - GLASS PLUS MILKY PARTICLES(GMAC+M)
WITH QXRD (GLX)

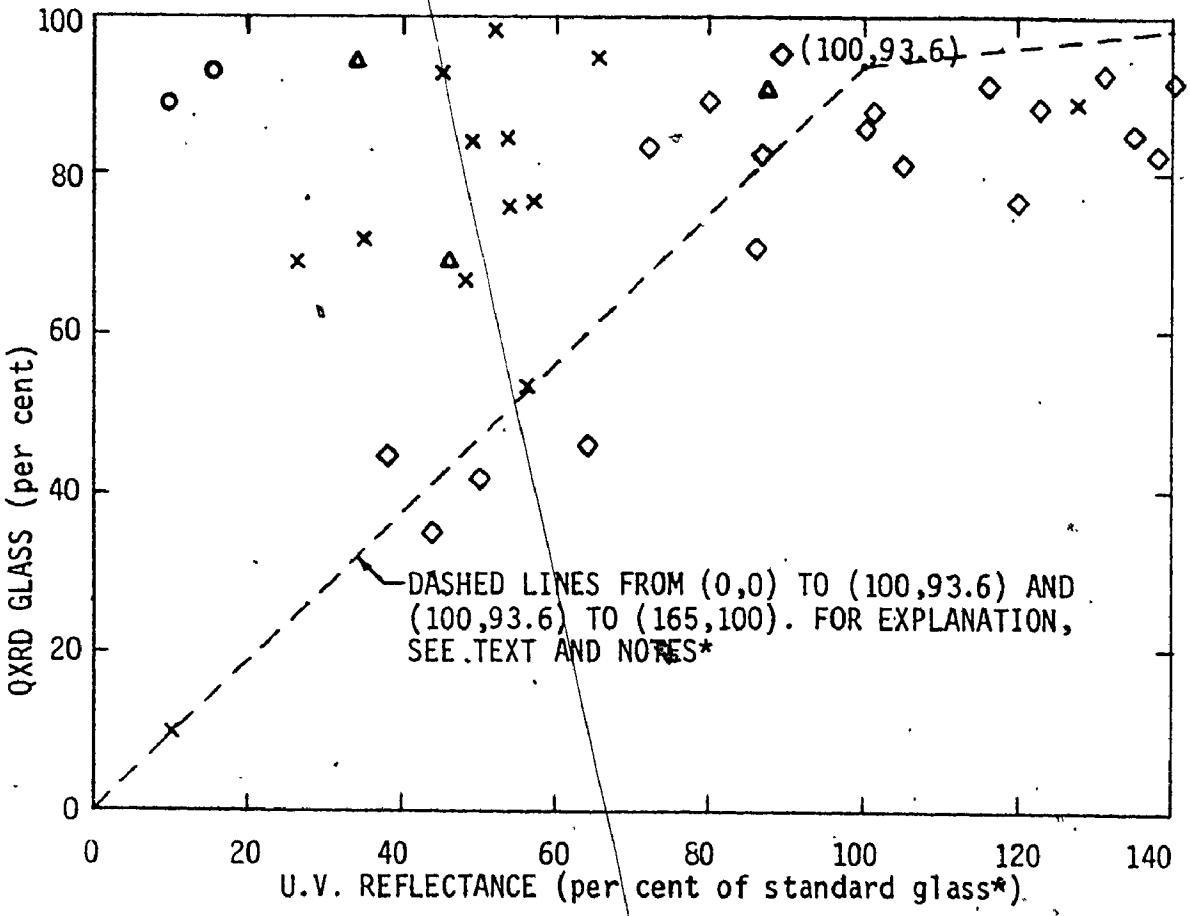

* The glass standard was found elsewhere to contain 93.6 per cent glass by QXRD. The maximum U.V. reading to date is 165 per cent.

SYMBOL	SLAG SOURCE
×	CANADIAN SLAGS
△	FOREIGN SLAGS (NON USA)
◇	AMERICAN SLAGS
○	ARTIFICIALLY QUENCHED SLAGS

FIGURE 3.5: COMPARISON OF GLASS CONTENT DETERMINATIONS: U.V. REFLECTANCE (GUV) WITH QXRD (GLX)

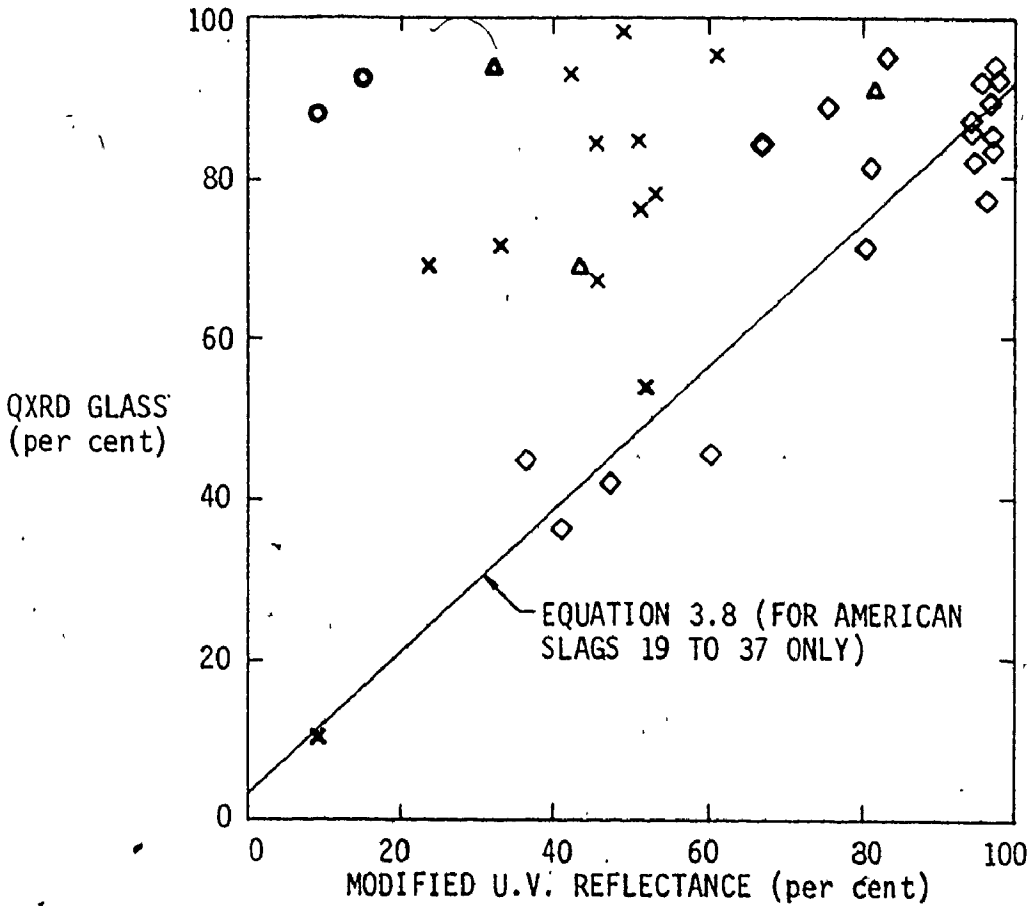

SYMBOL	SLAG SOURCE
×	CANADIAN SLAGS
△	FOREIGN SLAGS (NON USA)
◇	AMERICAN SLAGS
○	ARTIFICIALLY QUENCHED SLAGS

FIGURE 3.6: COMPARISON OF GLASS CONTENT DETERMINATIONS:
MODIFIED U.V. REFLECTANCE (GUV-N) WITH QXRD (GLX)

TABLE 3.4

MINERALOGICAL COMPOSITION OF SLAGS BY QXRD

SLAG NUMBER	MELILITE C_2MS_2-C_2AS (per cent)	MERWINITE C_3MS_2 (per cent)	DIOPSIDE CMS_2 (per cent)	CALCITE* $\overline{CC}$ (per cent)	TOTAL CRYSTALS (per cent)	GLASS CONTENT BY DIFFERENCE (GLX) (per cent)
1	6.1	0	10.3	0	16.4	83.6
2	27.1	6.1	0	0	33.2	66.8
3	23.9	7.0	0	0	30.9	69.1
4	2.0	0	0	0	2.0	98.0
5	9.0	37.5	0	0	46.5	53.5
6	2.4	6.4	0	0	8.8	91.2
7	7.9	7.7	0	0	15.6	84.6
8	6.1	0	0	0	6.1	93.9
9	15.2	8.7	0	0	23.9	76.1
10	12.1	18.8	0	0	30.9	69.1
11	2.9	4.0	0	0	6.9	93.1
12	21.5	6.5	0	0	28.0	72.0
13	85.4	0	4.0	0	90.2	9.8
14	1.9	5.1	0	0	7.0	93.0
15	16.4	6.4	0	0	22.8	77.2
16	2.1	2.8	0	0	4.9	95.1
17	2.5	8.9	0	0	11.4	88.6
18	10.8	0	0	0	10.8	89.2
19	6.8	8.9	0	2.5	18.2	81.8
20	0	11.4	8.0	3.2	22.6	77.4
21	0	9.3	0	3.0	12.3	87.7
22	2.7	8.6	0	0	11.3	88.7
23	3.4	6.1	0	1.7	11.2	88.8
24	6.3	7.9	0	0	14.2	85.8
25	5.3	9.8	0	2.5	17.6	82.4
26	0	5.5	0	2.7	8.2	91.8
27	3.7	10.4	0	3.1	17.2	82.8
28	3.6	11.1	0	0	14.7	85.3
29	23.9	40.5	0	0	64.4	35.6
30	0	6.9	0	0	6.9	93.1
31	0	6.9	0	1.9	8.8	91.2
32	0	5.0	0	0	5.0	95.0
33	54.6	0	0	0	54.6	45.4
34	20.1	9.2	0	0	29.3	70.7
35	10.9	5.5	0	0	16.4	83.6
36	58.5	0	0	0	58.5	41.5
37	43.2	11.2	0	0	54.4	45.6

*Calcite was only detected in slags from Neville Island Pa. According to Foster (1981), the slag is flushed from these blast furnaces between iron tappings and a small portion of the limestone burden may have been removed as well.

2. XRD Amorphous Hump (GAH)

As can be observed from Figure 3.2, there is a relationship between GLX and GAH values. However, it is not clear whether the relationship is linear, or curved, passing through the origin. The least squares linear equation relationship is given by Equation 3.1.

$$\text{GLX (per cent)} = 9.610 \times \text{GAH} + 32.7 \qquad (3.1)$$

(R= 0.849, S.E. =± 10.7) *

The value of the regression correlation coefficient is quite good considering the large variability which was found for repetitions of the XRD-GAH values. When slag Number 5 was removed from the regression and a third order polynomial used (Equation 3.2), the regression coefficient increased to 0.936.

$$\text{GLX (per cent)} = 0.298(\text{GAH})^3 - 5.495(\text{GAH})^2 + 36.67\ (\text{GAH}) \qquad (3.2)$$

(R= 0.936, S.E.=± 7.0)

(R= 0.905, S.E. =±8.5, for all 37 slags)

As shown by Millet and co-workers (1977), the position and area of the amorphous hump depends on the composition of the glass. Therefore it would be difficult to relate the GAH values to percentages of glass in the absence of standard glasses of a range of compositions. Also, as mentioned by Mather (1974-2), the use of copper radiation on iron also causes a halo due to secondary iron emissions. An advantage of this method is that

* R denotes the correlation coefficient for the equation . S.E. denotes the standard error of estimate.

calibration standards are not required and GAH values could be qualitatively compared to known, high glass content slags from the same source.

3. McMaster Individual Particle Analysis

As stated in 3.2.2 and shown in Table 3.4, two values were obtained using this method; GMAC, counting the clear, glassy particles only, and GMAC + M, counting the opaque, milky particles with the clear ones. These values are plotted against the GLX values in Figures 3.3 and 3.4 respectively. As can be observed from Figure 3.3, there is almost a one to one linear, correspondence of GMAC with GLX values. Least squares linear regression analysis resulted in Equation 3.3 for all 37 slags and Equation 3.4 for slags one to eighteen, which were used subsequently in Chapter 5.

$$\text{GLX (per cent)} = 0.9366\ (\text{GMAC}) + 8.6 \qquad (3.3)$$

$$(R = 0.890,\ \text{S.E.} = \pm 9.1)$$

$$\text{GLX (per cent)} = 0.8537\ (\text{GMAC}) + 14.9 \qquad (3.4)$$

$$(R = 0.889,\ \text{S.E.} = \pm 9.9)$$

The GMAC + M values were not as sensitive to lower glass contents, as can be seen in Figure 3.4. The regression equation is given by:

$$\text{GLX (per cent)} = 1.176\ (\text{GMAC} + \text{M}) - 25.3 \qquad (3.5)$$

$$(R = 0.698,\ \text{S.E.} = \pm 14.4)$$

Therefore it was deduced that the opaque, milky particles were in fact crystalline, perhaps microcrystalline in nature. This

was considered an important observation, since in previous inter-laboratory testing of optical procedures, the designation of these opaque, milky particles was a problem. (Weaver, 1974; Mather, 1974-1; Emery, Cotsworth and Hooton, 1976).

4. South African Optical Procedure (GSA)

The GSA values were not plotted against GLX. From Table 3.4, it can be easily observed that the glass contents determined by this procedure are not at all sensitive to changes in glass content, giving consistantly high values ranging from 88 to 99 per cent. A value of 97 per cent was obtained for the devitrified slag, Number 13, due to the fact that the majority of the crystalline particles were opaque but not birefringent. Therefore, while high glass contents were assigned using this method, it was of no use for quality control purposes.

5. Automated U.V.Reflectance (GUV)

From Figure 3.5, it can be observed that there was a wide scatter in results, especially with the non-United States slags. As can be seen, GUV values in excess of 100 per cent were obtained since the method compares each slag with a standard glass, which was subsequently found to contain only 93.6 per cent glass by XRD (Appendix F). The maximum value obtained to date was 165 per cent of the standard. The dotted line in Figure 3.5 connects these standard glass values (100 per cent GUV, 93.6 per cent GLX) with the origin, and also with 165 per cent GUV, 100 per cent GLX. Since one GUV value reached 165

per cent while the 100 per cent standard actually contained 93.6 per cent glass, it was deduced, as indicated by the dotted lines, that the GUV values do not vary linearly with glass content.

Therefore the GUV values were normalized to 100 per cent (GUV-N) by the following equations.

For $0<GUV\leq100$,

$$GUV\text{-}N = GUV \times 0.936 \qquad (3.6)$$

and for $GUV>100$,

$$GUV\text{-}N = 93.6 + (GUV-100) / (165-100) \qquad (3.7)$$

The normalized GUV-N values are given in Table 3.3 and plotted in Figure 3.6. There appears to be a linear relationship with GLX, but only for the slags from the United States, as given by Equation 3.8.

$$GLX(\text{per cent}) = 0.885 \times GUV\text{-}N + 3.3 \qquad (3.8)$$

$$(R= 0.899, \text{S.E.} = \pm 8.6).$$

The large variance with the other slags may be due to minor oxide contents affecting U.V. results as suggested by Schrämli (1963). The largest variations with GLX were for slags 14 and 18, which is evidence for this hypothesis. Both these slags were laboratory melted in an oxidizing atmosphere, which resulted in low sulphur contents and also left the glass particles slightly stained.

Therefore, using this method low glass content slags were distinguishable, but several slags of high glass content were

TABLE 3.5

QXRD GLASS CONTENT AND GRAIN SIZE

SLAG NUMBER	11		17	
SIZE FRACTION	-63μm,+45μm	Total Sample	-63μm,+45μm	Total Sample
Crystal Content				
Melilite (per cent)	3.8	2.9	0.0	0.0
Merwinite (per cent)	4.9	4.0	11.6	11.4
Total (per cent)	8.7	6.9	11.6	11.4
GLX Glass Content (per cent)	91.3	93.1	68.4	88.6
Difference (per cent)	1.8		0.2	

misrepresented as having much lower glass contents.

3.3.3 Glass Content and Grain Size Fraction

Since the optical glass count procedures use only a small proportion of the range of sizes found in ground slag cement (less than 20 per cent is retained on the 45μm sieve), it was thought worthwhile to check the assumption that the glass content of the minus 63μm to plus 45μm fraction used, was representative of the ground slag. Pirotte (1954) had stated that this assumption was poor due to differential grinding of crystals, glass, and portions of different chemical composition.

Therefore, the minus 63μm to plus 45μm portions of slags 11 and 17 were analysed by QXRD as well as samples of the total ground slag. Slag 17 was chosen since its GMAC glass count had been much lower than its glass content by GLX. The results are shown in Table 3.5. The small differences found were not considered significant, therefore the glass content of the minus 63μm plus 45μm fraction appears to be representative of the total ground slag.

3.3.4 Glass Content and Slag Hydraulicity

As mentioned previously, several interrelated parameters affect the hydraulicity of a slag (chemistry, mineralogy, temperature of vitrification, fineness of grinding), but the exact relationship to these parameters is unclear.

Therefore, while an accurate estimate of glass content can separate potentially inactive slags (i.e. air-cooled, or very poorly

quenched slags) from the rest, the use of glass content alone cannot be used to predict potential strength development among well vitrified slags as discussed in Chapter 5. The results support the conclusions of Keil (1954) and Lea (1971) in that physical strength testing should be used for the predominant assessment of slag quality. Of the tests available it is recommended that the Keil index approach be adopted (Keil, 1954).

$$\text{i.e., the Hydraulic Index } 70/30 = \frac{a-c}{b-c} \times 100 \qquad (3.9)$$

where a = 28 day strength of 70 per cent slag/30 per cent portland cement

b = 28 day strength of 100 per cent portland cement

c = 28 day strength of 70 per cent ground quartz/30 per cent portland cement

This index gives a range of values from 0 (for equivalence to inert quartz at room temperature curing) to 100 or greater (for equivalence to, or greater than, the portland cement being used). This index can be applied to other materials such as non-ferrous slags and flyash and gives a better range and index than the ASTM pozzolanic activity test, due to the inclusion of quartz as an inert material.

3.4 CONCLUSIONS AND RECOMMENDATIONS

While not a complete listing, eleven methods for estimating the glass content of slags have been discussed. Of these, six were evaluated and compared with the assistance of two industrial laboratories.

Calibrated X-ray diffraction was used as a realistic comparison standard for the other methods.

It was found that the often adopted South African optical procedure did not distinguish between air-cooled and glassy slags, and cannot be recommended.

The McMaster optical procedure based on glassy particles had an excellent correlation with XRD results, while results based on glassy plus milky particles provided a somewhat lower correlation and less sensitivity to low glass contents.

The automated Ultra-Violet reflectance method, while able to identify slags of low glass content, gave quite erroneously low results for some slags. However, for slags from one source, it may be accurate.

It is concluded that, of the methods evaluated, the McMaster optical method (GMAC) and quantitative X-ray diffraction are the only reliable methods.

However, a high glass content is not necessarily indicative of strength development in slag cements, since so many other physical and chemical factors are involved. The only value of a glass content is to ensure against using air-cooled or poorly quenched slags. Since some methods of glass content determination cannot even distinguish this, the acceptance or rejection of slag or slag cements on the basis of

glass content alone is unwise. The Keil index, which is a strength related physical test, is recommended for monitoring slag cement quality.

4. AUTOCLAVE REACTIVITY IN TERNARY BINDERS OF SLAG-PORTLAND CEMENT-SILICA FLOUR

4.1 INTRODUCTION

As described in Section 2.4, very little research has been done on the properties of pastes autoclaved for the short periods typically utilized in commercial practice. While slag has been studied in a few autoclave applications, as detailed in Section 2.5, there has been no extensive study of paste properties over a wide range of slags contents. Most work involving slag has concentrated on one or two arbitrary binder combinations. Also even fewer studies have used slag in conjunction with the portland cement-quartz binders commonly used in concrete block and brick.

Therefore, the purpose of the work in Chapter 4 is to elucidate the properties of a wide range of slag-portland cement-quartz binders for a typical commercial autoclave curing cycle. Then, in Chapter 5, the results of this work are applied to the study of variable slag properties with respect to autoclave reactivity.

4.2 EXPERIMENTAL

4.2.1 Materials

The chemical and mineralogical compositions as well as physical properties of the pelletized slag, portland cement and silica flour used are shown in Table 4.1. The sand used in the mortar cubes was standard ASTM C109 graded Ottawa quartz sand.

The pelletized slag cement used in this study was slag Number 17 from Chapter 3. This slag was selected since it was a commercially blended and ground product, and was thought to be typical of the material being used in construction.

The chemical analysis originally obtained for the normal portland cement (not shown), with the exception of free lime, was performed by X-ray fluorescence (XRF). However, after completion of much of the work, a subsequent, more detailed analysis, given in Table 4.1, showed that the portland cement contained 3.3 per cent calcium carbonate. However, this was not thought to be due to carbonation deterioration of the cement (Chen, 1979) and also other, more recently obtained samples from the same source were found to contain similar quantities of calcium carbonate. Calcium carbonate in the form of ground limestone may have been added as a dilutent material, which are now permitted by CSA (up to 5 per cent).

The silica flour, a widely used, commercially available, ground quartz was found by XRD and chemical analysis to contain 6.1 per cent sericite mica as an impurity, but autoclave testing showed this to be non-reactive. It also remained with the quartz residue in the unreac-

TABLE 4.1
PROPERTIES OF THE BINDER MATERIALS USED

CHEMICAL COMPOSITION BY XRF (Weight per cent)	PELLETIZED BLAST FURNACE SLAG 17	NORMAL PORTLAND CEMENT CSA TYPE 10	SILICA FLOUR
CaO	39.75	61.77*	0.12
SiO_2	36.95	20.27	95.83**
Al_2O_3	8.87	5.81	2.34
MgO	11.37	2.56	0.06
K_2O	0.44	1.25	0.62
Na_2O	-	0.21	0.08
S	2.06	3.32(SO_3)	-
Fe_2O_3	0.58(Fe)	2.11	0.38
Mn	0.51	-	-
TiO_2	-	-	0.12
LOI(1050°C)	Varies:0.10 at 20h,0.63 at 30h	1.55	0.45
Total	100.63	98.85	100.00
PHYSICAL PROPERTIES			
Specific Gravity	2.94	3.11	2.68
Blaine Fineness (m^2/kg)	409	343	274
MINERALOGICAL COMPOSITION	QXRD	BOGUE CALCULATION	QXRD, XRF
(Weight per cent)	glass =88.6 (of mainly C_2MS_2-C_2AS composition) crystals: C_3MS_2 = 8.9 melilite= 2.5	C_3S = 46.9 C_2S = 23.7 C_3A = 11.5 C_4AF = 6.4 $C\bar{S}$ = 5.5 $C\bar{C}$ = 3.3 Total = 97.3	quartz = 93.1 sericite= 6.1 ($KA_3S_6H_2$)

*Includes 0.24 per cent free lime by ethylene glycol extraction
**obtained by difference

ted silica test, described later.

Thus, due to these impurities, the effort to utilize commercially available portland cement and silica flour in the study tended to interfere with subsequent analysis to some extent.

4.2.2 Mortars

At each binder combination, three 51mm mortar cubes were mixed and compacted using the methods of ASTM C109 and C305. Constant workability (flow= 110 ±5) was obtained at a constant water content in most cases, except at high slag contents when the water content had to be reduced.

4.2.3 Pastes

All materials were passed through a 150μm sieve to remove large particles which might have acted as stress raisers in the small paste specimens. The powders were blended dry, distilled water was added, then the pastes mixed with a Sunbeam household mixer for 30s at low speed then 60s at high speed in a 0.5ℓ stainless steel bowl. A water/cement ratio* of 0.32 was used throughout, since preliminary trials had shown that the coefficient of variation of both compressive and split-tension test results for this W/C were lower than at either W/C equal to 0.25 or 0.40. After mixing, the pastes were cast in 30mm diameter by 50mm cylinder molds. The molds were compacted on a vibrating table for 5s to 10s without noticeable bleeding of the pastes.

---

*In this study, the terms water/cement ratio and W/C are meant to imply the water to total cementitious materials ratio.

4.2.4 Curing

After casting into the molds, the mortar and some paste specimens were stored for 14h to 22h at 23°C and 100 per cent relative humidity in order to set and develop initial (green) strength prior to autoclaving. In an effort to duplicate industrial pre-autoclave conditions, some pastes were initially cured for 3h to 5h at 70°C and 100 per cent relative humidity. It should be noted that the autoclave curing was held constant throughout and pre-autoclave conditions, after providing a minimum maturity factor (calculated by the curing time period (h) multiplied by temperature (°C + 10)), was not considered to be a significant factor as indicated by Menzel (1934) and Alunno-Rossetti and co-workers (1973).

After demolding, the specimens were placed on stainless steel racks in a Cenco laboratory autoclave. The maximum temperature of 185°C (1.03 MPa steam pressure) was reached in 1h to 1.5h, held for 4h, then the pressure was released slowly over 1.5h. The specimens were left in the autoclave for a further 16h to 18h before removal.

4.2.5 Strength Testing

All strength tests were performed using a Tinius Olson universal testing machine immediately after removal from the cooled autoclave. The compressive strengths reported for both the mortar cubes and capped paste cylinders are the average of three values. Two cylinders were subjected to splitting tension and the values averaged.

4.2.6 Density and Porosity Measurement

The solid density and apparent porosity of each paste was determined by displacement in methanol. Thin pieces (less than 2mm thick) of each paste were chipped from the split cylinder paste specimens until between 7g and 10g of paste was obtained. These were dried for 4h in vacuum at 110°C. This was similar to the equivalent "d"-drying used by Feldman (1971). Dry samples were weighed to 0.1mg then saturated with methanol under vacuum. The anhydrous methanol was kept dry with 4Å molecular sieves. The samples were transferred to a 150μm mesh basket suspended in a large jar of methanol and weighed, correcting for the weight of the basket (Wsusp). The temperature of the methanol was recorded, so that its specific gravity could be calculated (Dmeth). The sample pieces were then removed from the methanol and blotted on paper to the saturated-surface dry condition and immediately sealed in a pre-weighed glass vial and weighed (Wssd).

The calculations of solid density and apparent porosity are given by Equations 4.1 to 4.4.

$$\text{Volume of pores (Vpor)} = \frac{Wssd - Wdry}{Dmeth} \quad (ml) \qquad (4.1)$$

$$\text{Apparent volume (Vapp)} = \frac{Wssd - Wsusp}{Dmeth} \quad (ml) \qquad (4.2)$$

$$\text{Apparent porosity} = \frac{Vpor}{Vapp} \times 100 \text{ per cent} \qquad (4.3)$$

$$\text{Solid Density} = \frac{Wdry}{(Vapp - Vpor)} \quad (kg/m^3 \times 10^{-3}) \qquad (4.4)$$

The average coefficient of variation, based on three samples repeated four times each, was found to be 2.4 per cent for the apparent porosity results and 1.2 per cent for the solid density.

4.2.7 X-Ray Diffraction (XRD)

A Norelco diffractometer employing CuK_α radiation (λ=1.5418Å, settings 30 KeV, 16mA) and equipped with a graphite monochrometer and scintilation counter, was used at a scanning speed of 1^o 2θ/minute over the range $6^o 2\theta$ to $70^o 2\theta$. Several repeat scans at selected angles were made to verify the presence of weak peaks and to enable the averaging of intensities. Ten parts by weight of reagent grade CaF_2 was added to 100 parts of each sample (ground to minus 75μm) as an internal standard in order to calibrate both diffraction spacings and intensities. The CaF_2 and samples were ground together in an agate mortar in acetone to achieve a homogenous mixture. For intensity calculations, crystal peaks were expressed as a ratio to the height of the 111 spacing (Miller indices) of CaF_2 (3.15Å - $28.3^o 2\theta$). Peak height ratios were found in practice to give more reliable intensities than using peak areas and were also easier to calculate. This was also found in the calibration of quartz and αC_2SH by Dyczek and Taylor (1971).

4.2.8 Differential Thermal Analysis (DTA)

Dried paste samples were ground to pass a 300μm sieve, and re-dried at 110°C just prior to testing. Approximately 300mg of each sample was placed in a platinum sample cup. Calcined alpha-alumina was used as the reference material. Samples were heated in air at 12°C/minute up to 1100°C in a Dupont 900 analyser using platinum-rhodium thermocouples. In most cases the sensitivity was set at 0.03mv/m (0.06°C/m) of recording chart.

However, due to the age and condition of the DTA apparatus it was found that electrical instabilities resulting in spurious peaks, combined with steep background slopes, made interpretation of the results difficult. Therefore this method was only used as a rough check of the phase analysis obtained by XRD.

4.2.9 Scanning Electron Microscopy (SEM)

A Cambridge Stereoscan Mark 2 A electron microscope fitted with a KEVEX brand energy dispersive X-ray analyser (EDXRA) was used to observe the morphology of fracture surfaces. Each sample was dried at 110°C, mounted on a microscope specimen holder, then a conductive coating was evaporated on to the sample surface. A gold-palladium coating was normally used but chromium was used in some cases. For the EDXRA analysis, the 2.308 KeV ($K\alpha_1$) peak of sulphur was obscured by the 2.123 KeV ($M\alpha_1$) peak of gold, but the use of chromium eliminated this problem.

4.2.10 Non-Evaporable Water Content (Wn/C)

Measurement of the non-evaporable or chemically bound water content of pastes has been a problem in cement hydration research due in part to disagreement on the separation between evaporable and non-evaporable water (Feldman, 1972). Different methods have been developed (Powers and Brownyard, 1948; Copeland and Hayes, 1953; Mills, 1966; Kondo and co-workers, 1980), thus requiring the method utilized to be defined. A commonly used method has been to take the difference in weights between the paste dried at 110°C and ignited at 1050°C as a percentage of the dry weight (Mills, 1966). The method of Copeland and Hayes (1953) is more involved, providing corrections for the ignition loss of the unhydrated cement and expressing the values as a percentage of the ignited paste weights, which is almost the same as the percentage of the anhydrous materials.

The incorporation of slag in pastes further complicated non-evaporable water determinations, since slag typically gains weight on ignition due to the oxidation of sulphides (ASTM C114, 1980). It was found that while initially gaining weight during ignition at 1050°C, the slag was found to lose weight during continued ignition periods. This is likely due to volatization of the oxidized sulphides, as SO_2. After 20h to 30h of ignition, the weight change of each slag became consistent and levelled off(at a net loss in weight) in most cases parallel to the rate of weight change of the respective pastes. As an example, the ignition loss-ignition time curves for slag 17, and a paste

comprising 60 per cent slag 17, 20 per cent portland cement and 20 per cent silica flour, are shown in Figure 4.1. The Copeland and Hayes (1953) equation was then modified to include the three binder components based on the average loss on ignitions for each binder component and paste at ignition times of 20h and 30h. The calculated value of Wn was obtained by Equation 4.5.

$$Wn/C(t) = \left\{\frac{1}{1 - w(t)}\right. \left((Xbfx - Lbfs(t)) + (Xpc - Lpc(t)) + (Xsf - Lsf(t)) \right) \left.\right\} - 1 \qquad (4.5)$$

where,

Wn/C(t) = the non-evaporable water content per unit weight of anhydrous material (g/g).

w(t) = the paste ignition loss at time t (g/g).

(bfs=slag, pc=portland cement, sf=silica flour.)

Xbfs, Xpc, Xsf =the weight fraction of each binder material.

Lbfs(t), Lpc(t), Lsf(t) = the ignition loss of each binder material at time t (g/g).

This method had the advantage of correcting for volatile components in the raw materials, including the CO_2 in the portland cement, but did not correct for additional CO_2 in the pastes due to deterioration in storage. However samples were sealed in vials for storage, in an attempt to minimize this problem.

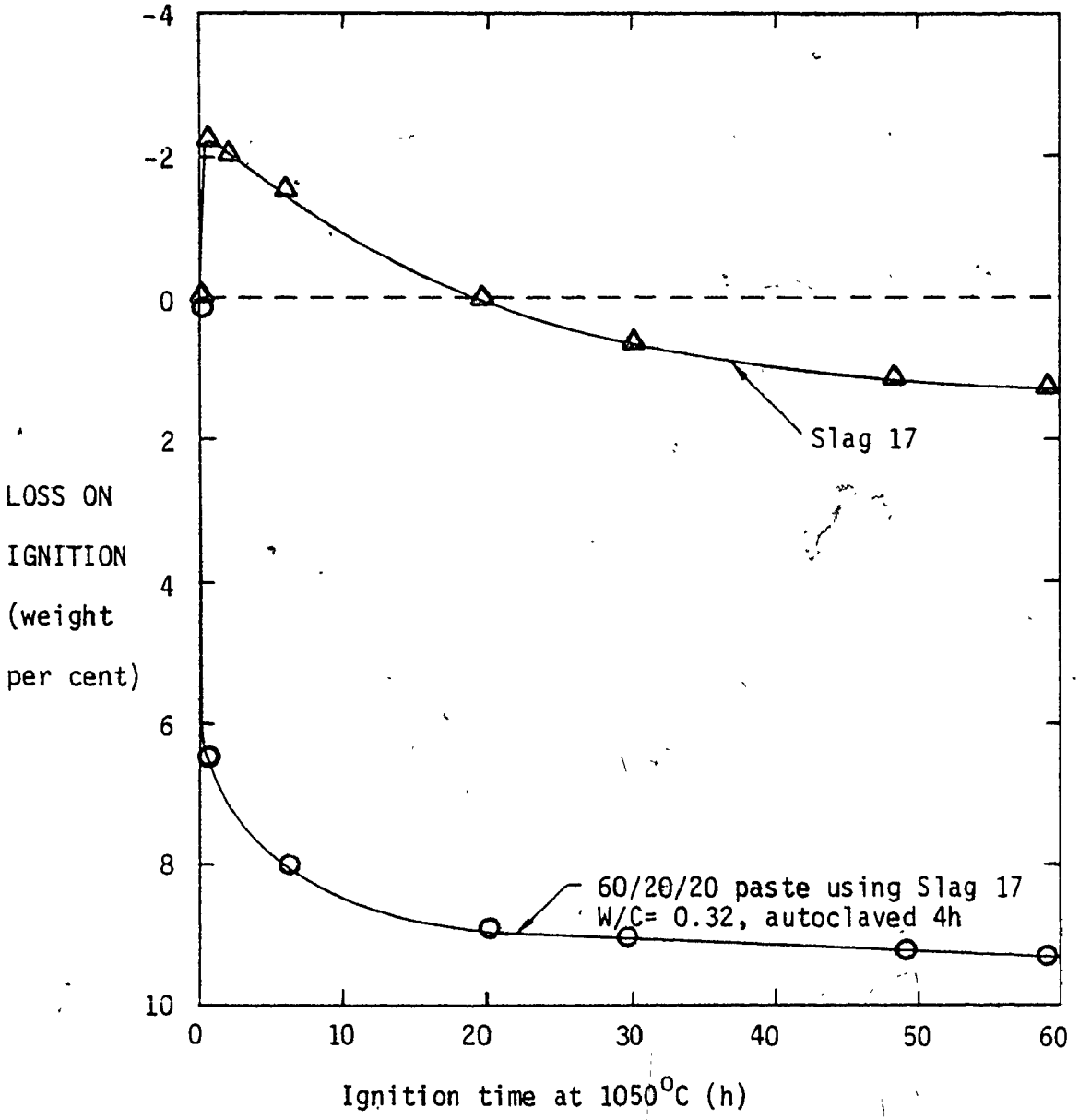

FIGURE 4.1: IGNITION LOSS - TIME CURVES FOR A PASTE AND ITS CONSTITUENT SLAG

4.3 QUANTIFICATION OF PASTE PHASES

4.3.1 Unreacted Slag

The determination of unreacted slag in pastes is difficult due to its glassy nature, and cannot be directly determined by QXRD. The minor crystalline components of slag, if any, were still found to be present at the same intensities as for the unreacted slag (multiplied by the slag fraction in the paste). This was taken as evidence of the lack of reaction of the crystalline components.

Kondo and Oshawa (1969) and later Kondo, and co-workers (1980) used an extraction method in which unreacted slag remained as the insoluble residual. However, in the first study (1969) it was found that autoclaved tobermorite was also insoluble, indicating that only the more poorly crystalline hydrates would be extracted by this method. Further study by Kondo and co-workers (1975) on hydrothermal reactions showed that this method could not be used. Therefore this method was not considered.

Another method considered was the measurement of crystalline slag (mainly melilite) intensities of ignited pastes as done by Kondo and co-workers (1975). However this may not be a valid method since slag hydrates may revert to melilite crystals upon ignition and hence be included in the unreacted fraction (Kondo et al., 1975). Also it was found, when this method was attempted that peaks of other minerals formed during ignition of hydrates overlapped the melilite 211 peak, making intensity measurements exceedingly difficult.

Simply summing the quantities of the other phases contained in

the pastes also proved to be an unsatisfactory method of determining the unreacted slag fraction. The values obtained were found to be in excess of the total slag content in many cases. This was likely due to inaccuracies in the measurement of the other paste components especially the C-S-H fraction which was complimented by its variable state of crystallinity as discussed Section 4.3.7.

Another method considered was measurement of the area of the amorphous halo in each paste and compare these values to the ones expected for the proportion of slag contained if none had reacted. However, amorphous C-S-H also exhibits an amorphous hump almost identical to the ore resulting from vitreous slag. The presence of an interfering halo resulting from amorphous C-S-H was confirmed in the XRD traces of the pastes not containing slag.

It appears then that the unreacted slag content of autoclaved pastes is not amenable to measurement at this time.

4.3.2 Unreacted Portland Cement (PC)

The quantity of portland cement remaining in the pastes was determined by QXRD, using the intensity ratio of the alite reflection at 2.77Å (32.3^{o} 2θ) to the 3.15Å calcium fluoride reflection. A five point calibration curve was developed using mixtures with the least squares linear fit given in Equation 4.6.

$$PC\ (\text{per cent}) = 40.919 \times \left(\frac{12.77\text{Å}}{13.15\text{Å}}\right) - 1.4 \qquad (4.6)$$

(R= 0.9975, SE =±2.8)

It was assumed that the different phases in portland cement reacted at equal fractional rates, which was considered to be reasonable by Crennan and co-workers (1972).

4.3.3 Unreacted Silica Flour

The extraction technique used by Kondo and co-workers (1975) was modified to make use of a centrifuge, instead of filtration, to isolate the insoluble residue. This modified technique is detailed in Appendix J. It was found by XRD analysis of the residues that the only mineral present, other than quartz, was the sericite mica impurity contained in the silica flour.

4.3.4 Calcium Hydroxide (CH)

An XRD calibration curve was developed using three mixtures with 5, 10 and 15 weight percentages of reagent grade calcium hydroxide. The purity of this calcium hydroxide was checked by its ignition loss compared to the theoretical losses expected for pure $Ca(OH)_2$ and $CaCO_3$, and the actual CH content determined by interpolation. The reflection at 2.63Å ($34.1^{o}2\theta$) was used to calculate intensity ratios and the CH quantity was found to be:

$$\text{CH (per cent)} = 10.83 \times \left(\frac{12.63\text{Å}}{13.15\text{Å}} \right) - 0.07 \qquad (4.7)$$

(R=0.996, SE =±1.1)

This provided an excellent fit for the limited data evaluated. *

4.3.5 Calcium Carbonate

Calcium carbonate contents of the binder materials and pastes were obtained using a Leco carbon analyser. The assumption was made that all of the carbon detected was present as CO_2 in the calcium carbonate. The calcium carbonate contents of the pastes at each binder combination were then adjusted, subtracting the amount originally present in the binder materials. The carbon analyser was not available until late in the study, so pastes had been stored for substantial periods of time before this analysis, perhaps affecting the results obtained.

*Since some CH can be amorphous, values obtained by XRD may be lower and less accurate than those obtained by thermal analyses.

4.3.6 Alpha Dicalcium Silicate Hydrate (αC_2SH)

No standard was made for this hydrate, but the XRD calibration equation of Dyczek and Taylor (1971) was used to estimate the quantity present. They also measured the 3.27Å (27.25°2θ) peak intensity as a ratio to the 3.15Å peak of calcium fluoride. The only difference between the procedures was that they added 10 parts CaF_2 to 90 parts sample, so the intensities found in this study had to be multiplied by 0.9.

$$\alpha C_2SH \text{ (per cent)} = 31.5 \times \left(\frac{13.27\text{Å}}{13.15\text{Å}} \right) + 0.8 \qquad (4.8)$$

(SE =±3.4)

4.3.7 C-S-H and Tobermorite

4.3.7.1 Background

As discussed in Section 2.4.2 , calcium silicate hydrates of the tobermorite group are very common in hydrated cements occurring over a wide range of compositions and temperatures of formation. These hydrates are not always well formed, and C-S-H is the term adopted by Taylor (1962) for poorly crystalline 11.3Å tobermorite, although it may include other semi-crystalline hydrates (Taylor and Roy,1980). Figure 4.2 shows the form of typical XRD patterns for crystalline 11.3Å tobermorite, semi-crystalline C-S-H, and near-amorphous C-S-H. From the wide range of crystallinities which may be encountered, the difficulties in quantitative XRD analysis of tobermorites can be

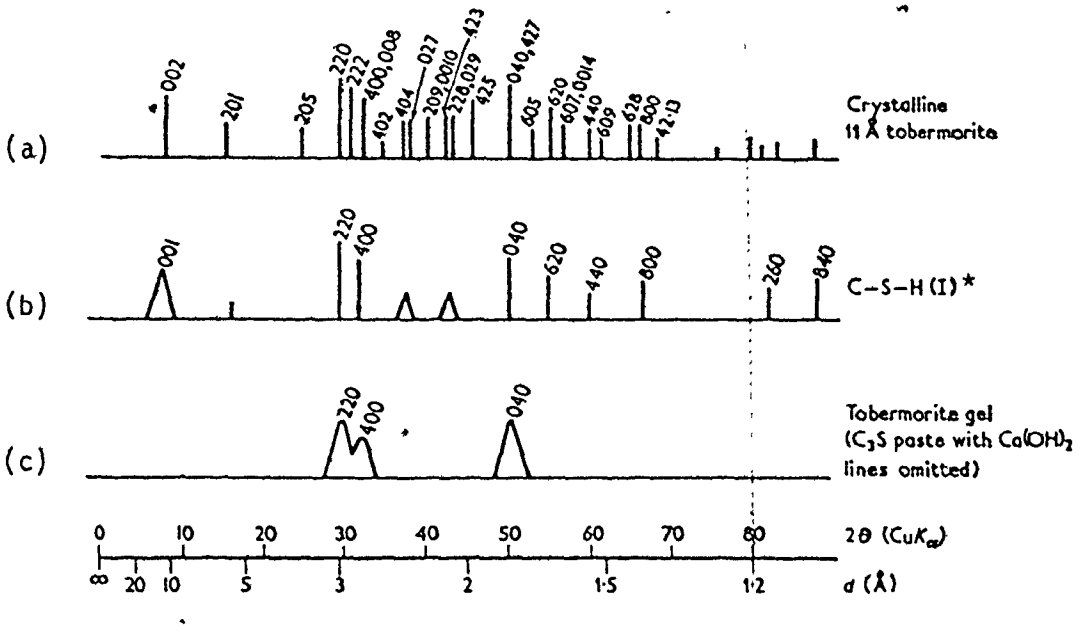

FIGURE 4.2: TYPICAL X-RAY POWDER PATTERNS FOR TOBERMORITES REPRESENTED AS LINE DIAGRAMS
(a) Crystalline 11Å tobermorite, similar to the synthetic material,
(b) semi-crystalline C-S-H similar to that found in most of the pastes in this work, and
(c) near-amorphous C-S-H found at high C/S ratios (Taylor, 1964).

---

*C-S-H(I) is a subdivision of poorly crystalline C-S-H with C/S less than 1.5.

appreciated. Therefore the experimental techniques are divided into two sections, for both amorphous and semi-crystalline C-S-H.

4.3.7.2 Tobermorite and Semi-Crystalline C-S-H

The methods available for the determination of C-S-H content in pastes containing slag are limited due to problems caused by the presence of slag.

The chemical extraction method of determining total C-S-H developed by Stokes (1971), and used by Hara and Midgley (1980) and Alexanderson (1979-1), was found not to be valid when unreacted slag (or unreacted portland cement) was present (Alexanderson, 1979-2).

The XRD method which was adopted to determine quantities of C-S-H is based on a similar calibration procedure used by Dyczek and Taylor (1971). They used intensity ratios of the 11.3, 3.07, 2.97 and 2.80Å reflections of synthetically produced tobermorite to the 3.15Å peak of the calcium fluoride standard. In this work, preliminary investigations showed that the 11.3 and 2.80Å reflections of many pastes were very weak due to a low degree of crystallinity of the C-S-H. Therefore, only the 3.07 and 2.97Å peaks were used for the most part in the determination of C-S-H.

In order to develop a calibration standard, a well crystallized 11.3Å tobermorite, with a molar C/S equal to 0.80, was synthesized from $Ca(OH)_2$ and silica flour as described in Appendix K. The synthesized product was found to contain 69.0 per cent tobermorite, 28.1 per cent xonotlite and 2.9 per cent unreacted silica flour (2.5 per

cent sericite, 0.4 per cent quartz). Due to the fact that both tobermorite and xonotlite exhibit tneir most intense XRD peak at 3.07 ± 0.2Å, the assumption of equal intensity ratios (to the CaF_2 standard) was made, so that a calibration curve for the 3.07Å peak could be developed. The 2.97Å peak is unique to 11.3Å tobermorite and the use of it for intensity calibrations was not a problem. To develop the calibration curves, the synthetic material was mixed with silica flour in 11 different proportions by weight and then calcium fluoride was added as discussed in Section 4.2.7. These mixtures were analysed by QXRD, as well as the silica and synthetic material alone, resulting in a 12 point calibration curve for each peak height ratio versus concentration. In addition, each mixture was scanned by XRD 3 to 7 times to obtain average peak height ratios for each point. Least squares linear regression equations were determined for the 2.97Å and 3.07Å peaks of tobermorite. The line fits were excellent with correlation coefficients of 0.9986 and 0.9985 respectively. As can be seen in Figure 4.3 there was only slight absorption of tobermorite by quartz as evidenced by the linearity of the calibration curves except at high tobermorite contents. The calibration equations developed were:

$$\text{C-S-H (weight per cent)} = 31.732(I_{3.07Å}/I_{3.15Å\ CaF_2}) - 3.3 \quad (4.9)$$

(R= 0.9986, SE = ±2.8)

$$\text{C-S-H (weight per cent)} = 54.805(I_{2.97Å}/I_{3.15Å\ CaF_2}) - 6.4 \quad (4.10)$$

(R= 0.9985, SE = ±1.5)

These equations were then applied to the peak height ratios of the same peaks in the autoclaved pastes to determine their C-S-H contents. The

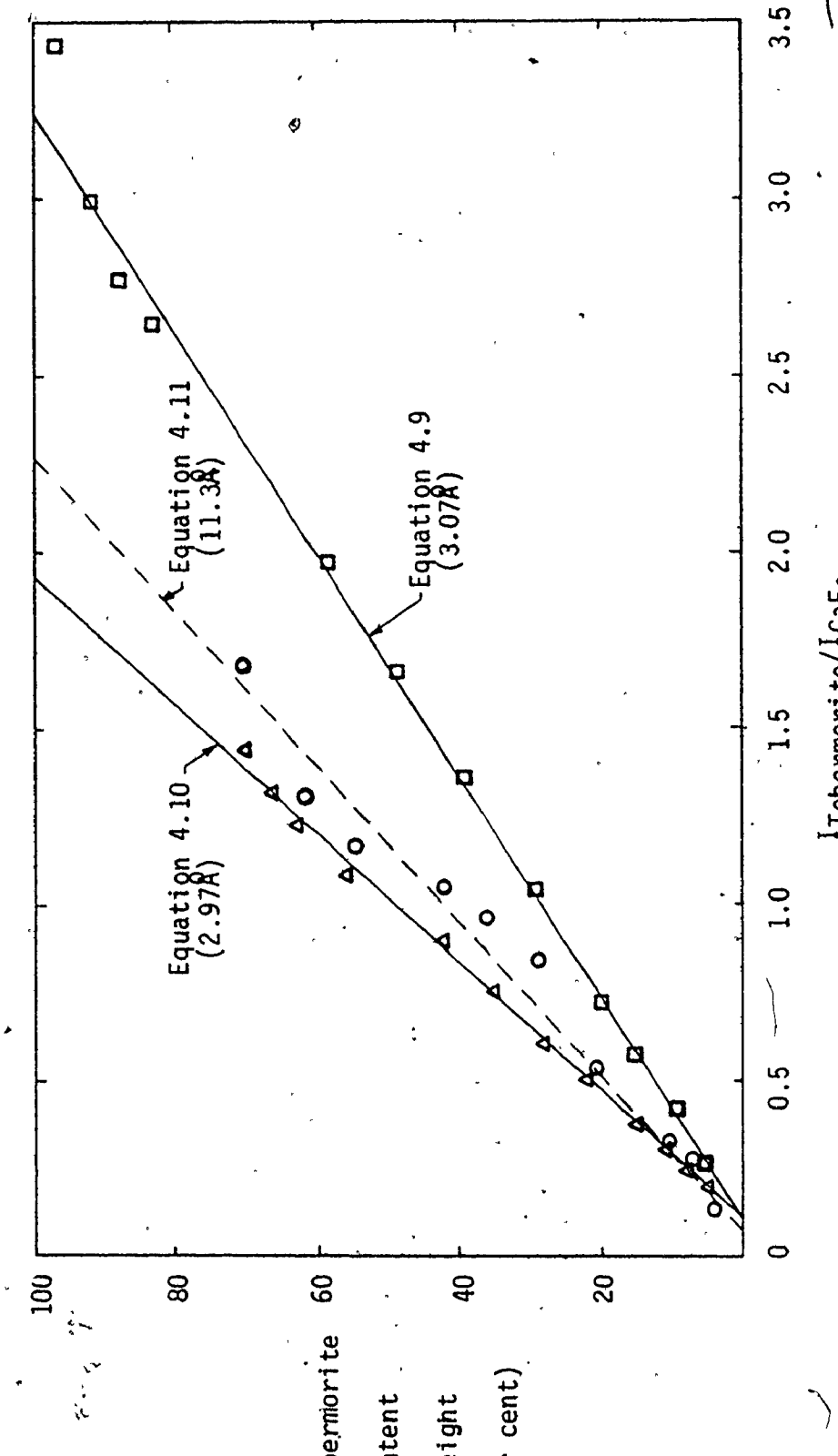

FIGURE 4.3: XRD CALIBRATION CURVES FOR PEAKS OF SYNTHETIC TOBERMORITE

values obtained from Equations 4.9 and 4.10 were then averaged. The 11.3Å intensity ratios were not used directly, but the curve is shown as a dotted line in Figure 4.3 and the linear fit is given in Equation 4.11.

$$\text{Tobermorite (weight per cent)} = 45.228(I_{11.3\text{Å}} / I_{3.15\text{Å}}) - 3.2 \quad (4.11)$$

($R = 0.986$, $SE = \pm 3.9$)

As Hara and Midgley (1980) pointed out, the use of a well crystallized tobermorite standard to determine the quantity of poorly crystallized C-S-H in hydrated pastes would tend to be inaccurate. They developed a crystallinity index (Yr) based on experimental results.

$$\text{Yr(per cent)} = \frac{0.25 + 47.1(I_{11.3\text{Å}} / I_{3.07\text{Å}})}{(1.28 - (I_{11.3\text{Å}} / I_{3.07\text{Å}}))} \quad (4.12)$$

Using mixtures of C-S-H and tobermorite, Hara and Midgley found that the intensity of the 3.07Å peak (relative to the 3.15Å peak of calcium fluoride) for a given amount of C-S-H depended linearly on its crystallinity index, for Yr values between 20 and 100 per cent. The intensity ratio for well crystallized tobermorite (Yr=100) was found to be 2.6 (calculating from their data) times greater than the same amount of poorly crystallized C-S-H (Yr=20). While for Yr values between 0 and 20 per cent, the intensity ratio did not change.

Therefore in this work, the equation for the crystallinity index was adopted to evaluate the pastes. The averaged amounts of C-S-H determined using Equations 4.9 and 4.10 were then corrected (C-S-Hc) for the influence of crystallinity.

For Yr values between 0 and 20 per cent:

$$\text{C-S-Hc (per cent)} = 2.6\ (\text{C-S-H}) \quad (4.13)$$

While for Yr values greater than 20 per cent:

$$\text{C-S-Hc (per cent)} = (\text{C-S-H}) \cdot (3.0 - 0.02(\text{Yr})) \quad (4.14)$$

However, as mentioned previously, the intensities of the 11.3Å peaks used in the calculation of Yr were very weak for some of the pastes. Due to this, the accuracy of the Yr values in these cases would be limited. However, the correction factor in Equation 4.13 does not change until the crystallinity index equals 20, and by that point the intensities of the 11.3Å peak would have to be quite substantial.

4.3.7.3 Amorphous C-S-H

The method of determining C-S-H content by the intensities of the 2.97Å and 3.07Å XRD peaks would not account for the presence of amorphous C-S-H which could only be detected by a hump in the base line of the XRD trace around 3Å.

The method of Berardi and co-workers (1975) of determining relative contents of amorphous C-S-H by measurement of the diffuse band around 3Å could not be used except for the portland cement -quartz paste due to the presence of the overlapping halo caused by unreacted slag glass which was discussed in Chapter 3. For pastes not containing slag, the amorphous C-S-H contents were estimated by difference after all other pastes were determined. However, in pastes containing slag the quantities could not be estimated.

4.4 RESULTS

4.4.1 Mortar Strengths

Mortar cubes were made at 10 per cent intervals over most of the range of the ternary system and the resulting compressive strengths are shown in Figure 4.4. The average coefficient of variation for all 50 sets of cube strengths was 4.1 per cent. It can be seen that at 20 per cent silica flour contents, high strengths were obtained over the whole range of slag cement/portland cement. The iso-bars delineate the areas of 35 and 45 MPa strength development. Maximum strengths greater than 45 MPa were obtained at three combinations with high slag contents: 60/20/20*; 70/20/10; and 75/15/10. From comparison of the strengths given in Figure 4.4 with the molar C/S ratios of the binder materials in Figure 4.5, it was observed that optimum strengths generally coincided with molar C/S ratios of the binder materials between 0.8 and 1.5.

In binders used for the production of commercial autoclave products, the C/S ratio is usually maintained in this range in order to optimize strength. This corresponds approximately to the range of C/S ratios for maximum tobermorite formation, between 0.75 and 1.1 (Verbeck and Copeland, 1972).

---

* For brevity, the ternary binder combinations have been designated throughout by weight per cent slag/ per cent portland cement/ per cent silica flour.

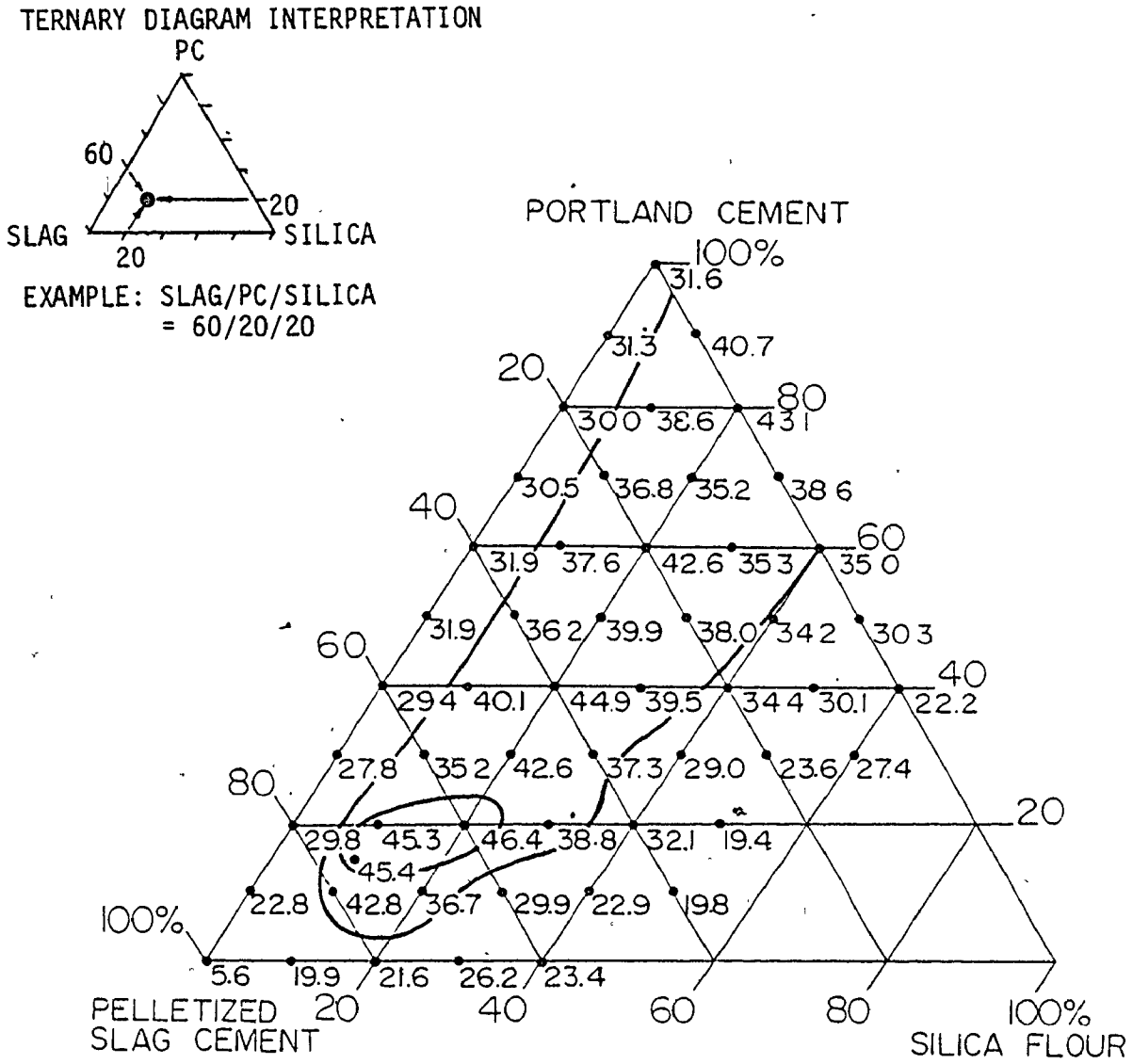

FIGURE 4.4: COMPRESSIVE STRENGTHS OF AUTOCLAVED MORTAR CUBES (MPa)

Strength isobars are shown for 35 and 45 MPa.

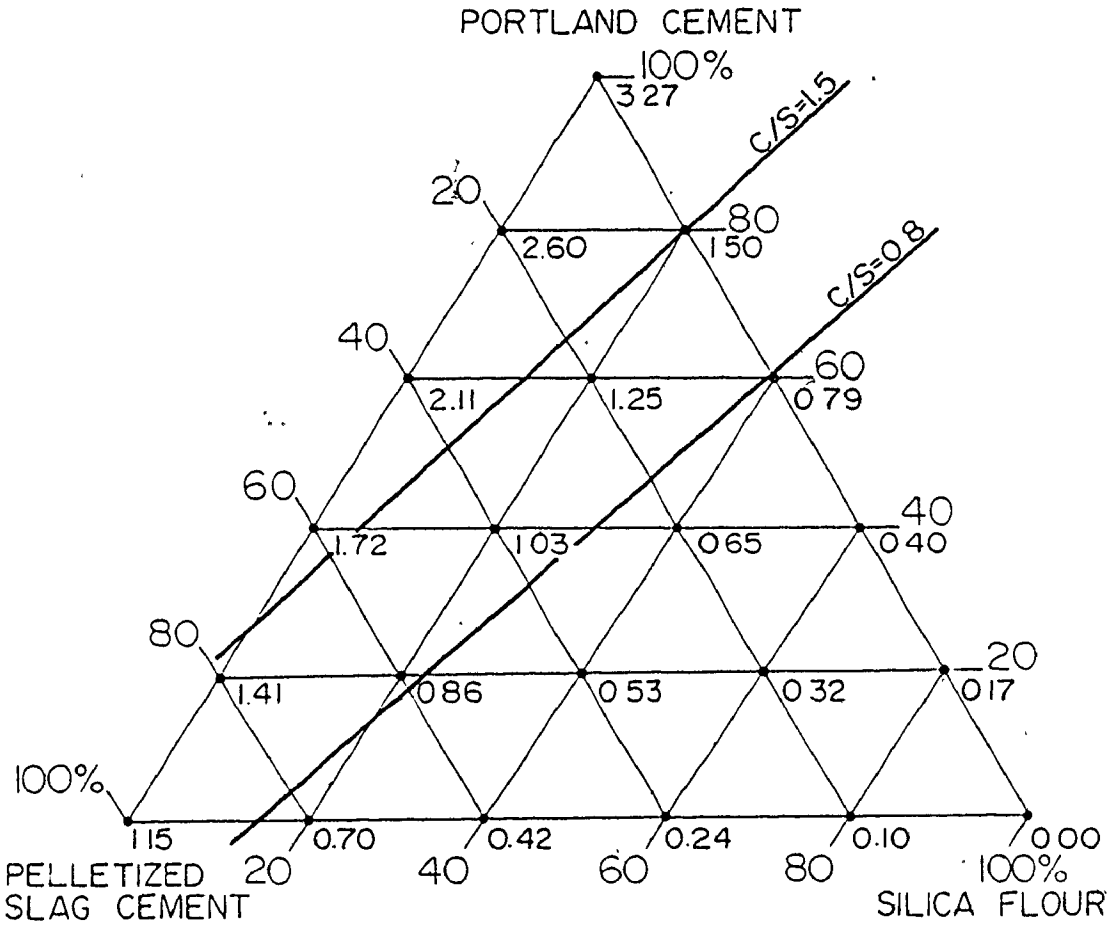

FIGURE 4.5: MOLAR C/S RATIOS OF INITIAL BINDER MATERIALS

The range of C/S commercially used is shown between C/S =0.8 and 1.5.

4.4.2 Paste Strengths

The compressive strengths of paste cylinders made at 20 per cent intervals in the ternary binder system are shown in Figure 4.6. Tensile to compressive strength ratios are given in Figure 4.7. The average coefficient of variation of all sets of cylinders was 8.9 per cent. While somewhat high, it was not possible within the context of the study to refine all data through repetitions, and it is doubtful that the trends would be changed significantly.

Comparison of these strengths with the mortar cube strengths in Figure 4.4 showed that the region of optimum strengths has shifted over to about 40 per cent silica flour. This seemed to indicate that some of the coarse quartz sand (0.15mm to 0.60mm) in the mortars had reacted to form hydration products. The hydrothermal reaction of coarse quartz sand was also found by Menzel (1934) who noted the reaction of 0.30mm to 0.58mm sand when autoclaved at 177°C. Also pastes initially containing 20 per cent silica flour, were still found to contain large quantities of unreacted silica as detected by XRD, but their strengths were less than the pastes containing 40 per cent silica flour. However, considering the calcium/silica ratios of the starting materials shown in Figure 4.5 and the unreacted components, the pastes containing 40 per cent silica were likely near the optimum C/S ratio of 0.8 for crystalline tobermorite formation. The strength of the 60/0/40 paste appears to be abnormally low, in view of the strengths of adjacent pastes, but the supply of Slag 17 was exhausted before this was concluded, preventing further testing.

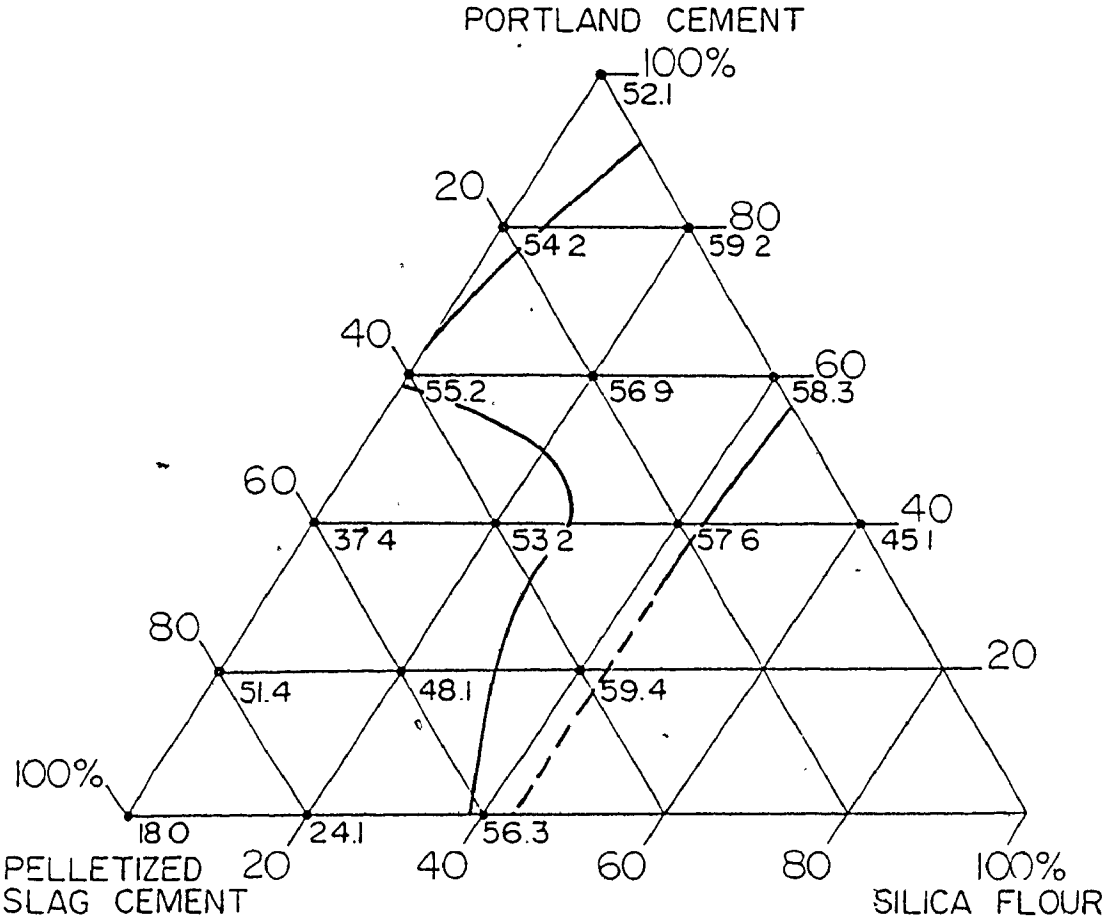

FIGURE 4.6: COMPRESSIVE STRENGTHS OF PASTE CYLINDERS (MPa)

The interpolated strength isobar at 55 MPa is shown.

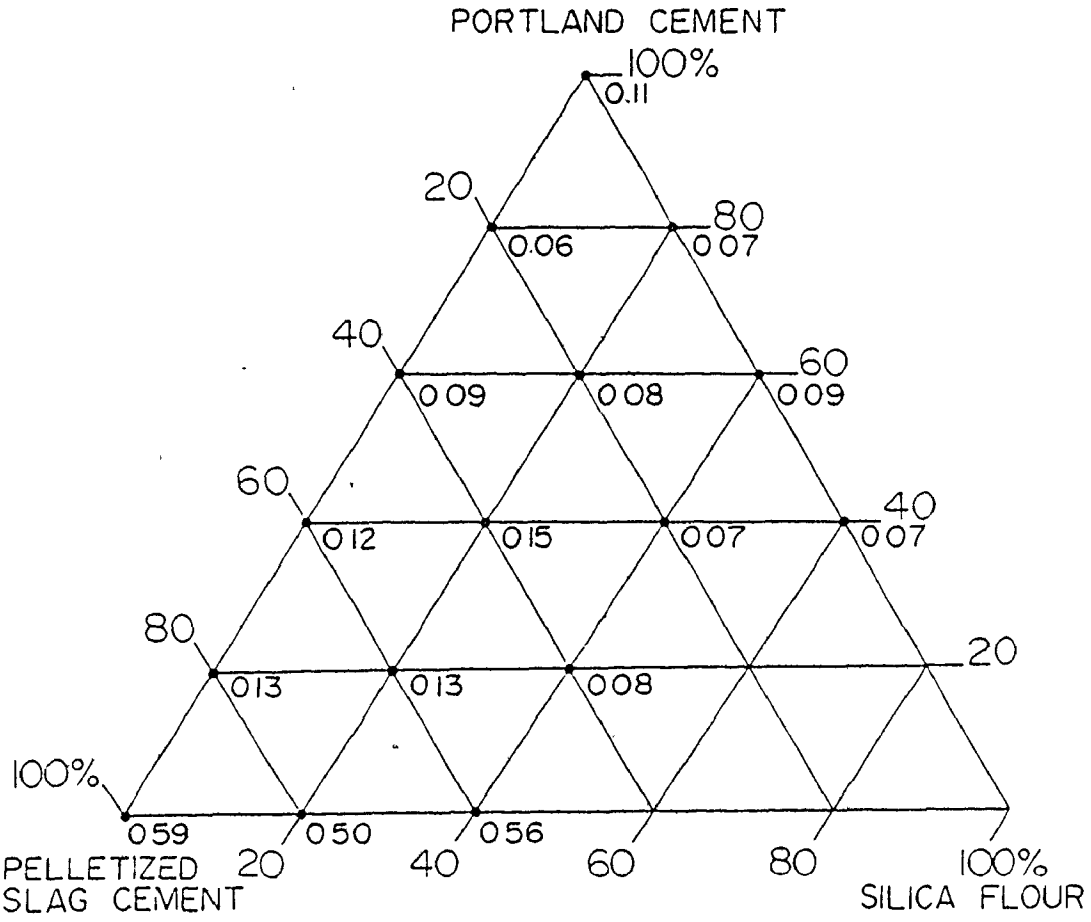

FIGURE 4.7: TENSILE TO COMPRESSIVE STRENGTH RATIOS OF PASTE CYLINDERS

4.4.3 Density and Porosity

The solid density at each binder combination is shown in Figure 4.8. Densities ranged from 2.35 to 2.62 $kg/m^3 \times 10^{-3}$ which was within the range of values found by Beaudoin and Feldman (1975) for autoclaved portland cement-silica pastes. However, unlike Beaudoin and Feldman's data, the solid densities of the portland cement-silica pastes in this study are almost constant. The slag paste (100/0/0) and slag-silica paste (80/0/20) exhibited the highest densities, likely due to large quantities of unreacted slag as evidenced by low strengths.

The apparent porosities shown in Figure 4.9 ranged from 23.4 to 37.2 per cent. The porosities of the three non-portland cement pastes and the high silica paste (0/40/60) were much higher than the others. These four pastes, as shown later in Figure 4.11, also had the lowest non-evaporable water contents which infers a low degree of hydration.

4.4.4 Unreacted Materials

The quantities determined for unreacted silica flour and portland cement are listed in Table 4.2. The binder combinations in which they were detected are also given in Figure 4.10. The amount of unreacted portland cement decreased with increasing slag and silica flour contents. At binder combinations containing 20 per cent silica flour, more silica flour was reacted at higher portland cement contents. This would be accounted for by the calcium hydroxide, liberated by the hydrating portland cement, reacting with the silica flour.

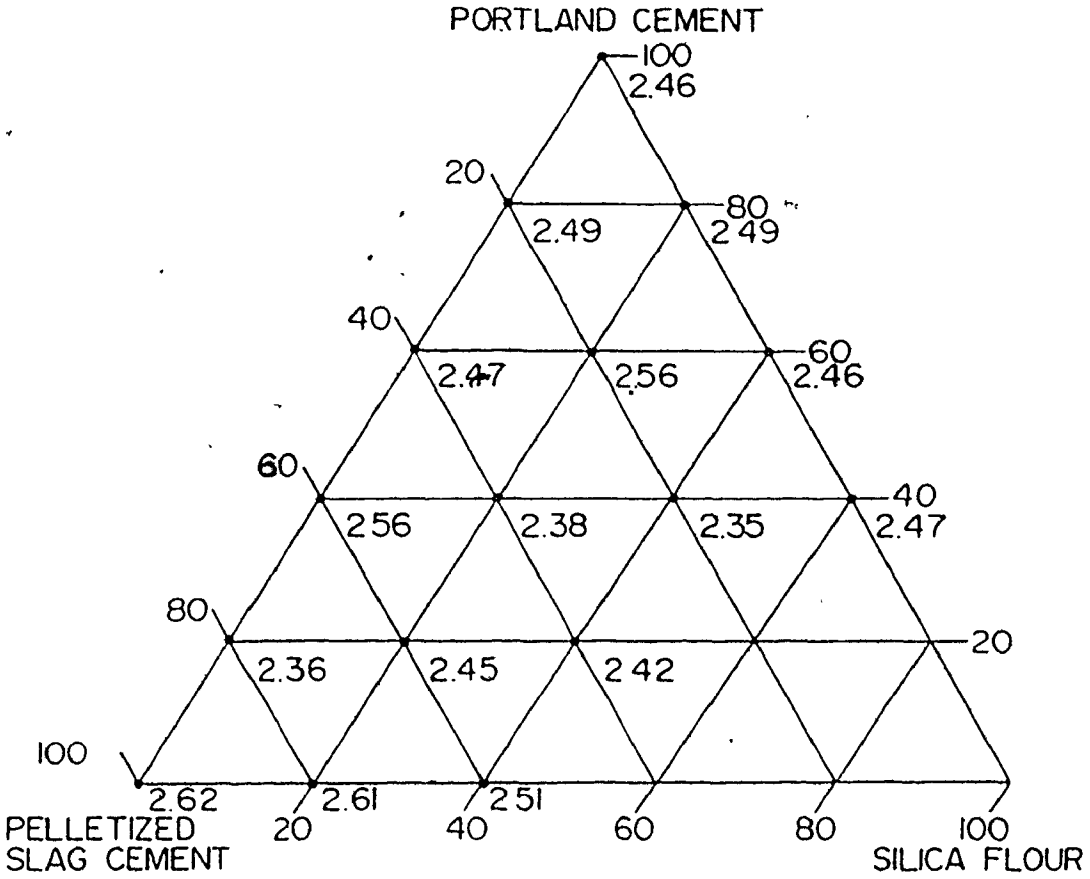

FIGURE 4.8: SOLID DENSITIES OF PASTES ($kg/m^3 \times 10^{-3}$)

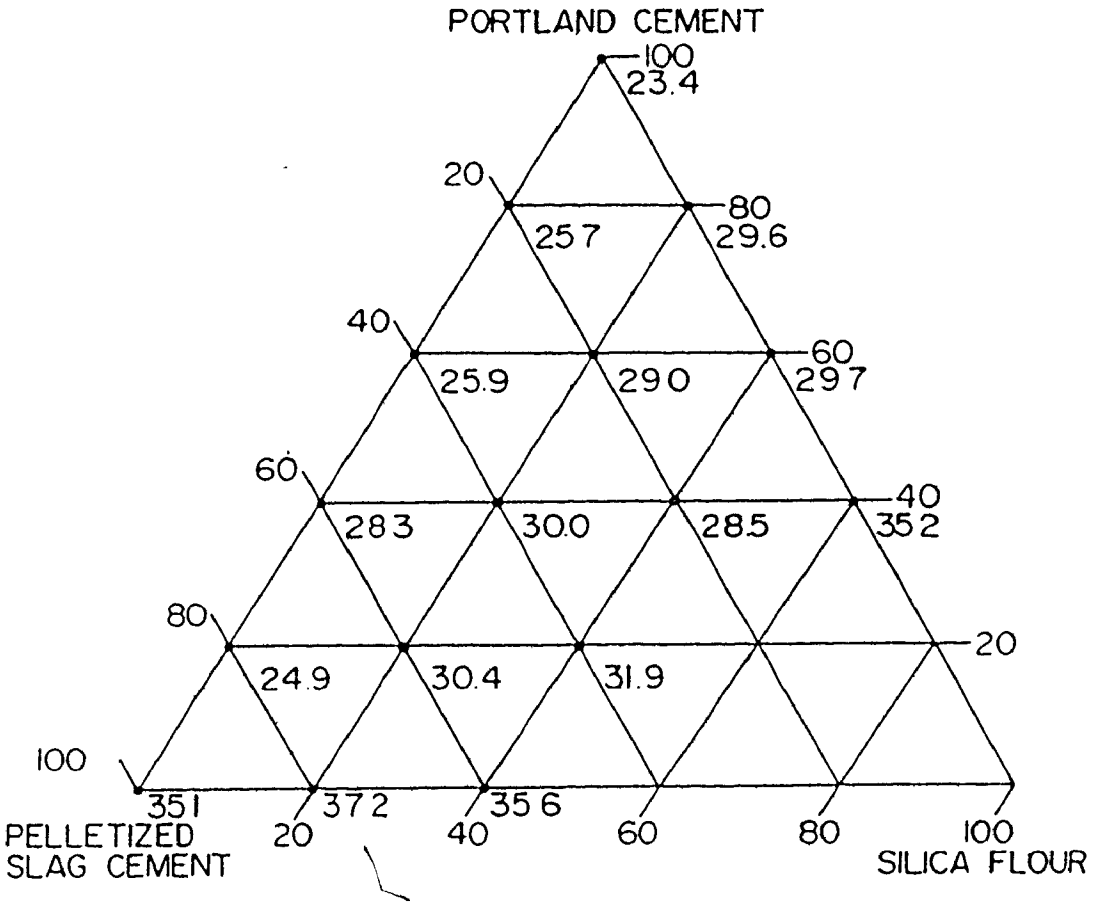

FIGURE 4.9: APPARENT POROSITES OF PASTES (per cent)

TABLE 4.2
QUANTITIES OF UNREACTED COMPONENTS AND LIME COMPOUNDS IN PASTES
(WEIGHT PER CENT)

PASTE COMPOSITION (BFS/PC/SF)	UNREACTED PORTLAND CEMENT PC	UNREACTED SILICA FLOUR SF	CALCIUM HYDROXIDE CH	CALCIUM CARBONATE* $\overline{CC}$
100/0/0	0	0	0	7.5
80/20/0	6.8	0	1.0	1.9
60/40/0	11.8	0	5.6	9.6
40/60/0	10.3	0	5.6	3.1
20/80/0	24.0	0	8.5	7.5
0/100/0	17.3	0	17.5	0.7
80/0/20	0	17.6	0	1.1
60/20/20	4.8	13.7	0	3.6
40/40/20	9.6	12.3	0	2.6
20/60/20	14.7	11.8	1.3	0.7
0/80/20	15.0	9.8	1.5	0.2
60/0/40	0	32.2	0	1.6
40/20/40	0	19.8	0	2.1
20/40/40	14.5	29.0	0	0.6
0/60/40	11.5	24.7	0	2.3
0/40/60	5.8	46.3	0	2.8

* Based on CO_2 Contents of paste minus the CO_2 contents in the raw materials, using a LECO carbon analyser.

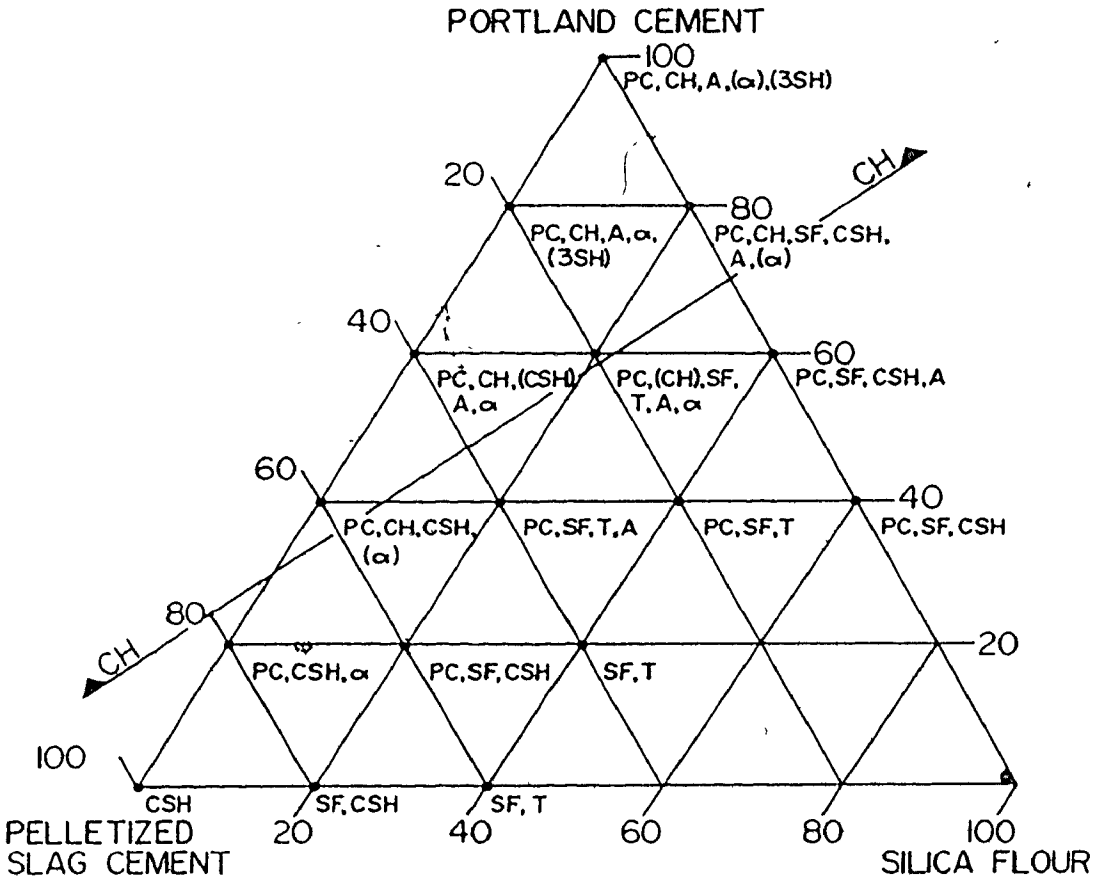

FIGURE 4.10: PHASE COMPOSITION OF HYDRATED PASTES

Legend:
- SF = unreacted silica flour
- PC = unreacted portland cement
- CH = calcium hydroxide
- A = amorphous C-S-H
- CSH = semi-crystalline calcium silicate hydrate (C-S-H)
- T = more crystalline C-S-H
- α = αC_2SH
- 3SH = tricalcium silicate hydrate
- ( ) = less than 5 per cent detected

4.4.5 Lime Compounds

The calcium hydroxide (CH) contents of the pastes are given in Table 4.2. Calcium hydroxide was consumed readily by silica flour and to a lesser extent by slag as indicated in Figure 4.10, and was not detected by XRD or DTA below the isobar labelled CH.

The calcium carbonate contents of the paste are also given in Table 4.2. The values given are the net contents after correcting for the calcium carbonate detected in the unreacted materials. The pastes were stored as powder for over one year before the carbon analysis so much of the carbonation of calcium hydroxide or C-S-H likely occurred during storage.

4.4.6 Hydration Products

4.4.6.1 Semi-Crystalline C-S-H and Tobermorite

The hydration products detected are given in Table 4.3 and are also shown in Figure 4.10. 11.3Å tobermorite in various degrees of crystallinity, was found to be the main hydrated phase in all binders containing silica flour, and for 100 per cent slag cement. Poorly crystalline tobermorite was also found by Midgley and Chopra (1960) when an unactivated granulated slag was autoclaved at 188°C. T denotes a relatively well crystallized tobermorite (Yr greater than 18 per cent) having a well formed 11.3Å peak and CSH denotes poorly crystalline tobermorite (C-S-H). The maximum content of C-S-H, between 46 and 52 perccent by weight, was found along the line of binders containing 40 per cent silica flour, coincident with high strengths. The degrees of

TABLE 4.3
QUANTITIES OF HYDRATED PHASES IN PASTES
(WEIGHT PER CENT)

PASTE COMPOSITION (BFS/PC/SF)	C-S-H CONTENT CSH	CRYSTALLINITY INDEX Yr	CORRECTED C-S-H CONTENT C-S-H c*	αC_2SH CONTENT α	SUM OF C-S-Hc AND αC_2SH
100/0/0	8.4	very low	21.8	0	21.8
80/20/0	6.2	11.2	16.1	7.1	23.2
60/40/0	9.4	14.9	24.4	4.1	28.5
40/60/0	4.5	28.8**	10.9	5.5	16.4
20/80/0	0	-	0	8.0***	8.0
0/100/0	0	-	0	4.0***	4.0
80/0/20	12.1	14.3	31.5	0	31.5
60/20/20	12.0	10.6	31.2	0	31.2
40/40/20	6.1	18.0	15.9	0	15.9
20/60/20	10.8	20.3	28.0	3.3	31.3
0/80/20	10.8	12.7	28.1	2.8	30.9
60/0/40	17.7	35.9	46.0	0	46.0
40/20/40	19.9	18.1	51.7	0	51.7
20/40/40	19.0	21.1	49.0	0	49.0
0/60/40	18.1	14.9	47.1	0	47.1
0/40/60	17.5	5.8	45.5	0	45.5

* Not including amorphous C-S-H.
** This value of Yr is suspect due to poorly formed C-S-H peaks.
*** Tricalcium silicate hydrate was also detected but not quantified. In the 20/80/0 paste, $C_3SH_{1.5}$ was just detected, while stronger intensities were observed in the 0/100/0 paste.

crystallinity were also relatively high for these pastes as shown in Table 4.3, but were still low in absolute terms. As Crennan and co-workers (1977) found, the crystallinity of C-S-H is dependent on the fineness of the quartz employed.

4.4.6.2 Amorphous C-S-H

The presence of amorphous C-S-H, which was not included in the C-S-H values determined in Table 4.3, was detected in pastes not containing slag by the amorphous hump in each XRD trace . By difference, the amorphous C-S-H contents as indicated in Table 4.4 were estimated to be: 60.1 per cent at 0/100/0, 42.6 per cent at 0/80/20, 14.5 per cent at 0/60/40, and 0 per cent at 0/40/60. The content of this amorphous hydrate increased with increasing portland cement contents and increasing C/S ratios.

While the quantity of amorphous C-S-H could not be determined in pastes containing unreacted slag, its presence was indicated at some combinations by the fact that the maximum unreacted slag content, assuming none had reacted, could not account for the differences shown in Column 2 in Table 4.4. Therefore amorphous C-S-H was included in the paste phases given in Figure 4.10 for the 40/60/0, 20/80/0, 40/40/20 and 20/60/20 binder combinations.

Since at other combinations, the unreacted slag could possibly account for the differences in the total phase content of the pastes, the presence of amorphous C-S-H was not certain. This was indicated by the question marks in the Column 5 in Table 4.4. However, it appears that amorphous C-S-H was mainly formed at slag contents of 40 per cent or

TABLE 4.4
SUMMATION OF PASTE PHASES

PASTE COMPOSITION (BFS/PC/SF)	SUM OF PHASES QUANTIFIED IN TABLES 4.2 AND 4.3 (per cent)	DIFFERENCE FROM 100 (per cent)	MAXIMUM UNREACTED SLAG CONTENT OF PASTES * (per cent)	POSSIBILITY OF DIFFERENCE ONLY BEING DUE TO UNREACTED SLAG	PART OR ALL OF DIFFERENCE DUE TO AMORPHOUS C-S-H
100/0/0	29.3	70.7	96.2	yes	?
80/20/0	32.9	67.1	74.1	yes	?
60/40/0	55.5	44.5	55.4	yes	?
40/60/0	35.4	64.6	36.0	no	yes
20/80/0	48.0	62.0	18.0	no	yes
0/100/0	39.9	60.1	0	-	yes(all)
80/0/20	50.2	49.8	76.7	yes	?
60/20/20	53.3	46.7	55.8	yes	?
40/40/20	40.4	59.6	36.9	no	yes
20/60/20	59.8	40.2	18.4	no	yes
0/80/20	57.4	42.6	0	-	yes(all)
60/0/40	79.8	20.2	56.9	yes	?
40/20/40	73.6	26.4	37.3	yes	?
20/40/40	93.1	6.9	18.6	yes	?
0/60/40	85.5	14.5	0	-	yes(all)
0/40/60	100.4	-0.4	0	-	no

*Calculation = (per cent slag in combination) / (1+ Wn/C)

less and silica flour contents of 0 and 20 per cent. This agrees with Taylor (1964) who commented that near-amorphous tobermorites generally have high C/S ratios. Also, it is clear by comparison of Columns 2 and 3 in Table 4.4 that a larger fraction of slag was reacted at higher slag contents.

4.4.6.3 αC_2SH

The presence of αC_2SH was detected mainly in the slag-portland cement binary combinations as shown in Figure 4.10 and Table 4.3, but was never detected in quantities greater than eight per cent. All of the pastes containing αC_2SH, including pastes containing silica flour, had molar C/S ratios (Figure 4.5) exceeding 1.0, which agreed with the results of Aitken and Taylor (1962) shown in Figure 2.4. However, high strengths were also obtained for the pastes containing αC_2SH, perhaps due to optimum mixtures of dense, well crystallized αC_2SH and less dense, poorly crystallized C-S-H as suggested by Feldman and Beaudoin (1976) and Taylor (1977). In other studies, pastes containing large quantities of αC_2SH were found to exhibit low strengths (Kalousek,1954-2; Sanders and Smothers, 1957). The surprisingly low quantity of αC_2SH found in the portland cement paste was also found by Alunno-Rossetti and co-workers (1973) for C_3S pastes autoclaved at 190°C for 5h. However, according to Taylor (1964) and Verbeck and Copeland (1972), αC_2SH is usually the predominant hydrated phase found in autoclaved portland cement.

In the original analysis (Hooton and Emery, 1980), DTA endotherms, with characteristic temperatures at 475°C were found and attri-

buted to αC_2SH (Kalousek, 1954-1; Midgley and Chopra, 1960). However, later Krüger (1980) suggested that this endotherm might be due to $Ca(OH)_2$ instead, although published DTA data suggested the $Ca(OH)_2$ endotherm to occur at about 550°C (Kalousek, 1954-2). Subsequent DTA analysis of autoclaved reagent grade calcium hydroxide did not produce a similar endotherm to those found for the pastes. However, when the portland cement paste was subjected to methanol-ethylene glycol extraction (to remove the calcium hydroxide), then re-analysed by DTA, the endotherm was not present. Therefore the endotherm was concluded to be calcium hydroxide, and the change in characteristic temperature was attributed to factors such as machine sensitivity, sample packing, grain size and/or crystallinity.

4.4.6.4 Tricalcium Silicate Hydrate

Tricalcium silicate hydrate ($C_3SH_{1.5}$) was only detected in small quantities in the portland cement paste and the 20/80/0 paste as shown in Figure 4.10. According to Aitken and Taylor (1962), the presence of $C_3SH_{1.5}$ would be expected for molar C/S ratios of greater than 2.6 when autoclaving at 185°C as shown in Figure 2.4. These two paste combinations were the only ones which met this criteria, having molar C/S ratios of 3.27 and 2.60 respectively. The phases detected in the portland cement paste (Figure 4.10) agree with the phases detected by Akaiwa and Sudoh (1966) for portland cement autoclaved 5h at 200°C. However, portland cement autoclaved for 5h at 150°C did not contain $C_3SH_{1.5}$. Therefore, the limit of formation of $C_3SH_{1.5}$ for short autoclave periods must be between 150°C and 185°C.

4.4.7 Non-Evaporable Water Content

In Figure 4.11, estimates of the non-evaporable water, uncorrected for any carbonation of the hydrates, are given as percentages of the ignited weights. The non-evaporable water content generally increased with increasing portland cement content, which would seem to indicate more complete hydration of pastes containing large quantities of portland cement after 4h autoclaving at 185°C. However, the presence of increasing quantities of $Ca(OH)_2$ with increasing portland cement content accounted for some of this increase. The non-evaporable water contents, corrected for $Ca(OH)_2$, are also shown in parentheses in Figure 4.11. The non-evaporable water contents corrected for the net (total minus the $CaCO_3$, in binder materials) $CaCO_3$ contents in the pastes are also given. As described in Section 4.2.9, the CO_2 contents of the binder materials were taken into account in the original Wn/C values. As indicated, in Table 4.2, the CO_2 corrections for some of the pastes may be excessive due to carbonation during storage. The non-evaporable water contents of the non-portland cement (slag-silica flour binary) pastes were much lower than the rest, most likely due to slower reaction kinetics.

4.4.8 Scanning Electron Microscopy

The SEM study was kept very limited in this work since it was considered to be more of a visual aid than an analytical tool, although recent advances have been made in analytical electron microscopy as discussed by Taylor and Roy(1980). The morphologies of cement hydrates

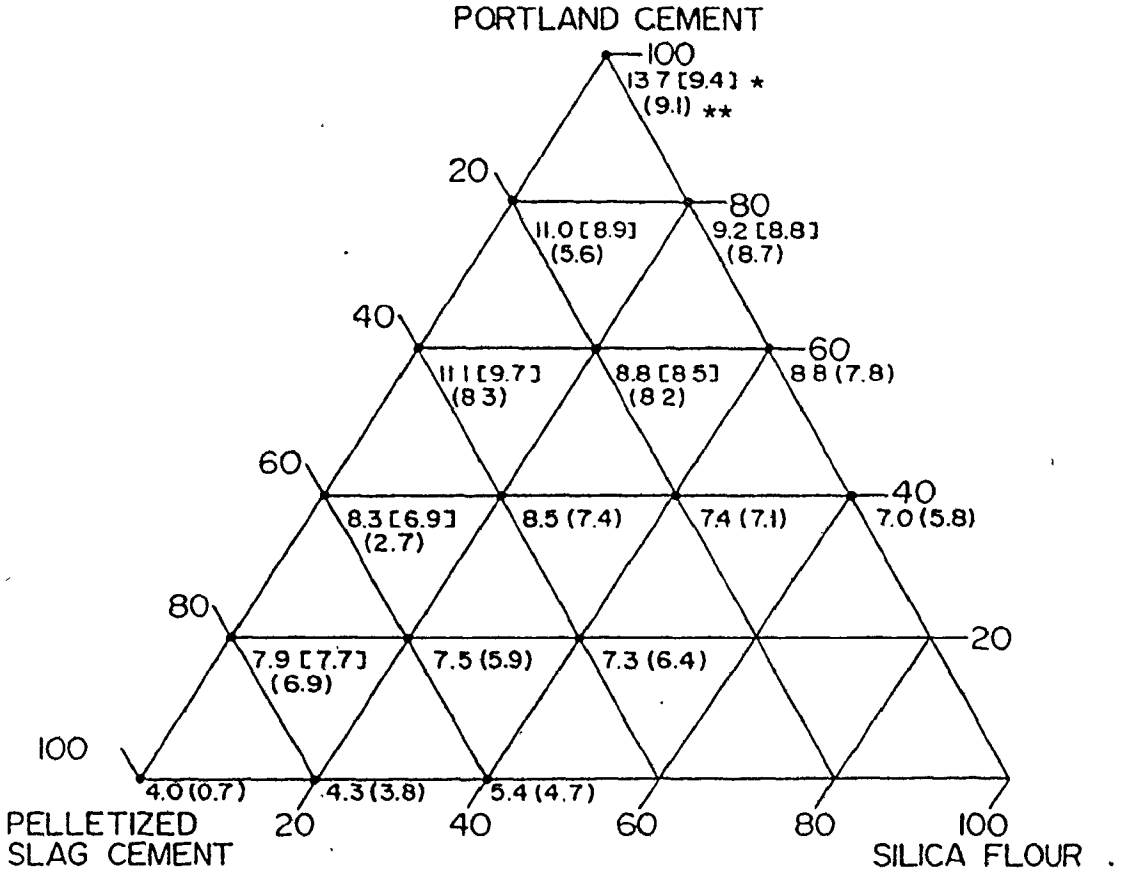

FIGURE 4.11: NON-EVAPORABLE WATER CONTENT OF PASTES (WEIGHT PER CENT)

* Values in [ ] parentheses are corrected for $Ca(OH)_2$ content.

** Values in ( ) parentheses are corrected for $CaCO_3$ and $Ca(OH)_2$ contents.

are quite variable and in many cases it is difficult to distinguish one from another. However, it was thought that a limited study was required in order to provide an indication as to the nature of hydrates in general.

The morphology of the synthetic tobermorite material was examined in the SEM. As shown in Figures 4.12 to 4.14, the material is composed of radiating fibres which may be due to either tobermorite or xonotlite. Small plates, which may be unreacted CH, appear at the interior of the radiating fibre clusters.

While several pastes were examined in the SEM, surface charging problems, resulted in poor quality micrographs. As the samples were evacuated in the microscope, hydrate shrinkage caused cracking of the conductive surface coating which resulted in the "charging" problems.

Figures 4.15 and 4.16 show fracture surfaces of the 80/20/0 paste. The crumpled foil structure of the C-S-H is typical of semi-crystalline C-S-H according to Taylor (1964). The EDXRA results show the elements found but little reliability is given to the intensity ratios since they are affected by experimental conditions such as surface roughness nad the prominence of the feature being examined. (Grattan-Bellow et al, 1978). The areas of influence of the electron beam maybe larger than a small particle chosen for analysis and the composition of some of the surrounding material may also be included. For these reasons, the hexagonal plates in Figure 4.16 are likely CH inspite of the other elements given in the EDXRA analysis. The structures of 60/20/20 pastes are given in Section 5.4.11.

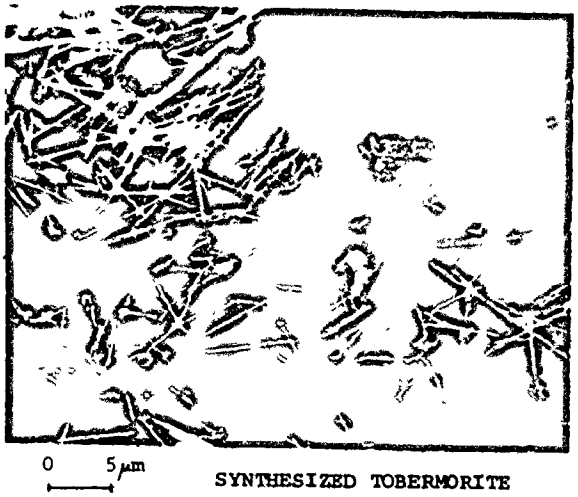

FIGURE 4.12: FIBROUS HYDRATES

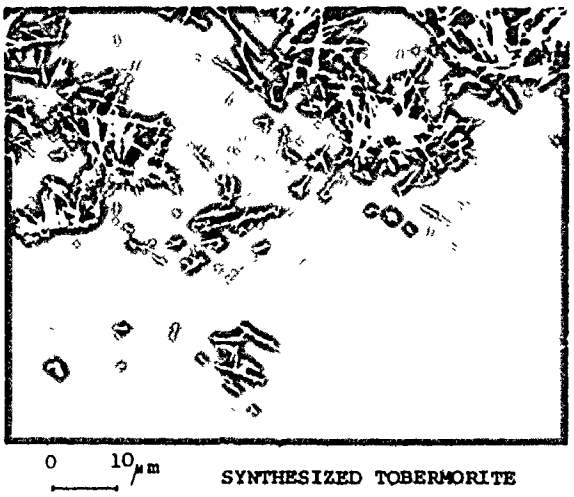

FIGURE 4.13: RADIATING CLUSTERS OF FIBROUS HYDRATES

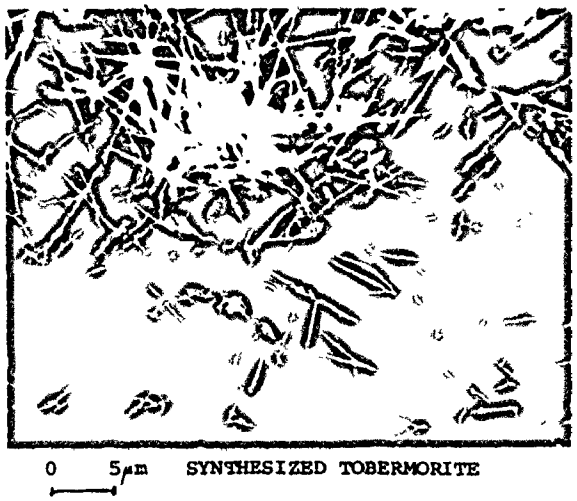

FIGURE 4.14: ENLARGED CLUSTER FROM FIGURE 4.13, EXHIBITING RADIATING FIBRES(Ca/Si=1.18,EDXRA) AND PLATES (Ca/Si=0.95,EDXRA).

EDXRA ELEMENTAL COUNT RATIOS				
SYMBOL	ELEMENT			
	Ca	Si	Al	S
△	3.75	1.00	0.56	1.10

FIGURE 4.15: EXFOLIATED SHEETS SURROUNDED BY POROUS HYDRATES

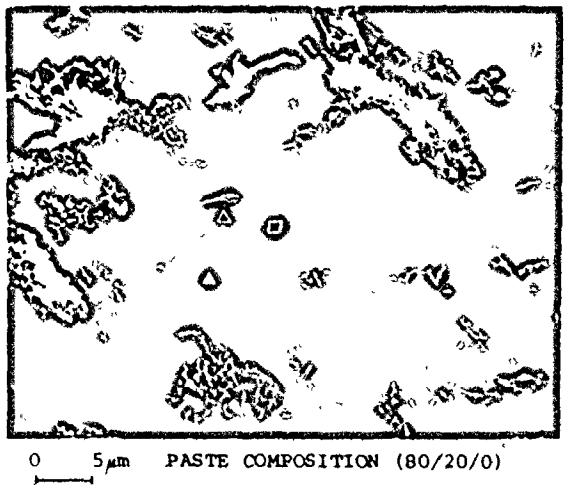

FIGURE 4.16: CRUMPLED FOIL STRUCTURE OF C-S-H AND HEXAGONAL PLATES - LIKELY CH.

EDXRA ELEMENTAL COUNT RATIOS							
SYMBOL	ELEMENT						
	Ca	Si	Al	Mg	S	K	Mn
△	2.52	1.00	0.04	0.05	0.01	0.02	0.02
▲	4.06	1.00	0.38	--	0.53	0.03	0.03
□	1.89	1.00	0.17	0.15	0.05	0.06	--

4.4.9 Non-Portland Cement Combinations

One important observation was that in binders not containing portland cement, the silica flour reacted hydrothermally with the slag cement in both mortars and pastes resulting in higher strengths than that obtained by slag cement alone. A further point of interest is observed from Figure 4.7 which gives tensile to compressive strength ratios for the ternary combinations of pastes. While ratios for binders including any proportion of portland cement did not exceed 0.15, ratios for slag cement and slag cement/silica flour combinations were at least 0.50. Along the slag cement/silica flour binary, the maximum compressive (56.3 MPa) and split tension (31.4 MPa) strengths occurred using 60 per cent slag cement and 40 per cent silica flour. From XRD analysis, it was found that relatively well crystallized 11.3Å tobermorite was the only hydrated phase formed at this combination. Using the method of Hara and Midgley (1980) the crystallinity factor Yr was 36. Kamel (1973-1) also found that a paste of composition 67/0/33 reacted to form 11Å tobermorite after autoclaving for 5h at 193°C. Autoclaving for 6h resulted in lower combined water contents attributed to partial conversion to xonotlite. However no strength testing of this composition was provided (Kamel, 1973-1,2).

The small quantity of free lime liberated by the slag is unlikely to have produced tobermorite to the extent it was found. Therefore reactions, the determination of which was beyond the scope of the study, must have occurred between the calcium silicates in the slag glass and the silica flour. The mechanism of these reactions must

certainly be different than the commonly accepted theory of alkali activation, originally proposed by D'Ans and Eick (1954) and adopted later by Kondo and Ueda (1969) and Kondo and co-workers(1975). Although not considering autoclave termperatures, D'Ans and Eick proposed that hydration-inhibiting, acidic gels initially coated the surfaces of the slag grains and could only be penetrated by a sufficient concentration of externally supplied alkali. This mechanism probably explains the low strengths of the slag paste (100/0/0) but not the higher strengths developed in the slag-silica flour pastes.

The practicality of these non-portland cement binders was questioned due to the slow setting and low green strengths obtained in the pastes. However, in a related industrial application study described in Section 4.5, full scale, 200mm width, masonry blocks were successfully produced, with a binder of 67 per cent slag (285 m^2/kg Blaine fineness) and 33 per cent silica flour (Emery and Hooton, 1978).

4.5 INDUSTRIAL APPLICATIONS OF TERNARY BINDERS

Previous sections in this chapter have dealt with strengths of miniature laboratory specimens, but using commercially applicable cementitious systems. In a parallel applied study, similar strength trends were found for full size concrete blocks with regard to binder composition. In this section this work is described and similarities to the laboratory results are discussed.

Full scale, 200mm by 200mm by 400mm, hollow masonry blocks were produced at a local commercial plant, incorporating slag into the normally used portland cement-silica flour binders. However, the slag ground to 400 m^2/kg Blaine fineness, used in the laboratory studies was not employed due to its cost relative to less expensive silica flour. In order to obtain maximum economic benefits, unground, pelletized slag, commonly used as a light weight aggregate in masonry blocks, was partially ground using methods developed by Kim (1975) and Gupta (1976) for base stabilization and autoclave brick use. Essentially this concept consisted of partial pre-grinding some of the moist slag pellets in an Eirich R7 intensive mixer with a high speed rotor, then introducing this material to the concrete batch mixer along with the aggregates. A schematic diagram of the materials required is given in Figure 4.17. Between 20 and 30 per cent of minus 75μm (Blaine fineness = 285 m^2/kg) slag fines were produced in six minutes grinding (depending on the slag moisture content, increased moisture having a beneficial effect on grinding) with the plus 75μm material used to augment the fine end of the aggregate gradation. Over 50 different

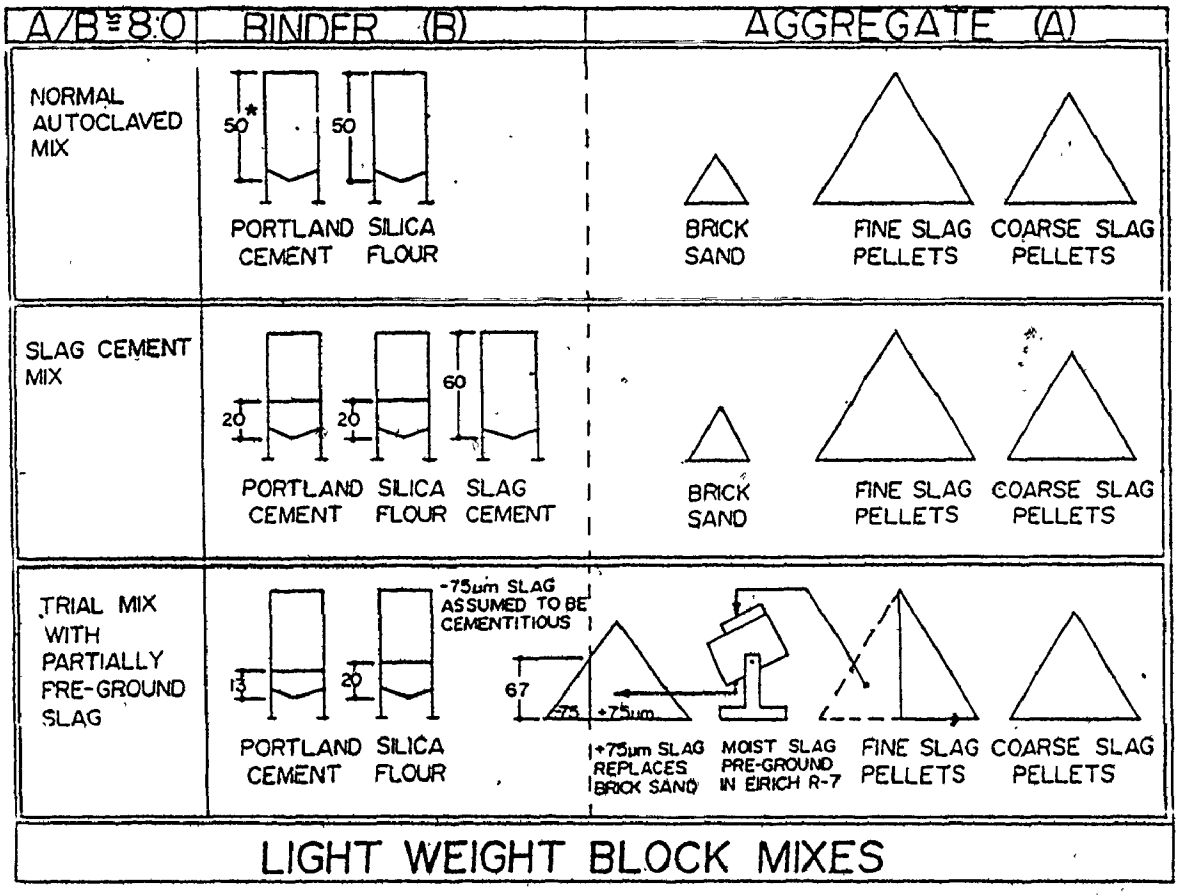

FIGURE 4.17: SCHEMATIC DIAGRAM OF MATERIAL REQUIREMENTS IN THE MANUFACTURE OF LIGHT WEIGHT AUTOCLAVE BLOCKS

1. Without slag as a binder component
2. With separately ground slag cement as a binder component
3. With partially pre-ground pelletized slag as a binder component

* Numbers refer to weight percentages of binder components

batches of blocks were produced industrially, based on data developed in the laboratory, and variables such as binder composition, aggregate types and autoclave cycles were considered.

The effects of variations in the binder composition on strength are shown in Figure 4.18 for light weight pelletized slag aggregate and in Figure 4.19 for normal weight dolomitic limestone and sand aggregates. (Autoclave cycles noted on figures). It can be seen that the compositions providing maximum strength in both figures are similar to the mortar cube compositions in Figure 4.4. Comparing Figures 4.18 and 4.19, it can be observed that presence of slag aggregate causes the maximum strength compositions to shift towards a higher silica flour content. This would be expected, since with standard portland cement-silica binders, the use of slag aggregate allows the use of more silica flour than the limestone aggregate for optimum strength.

Also in one limestone aggregate batch, waste cement kiln dust was substituted for the portland cement at a binder combination of 50/31/19. For total autoclave cycles of 4.5, 5.5, and 6.5h at 177°C, the respective strengths were 8.9, 9.3 and 10.4 MPa, while a similar mix using portland cement had strengths of 10.4, 10.5 and 9.6 MPa. While the strengths obtained using kiln dust were slightly lower at the shorter autoclave cycles, they exceeded the CSA minimum requirement of 6.9 MPa. While the industrial study has not been covered in detail here (Emery and Hooton, 1978), the effect of composition variables on block strengths is of considerable interest given the comparison with the influence of the same variables on strengths of pastes and mortars.

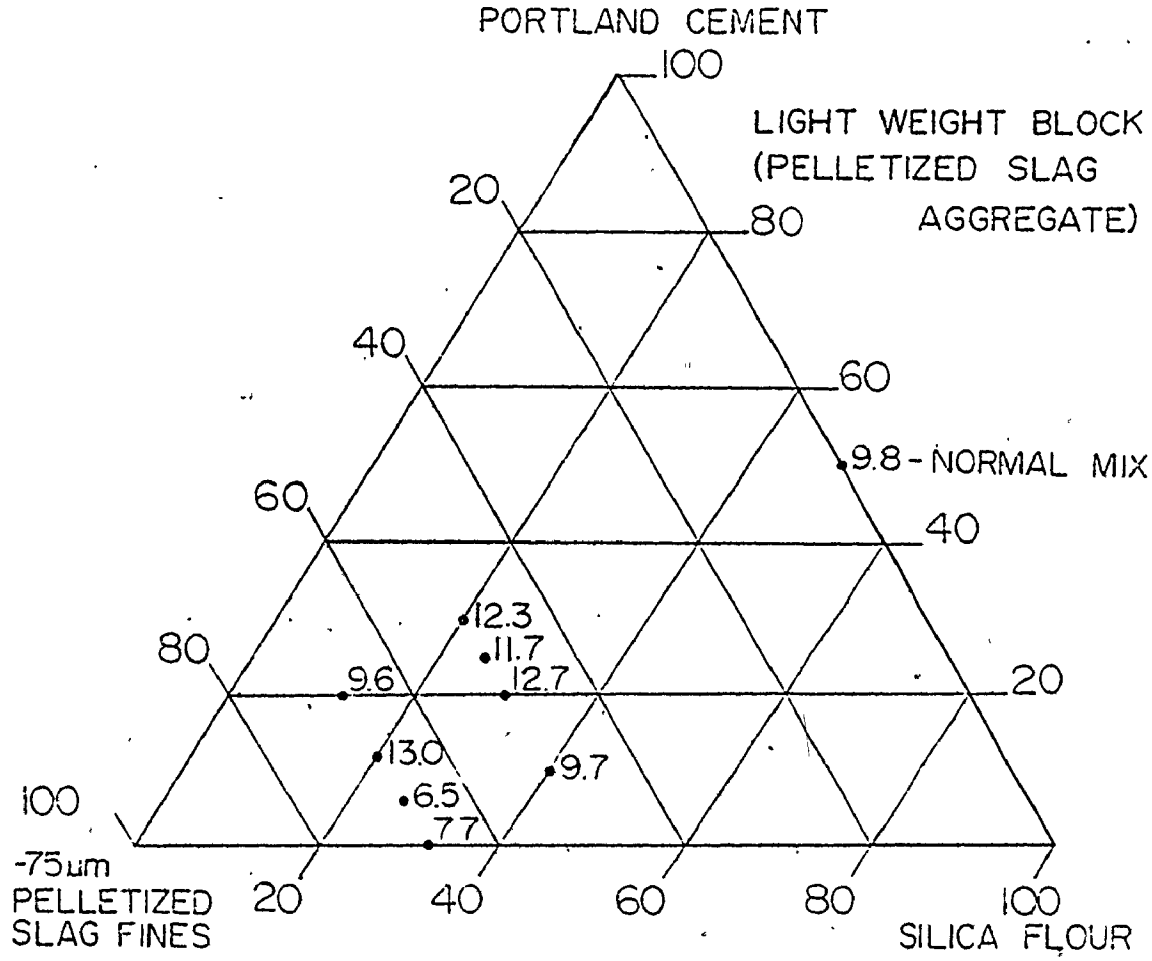

FIGURE 4.18: COMPRESSIVE STRENGTHS OF LIGHT WEIGHT AUTOCLAVED BLOCKS (MPa)

200 x200x400mm (MPa, Gross Area)
CSA minimum = 6.9 MPa
Autoclave cycle 8h total, 6.2h at 185°C

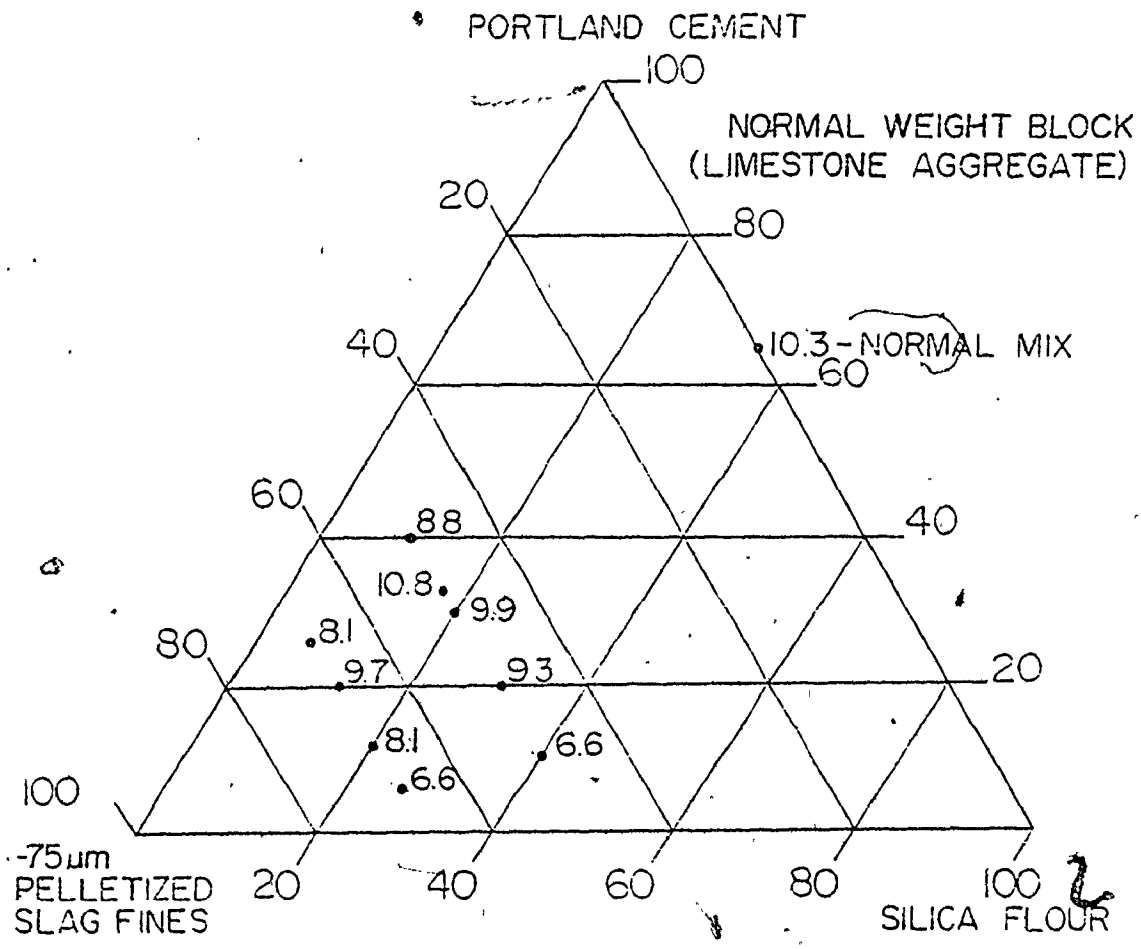

FIGURE 4.19: COMPRESSIVE STRENGTHS OF AUTOCLAVED BLOCKS CONTAINING LIMESTONE AGGREGATE

200x200x400mm (MPa, Gross Area)
CSA minimum = 6.9 MPa
Autoclave cycle 45h total, 2.5h at 180°C

4.6 CONCLUSIONS

Ternary binder compositions of slag, portland cement and silica flour were studied for a typical commercial autoclaving curing regime of 185^{o}C for 4h.

For autoclaved mortars, higher strengths were obtained with pelletized slag cement as the principal constituent in the ternary system slag/portland cemnt/silica flour than with any binary portland cement/silica flour binder combination. While the strength of mortar cubes for unactivated slag was low, high strengths resulted with as much as 80 per cent slag as long as the combination contained both portland cement and silica flour. Optimum strengths were found for 60 to 75 per cent slag contents.

Paste combinations resulting in high strengths generally contained more silica flour than in mortars. These increases in strength with added silica was attributed to the formation of larger quantities of C-S-H and a higher degree crystallinity. Relatively high compressive strengths were also obtained for pastes not containing silica flour. Mixtures of αC_2SH and poorly crystalline to amorphous C-S-H were found and the presence of calcium hydroxide was detected in all the portland cement-slag binary combinations. The presence of CH indicated that slag, unlike silica flour, did not require large quantities of lime to hydrate.

Pelletized slag was activated by silica flour alone, forming relatively well crystallized tobermorite and resulting in high strengths

at one combination without the use of portland cement. These slag-silica binders also showed very high tensile to compressive strength ratios. The mechanism of the slag reaction in these pastes is unclear. It is certainly different than the commonly accepted mechanism of alkaline activation and this is an area for future study.

Using a partially ground pelletized slag to replace part of the binder and fine aggregate, in a parallel applied study, full scale, 200mm width concrete blocks were commercially produced. In light weight (slag aggregate) blocks, the slag replaced up to 67 per cent of the binder required without loss in strength.

5. EFFECTS OF SLAG PROPERTIES ON AUTOCLAVE REACTIVITY

5.1 INTRODUCTION

After the establishment of slag cement reactivity when used in ternary slag-portland cement-silica flour autoclaved binders as described in Chapter 4, the next logical step in this work was to study the effects of variable slag properties on reactivity. Slags from different sources were obtained having a range of glass contents and chemical compositions. As well, some slags were ground to different finenesses, and others altered to extend the range of glass contents available.

To study the variations in slag properties, it was necessary to choose a single, ternary, binder composition. Initial studies with pure slag pastes were abandoned due to slow setting times and low green strengths which resulted in unacceptable specimen losses. Also, as Krüger (1976) found, the strength development of unactivated slags (at 20°C) could not be used to predict strength development of the same slags activated with $Ca(OH)_2$. Therefore, a study of unactivated slags appeared to have little practical value.

The results obtained from the applied, industrial trials discussed in Section 4.5 indicated that an optimum, practical composition would contain around 60 per cent slag, with the ratio of portland cement to silica flour dependent on the aggregates used. Combined with the mortar cube strength results, this led to the selection of 60 per

cent slag / 20 per cent portland cement / 20 per cent silica flour as the binder composition to be used in this work. Since paste experiments in both Chapters 4 and 5 were carried out concurrently, the fact that the 60/20/20 binder composition was not the overall optimum with regard to paste strengths and hydration products, was not realized until later.

However, the selection of an optimum paste composition found along the 40 per cent silica flour line, along with the practical requirement of some portland cement content (to develop green strength in a practical time frame), would have necessitated reducing the slag content to 40 per cent. Therefore, in order to retain slag as the dominant component for this study, the 60/20/20 binder was chosen.

5.2 EXPERIMENTAL METHODS

5.2.1 Materials

The portland cement and silica flour used were the same as described in Section 4.2.1 with physical and chemical properties listed in Table 4.1. The sources and properties of the slags used are given in Tables 3.2 and 3.4. (The numbering system adopted in Chapter 3 is continued). In this chapter, eight Canadian pelletized slags, three foreign pelletized slags, four physically altered Canadian slags and one synthetic slag have been studied. Also, paste Series 19, using slag Number 9 but with CSA Type 50, sulphate resisting portland cement, was included to observe the effect of portland cement type on hydration. The properties of the Type 50 portland cement are given in Table 5.1. A set of control pastes, designated C, were made using 70 per cent normal portland cement and 30 per cent silica flour. This is typical of binders used commercially.

5.2.2 Paste Specimens and Casting

Due to the limited quantity of some slags available for this study, the 30mm diameter and 50mm long cylinders used in Chapter 4 were not adopted here. Instead, smaller paste prisms 15mm by 15mm by 90mm long were cast in machined plexiglass gang molds. This allowed more repetitions of tensile (modulus of rupture) and compressive (equivalent cube) strength tests. For each slag tested, the pastes made with 60 per cent slag, 20 per cent portland cement and 20 per

TABLE 5.1

PROPERTIES OF THE SULPHATE RESISTANT PORTLAND CEMENT

(CSA TYPE 50)

XRF CHEMICAL COMPOSITION		MINERALOGICAL COMPOSITION		
COMPONENT	QUANTITY (per cent)	COMPOUND	BOGUE CALCULATION (per cent)	QXRD (per cent)
CaO_{Total}	62.52	C_3S	48.73	78.4**
CaO_{free}*	0.62	C_2S	25.59	
SiO_2	21.75	C	0.62	
Al_2O_3	3.49	C_3A	3.07	2.0
MgO	3.75	C_4AF	12.35	12.3
K_2O	0.71	$C\bar{S}$	4.20	4.2
Na_2O	0.37	Total	94.56	96.5
SO_3	2.47			
Fe_2O_3	4.06	PHYSICAL PROPERTIES		
SrO	0.04	Specific Gravity = 3.18		
P_2O_5	0.09	Blaine Fineness = 345 m^2/kg		
TiO_2	0.17			
LOI	1.15			
Total	100.57			

* By ethylene glycol extraction

** By salicylic acid extraction

cent silica (60/20/20), were mixed at water/binder ratios of 0.28, 0.32 and 0.40, designated A, B and C respectively. The mixing procedure was the same as described in Section 4.2.3, but vibration was not used on the 0.40 W/C pastes, which were simply tamped with a small rod in order to minimize bleeding.

5.2.3 Curing Conditions

After casting, the paste prisms were stored at 23°C and 100 per cent relative humidity for 15 to 23h prior to demolding and autoclaving. The autoclave cycle was the same as described in Section 4.2.4 with the maximum temperature of 185°C and 1.03 MPa steam pressure maintained for 4h. Specimens were left in the autoclave overnight, and after removal, were placed in a saturated solution of calcium hydroxide, vacuum de-aired and allowed to soak at least 24h prior to strength testing. This ensured that the paste prisms were saturated throughout for testing since variable moisture conditions have been found to have a major influence on strengths especially at low moisture contents (Mills, 1960; Feldman and Sereda, 1970).

5.2.4 Strength Testing

Two modulus of rupture tests, with span equal to 45mm and using third point loading(Figure 5.1),were performed on each paste prism using a small stiff testing machine (Instron). The cast face of each prism was maintained parallel to the applied load. Values obtained where the failure occurred outside of the centre span (the region of

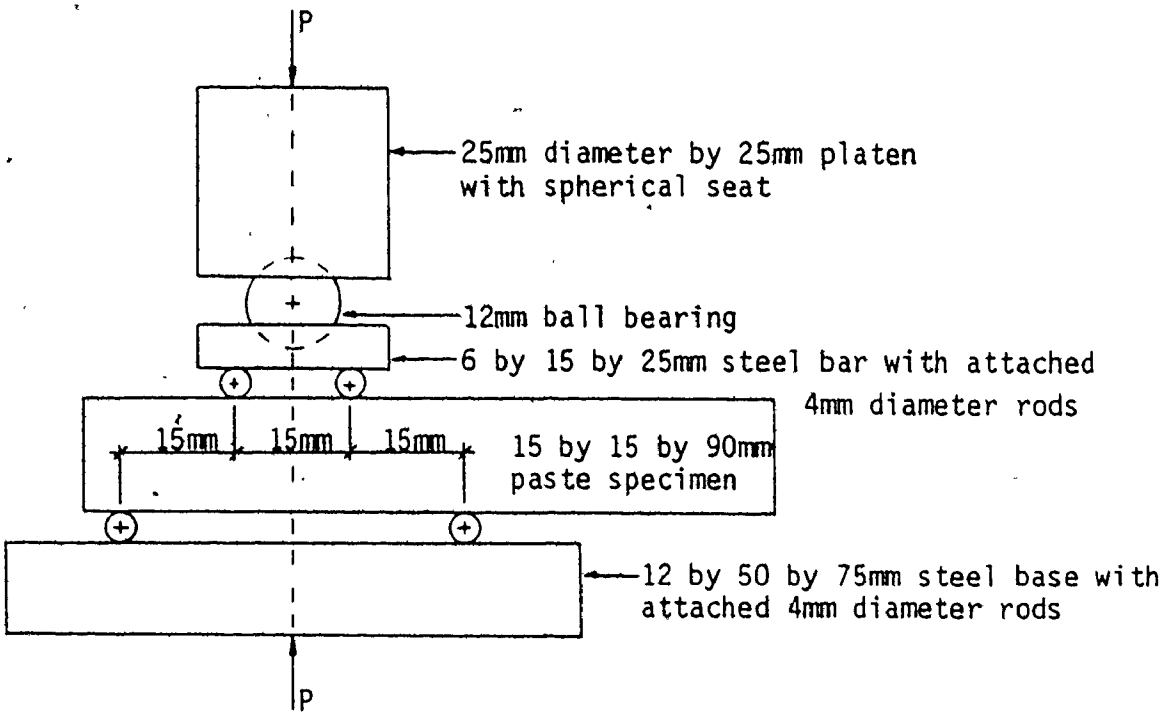

FIGURE 5.1: MODULUS OF RUPTURE TEST

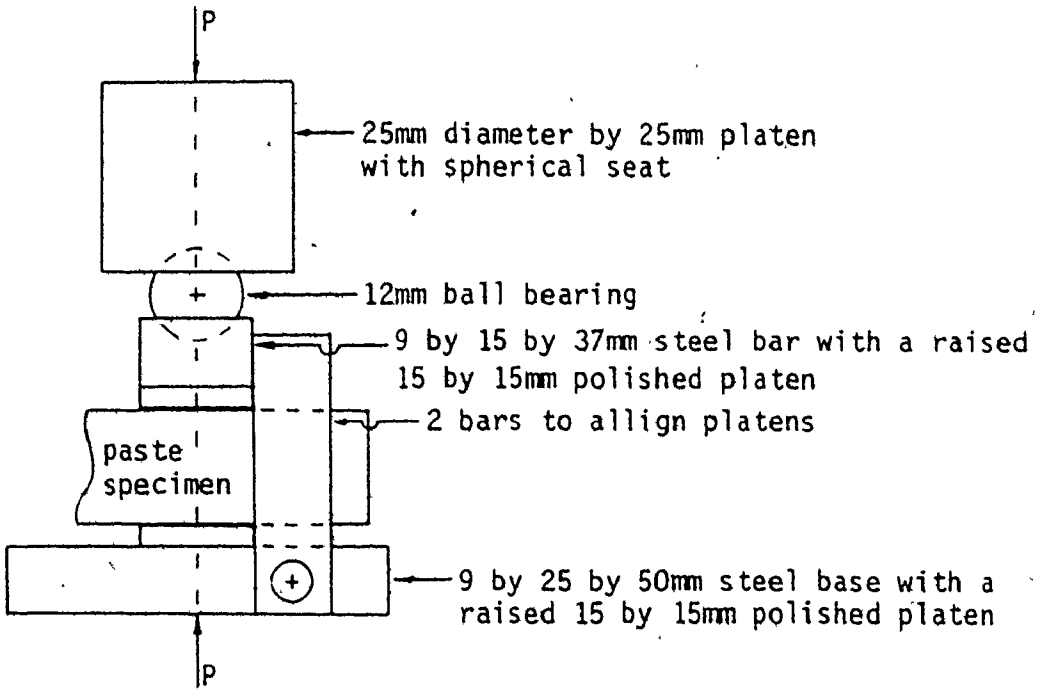

FIGURE 5.2: EQUIVALENT CUBE COMPRESSION TEST

constant, maximum, bending moment) were discarded. The modulus of rupture strengths were found to be an average of 81 per cent higher than splitting strengths obtained using the paste cylinders described in Section 4.2.3. These results were not unexpected since it has been found elsewhere that the direct tensile strength is less than the split cylinder strengths and both are less than the modulus of rupture strength for identical samples (for example; Neville, 1972).

Equivalent cube compression tests were performed on each of the three pieces of each prism remaining after the modulus of rupture testing (Figure 5.2). Between tests, the pastes were stored in the saturated lime solutions. The compression tests were performed in a Tinius Olson universal testing machine. It was found experimentally that the equivalent cube compressive strengths were an average of 48 per cent higher than those obtained using the paste cylinders described in Section 4.2.3. This was expected (for example; Neville, 1972) due to:

1) the lower height/width ratio
2) the smaller size
3) the effect of restraint from the overhanging sections in the equivalent cube test.

Three prisms were tested at each water/cement ratio, providing up to six modulus of rupture and nine compression test results for each variable. The only exception to this was with slag Number 18, the synthetically produced and quenched C_2MS_2 glass, where no modulus of rupture tests and only four compression tests were performed due to the limited availability of this material.

5.2.5 Density and Porosity Measurement

The solid density and apparent porosity of each paste were determined by the displacement method using methanol, as described previously in Section 4.2.6. As a check, solid densities of most of the pastes were measured using a Beckman air comparison pyncnometer in a helium atmosphere as described by Feldman (1971). The paste samples were dried by the same technique and were of the same size as described previously in Section 4.2.6. However,due to the irregular shapes of the samples,the bulk volumes and hence the porosities could not be checked by this method.

Also, mercury intrusion pore size distributions were obtained for a few of the pastes in order to more fully characterize the physical state of the pastes. These were performed using an Aminco, Porosimeter capable of 413 MPa intrusion pressure (29.5Å diameter pores intruded).

5.2.6 X-Ray Diffraction

The apparatus and techniques described in Section 4.2.7 were also used in this work.

5.2.7 Differential Thermal Analysis

The same methods as described in Section 4.2.8 were used. In most cases, only the pastes with initial water/cement ratio equal to 0.32 were examined.

5.2.8 Scanning Electron Microscopy

The apparatus and coating techniques described in Section 4.2.9 were also used in this work.

5.2.9 Non-Evaporable Water Content

The same methods and calculations previously described in Section 4.2.10 were used in this work.

5.3 QUANTIFICATION OF PASTE PHASES

5.3.1 Unhydrated Slag

The difficulties in determining quantities of unreacted slag were discussed Section 4.3.1. In this work, the unreacted slag was estimated by difference after all other phases were determined.

5.3.2 Unreacted Portland Cement

The quantity of unreacted portland cement was determined in most cases by the QXRD method described in Section 4.3.2. However, in some cases, the small quantities of portland cement combined with overlap by the 2.75Å peak of crystalline C_3MS_2 made the measurement of the 2.77Å peak of alite difficult. For these cases, an alternate calibration equation was developed using the intensity 2.60Å (34.45°2θ) peak of alite. Equation 5.1 was calculated by linear regression of four mixtures.

$$PC \text{ (per cent)} = 29.583 \, (I_{2.60Å} / I_{3.15Å}) + 0.2 \qquad (5.1)$$

$$(R \doteq 0.997, \; SE = \pm 1.3)$$

Both Equations 4.7 and 5.1 gave similar results for pastes in which both peaks could be measured.

5.3.3 Calcium Hydroxide

From previous experience, for example as shown in Figure 4:8, calcium hydroxide was not expected to be detectable at the 60/20/20 binder combination chosen for this study. However, the calcium hydroxide content of the control pastes was determined using Equation 4.7.

5.3.4 Unreacted Silica Flour

In order to bring the task within manageable limits, the extraction technique described in Section 4.3.3 was not adopted. However, using the values obtained by extraction on pastes in Chapter 4, together with their XRD relative intensity data, an excellent XRD calibration curve was obtained for the peak height intensity of the major 3.435Å (26.65^{o} / 2θ, CuKα) reflection of quartz relative to the 3.153Å peak of the CaF_2 standard. In addition, several of the pastes in this study were checked by the extraction technique, resulting in 28 data points for the calculation of Equation 5.2.

Silica Flour (Weight per cent) = 2.9 + 3.674 (I3.345Å / I3.153Å CaF_2) (5.2)
(R=0.992, SE=±2.1)

Where the unreacted silica flour content was checked by the extraction technique, the value obtained by extraction was reported in the results.

5.3.5 C-S-H and Tobermorite Contents

The QXRD method described in Section 4.3.7.2 was also used in this work. However as shown in Table 3.3, some of the slags used in this study contained substantial quantities of crystalline melilite. These crystalline peaks remained in the autoclaved pastes and the 201 (Miller indices) melilite was found to overlap the 3.07Å C-S-H peak. In these cases the intensity ratios of the 201 to the 211 melilite peaks were determined from XRD traces of the original slags. Then using these ratios, together with the 211 peak intensities found in the

pastes, the proportion of the 3.07Å reflections due to the overlapping 201 peaks were determined and the C-S-H intensities corrected. This method of correcting for overlapping peaks was also used by Midgley (1976).

Amorphous C-S-H could only be determined as described in Section 4.3.7.3. However, from the results of Chapter 4, it was not expected to be a major component at the 60/20/20 binder combination used in this work. For the 0/70/30 control paste, the amorphous C-S-H could be estimated by difference.

5.4 RESULTS

5.4.1 Strength Tests

The equivalent cube compressive strengths are given in Table 5.2. The average coeffieients of variation were 8.1, 8.9 and 7.0 per cent for W/C equal to 0.28, 0.32, and 0.40 respectively. The modulus of rupture tensile strengths are given in Table 5.3 along with tensile to compressive strength ratios. The average coefficients of variation for these tests results were 9.5, 8.5 and 8.7 per cent for W/C equal to 0.28, 0.32, and 0.40 respectively. The coefficients of variation for both sets of tests are on the high side, but study of the literature suggests that this is common with very small specimens (Mathews and Baker, 1976; Crennan et al, 1977).

Comparing compressive strengths for paste Series 9 and 19, it can be observed that the sulphate resistant portland cement reduced strengths by an average of 12 per cent. From paste Series 13 (glass content GLX = 10 per cent) the drastic reduction in strength caused by devitrigication can be observed. Comparison of the results for paste Series 9 and 14 (GLX = 76 and 93 per cent respectively), which contained slags of approximately the same chemical composition and had similar compressive strengths, showed that while vitrification is important for reactivity, a higher glass content is not necessarily indicative of higher strength potential as was also observed by Demoulian and co-workers (1980). As Fierens (1979) cautioned, differences in minor oxides resulting from remelting slag Number 14 may also have influenced strength. However, the only significant

TABLE 5.2

EQUIVALENT CUBE COMPRESSIVE STRENGTHS OF PASTES

PASTE	COMPRESSIVE STRENGTHS (MPa)		
SERIES	A	B	C
1	74.1	66.3	49.0
2	90.3	78.8	59.7
3	69.8	63.4	52.5
4	89.8	79.6	62.5
5	76.7	73.7	55.8
6	86.2	77.2	58.3
7	76.5	71.0	58.8
8	55.0	55.6	46.1
9	96.6	81.2	61.3
10	85.7	71.2	52.9
11	99.2	83.2	64.1
12	62.5	57.4	41.9
13	23.6	20.9	15.3
14	99.8	89.4	64.5
15	91.8	77.7	64.1
16	80.3	71.2	54.5
17	89.5	75.5	62.0
18	102.7	94.1	66.5
19	83.9	71.0	54.7
C	76.4	61.5	40.1

TABLE 5.3

MODULUS OF RUPTURE TENSILE STRENGTHS OF PASTES

PASTE	MODULUS OF RUPTURE (MPa)			FRACTION OF COMPRESSIVE STRENGTH		
SERIES	A	B	C	A	B	C
1	12.5	10.5	8.9	.169	.158	.182
2	13.5	11.6	8.3	.150	.147	.139
3	12.8	12.9	10.9	.183	.203	.208
4	19.2	20.3	14.1	.214	.255	.226
5	12.1	10.9	8.8	.158	.148	.158
6	13.4	11.4	10.2	.155	.148	.175
7	13.4	11.8	9.8	.175	.166	.167
8	10.5	10.8	8.8	.191	.196	.191
9	15.4	14.1	10.4	.159	.174	.170
10	14.8	13.0	9.4	.173	.183	.178
11	21.0	17.0	12.6	.212	.204	.197
12	9.9	9.5	6.5	.158	.166	.155
13	6.1	5.3	4.1	.292	.254	.268
14	13.9	13.3	10.3	.139	.149	.160
15	16.8	15.7	10.4	.183	.202	.162
16	20.3	17.1	12.6	.253	.240	.231
17	14.1	11.4	10.3	.158	.151	.166
18	-	-	-	-	-	-
19	14.3	13.3	10.0	.170	.187	.183
C	3.7	3.2	2.8	.048	.052	.070

chemical change noted from Table 3.2 was the reduction in sulphur content from 1.83 to 0.53 per cent and this was not considered a major influencing factor on strength, for reasons given later in Section 5.5.3.

As shown in Table 5.3, the tensile to compressive strength ratios for the control pastes (0/70/80) were only a fraction of the 60/20/20 paste ratios.

5.4.2 Paste Density

The solid densities of the dried pastes obtained by methanol displacement, are given in Table 5.4. The solid densities for most of the pastes obtained by helium comparison pycnometry are also given. The close correspondence between the two methods was also found by Feldman (1972).

Due to the smaller diameter of helium molecules, it might be expected that solid densities obtained using helium would be higher than those obtained by methanol displacement. However, as mentioned in Section 5.2.5, these densities were calculated using the solid volumes obtained just after introduction of helium to the sample (after 2m, Feldman, 1972). Small pores, that helium did not fill "instantaneously", were regarded as part of the solid. As shown by Beaudoin and Feldman (1978), helium, due to its small molecule, will continue to flow or diffuse into very small and/or blocked pore space for periods of 48h or more. Therefore, helium will eventually flow into smaller pores than methanol, but helium "instantaneous" densities do not reflect this. For example, the specific gravities after 50h helium inflow were found to

TABLE 5.4

SOLID DENSITIES OF DRIED PASTES USING METHANOL AND HELIUM AS FLUIDS

	DENSITY BY METHANOL DISPLACEMENT			DENSITY BY HELIUM DISPLACEMENT		
PASTE SERIES	($kg/m^3 \times 10^{-3}$) A	B	C	($kg/m^3 \times 10^{-3}$) A	B	C
1	2.30	2.31	2.33	nd*	nd	nd
2	2.30	2.29	2.39	nd	2.33	nd
3	2.26	2.21	2.35	nd	nd	nd
4	2.24	2.21	2.24	2.29	2.23	2.24
5	2.45	2.48	2.49	2.43	2.45	2.53
6	2.36	2.41	2.41	2.28	2.31	2.29
7	2.33	2.31	2.35	2.29	2.27	2.31
8	2.38	2.38	2.38	2.28	2.28	2.28
9	2.35	2.37	2.40	2.32	2.33	2.30
10	2.30	2.38	2.38	2.33	2.35	2.35
11	2.22	2.20	2.30	nd	nd	nd
12	2.41	2.41	2.35	2.41	2.41	2.35
13	2.67	2.63	2.61	2.64	2.60	2.58
14	2.31	2.33	2.31	2.28	2.30	2.26
15	2.21	2.26	2.28	nd	nd	nd
16	2.19	2.15	2.16	nd	nd	nd
17	2.19	2.17	2.24	nd	nd	nd
18	2.33	2.39	2.46	2.32	2.33	2.37
19	2.39	2.39	2.40	2.37	2.36	2.38
C	2.44	2.38	2.42	2.31	2.31	2.29

*nd= not determined

be 2.58 for Paste 7B, 2.77 for Paste 13B, 2.57 for Paste 18B, and 2.42 for Paste CB. However, the size of pore spaces filled by helium after this inflow period would be much smaller than detectable by mercury intrusion and could only be measured by adsorption techniques.

While inclusion of the densities obtained by helium displacement in Table 5.4 was thought to be valuable as a confirmation of the accuracy of values obtained by the methanol displacement technique (which was also used to calculate the apparent porosities), only the methanol displacement densities are referred to in subsequent discussion.

The average coefficient of variation for the methanol displacement technique was found to 1.2 per cent. The differences between the solid densities of the different pastes could either be attributable to the type of hydration product formed or to the degree of hydration. In this light, it is instructive to review the published specific gravities of some of the common hydrated compounds, for example; 11Å tobermorite= 2.42 to 2.46, C-S-H(I) = 2.0 to 2.2, xonotlite = 2.71, αC_2SH= 2.80 and C_3S hydrate = 2.56. (Taylor, 1964). In general, the specific gravities of the hydrated components are less than those of the unreacted materials, which were given in Tables 3.2, 4.1 and 5.1.

As exhibited by the high densities of pastes containing slag Number 13, the devitrified slag, densities were obviously affected by the low degree of hydration. The influence of the degree of hydration on the paste solid densities is shown indirectly in Figure 5.3. From discussions in Chapters 2 and 3, the glass content of slags was thought to be the dominant factor influencing reactivity, and since

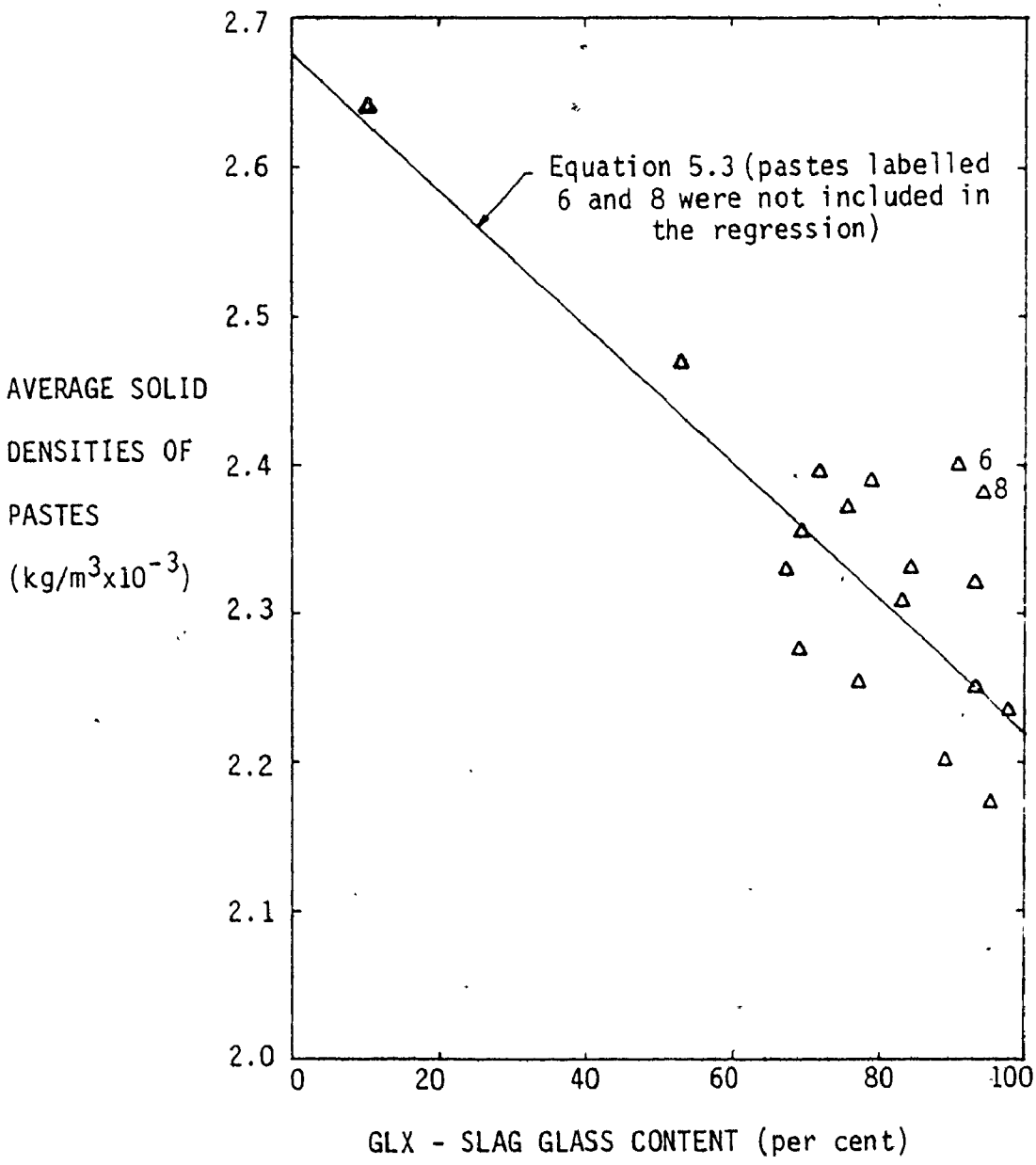

FIGURE 5.3: RELATIONSHIP BETWEEN AVERAGE SOLID DENSITIES OF DRIED PASTES (BY METHANOL DISPLACEMENT) AND GLASS CONTENTS (QXRD METHOD) OF THEIR CONSTITUENT SLAGS

the paste binders contained 60 per cent slag, the slag glass contents were used as a measure of the degree of hydration in Figure 5.3.

Linear regression analysis of the average paste densities with the glass contents of their constituent slags resulted in the relationship given by Equation 5.3.

$$\text{Paste Density} = 2.676 - 0.0046\ (\text{GLX}) \qquad (5.3)$$

$(R = -0.856,\ SE = \pm 0.061)$

The values for the pastes containing slags Number 6 and 8 were not included in the regression. Both these slags from foreign sources had much different chemical compositions than the others with higher alumina and lower magnesia contents. Substitution of the GMAC glass contents for the GLX values resulted in a similar trend, with the correlation coefficient equal to -0.781.

Therefore it was concluded that while the specific gravities of the hydration products maybe an influencing factor on the observed paste densities, the major factor appears to be the degree of hydration of the pastes as controlled by the reactivity of the slag.

5.4.3 Paste Porosity

The apparent porosities obtained by methanol displacement are given in Table 5.5. The average coefficient of variation for the technique was found to be 2.4 per cent.

In the early part of this experimental program, it was found that prolonged, moist storage of the autoclaved paste specimens, between the time of strength testing and preparation for porosity testing resulted in additional hydration reactions. This resulted in abnormally low densities and porosities due to these hydration products filling in and also blocking pore space. (All of these pastes were re-made and re-tested.) Mercury intrusion porosimetry showed these re-hydrated pastes to have very fine pore size distributions (almost all less than 0.009μm diameter). This has only been mentioned since it was thought that this might be of interest for future research, as the very fine pore size distributions could be indicative of high mechanical strengths.

The pore size distributions for some pastes were obtained by mercury intrusion porosimetry and these are plotted in Figure 5.4. Except for paste 13B, made from the devitrified slag, and the control paste, CB, it can be seen by the steep slopes at 30Å that much of the pore space is smaller than 30Å in diameter. Therefore the generally lower total porosity values obtained by mercury porosimetry are explained by the ability of methanol to penetrate pores with diameters smaller than 30Å. Adsorption techniques would have to be employed to obtain pore size distributions smaller than those obtainable by mercury intrusion. The coarse pores of the control paste, acting as Griffeth cracks, are

TABLE 5.5

PASTE POROSITIES

PASTE SERIES	APPARENT POROSITY (PER CENT)		
	A	B	C
1	28.5	31.2	40.4
2	27.0	29.7	40.0
3	25.5	29.7	40.6
4	26.3	29.1	38.5
5	30.1	35.5	43.6
6	27.9	33.6	40.9
7	26.6	30.4	39.5
8	30.9	33.9	39.9
9	27.6	32.1	40.5
10	27.7	34.3	41.1
11	26.2	27.4	37.3
12	33.4	36.6	42.1
13	39.9	42.2	48.3
14	28.3	31.5	38.1
15	27.4	31.8	38.2
16	23.3	26.3	34.0
17	27.3	29.3	36.3
18	26.9	32.0	43.9
19	28.9	33.5	39.8
C	27.4	32.4	38.1

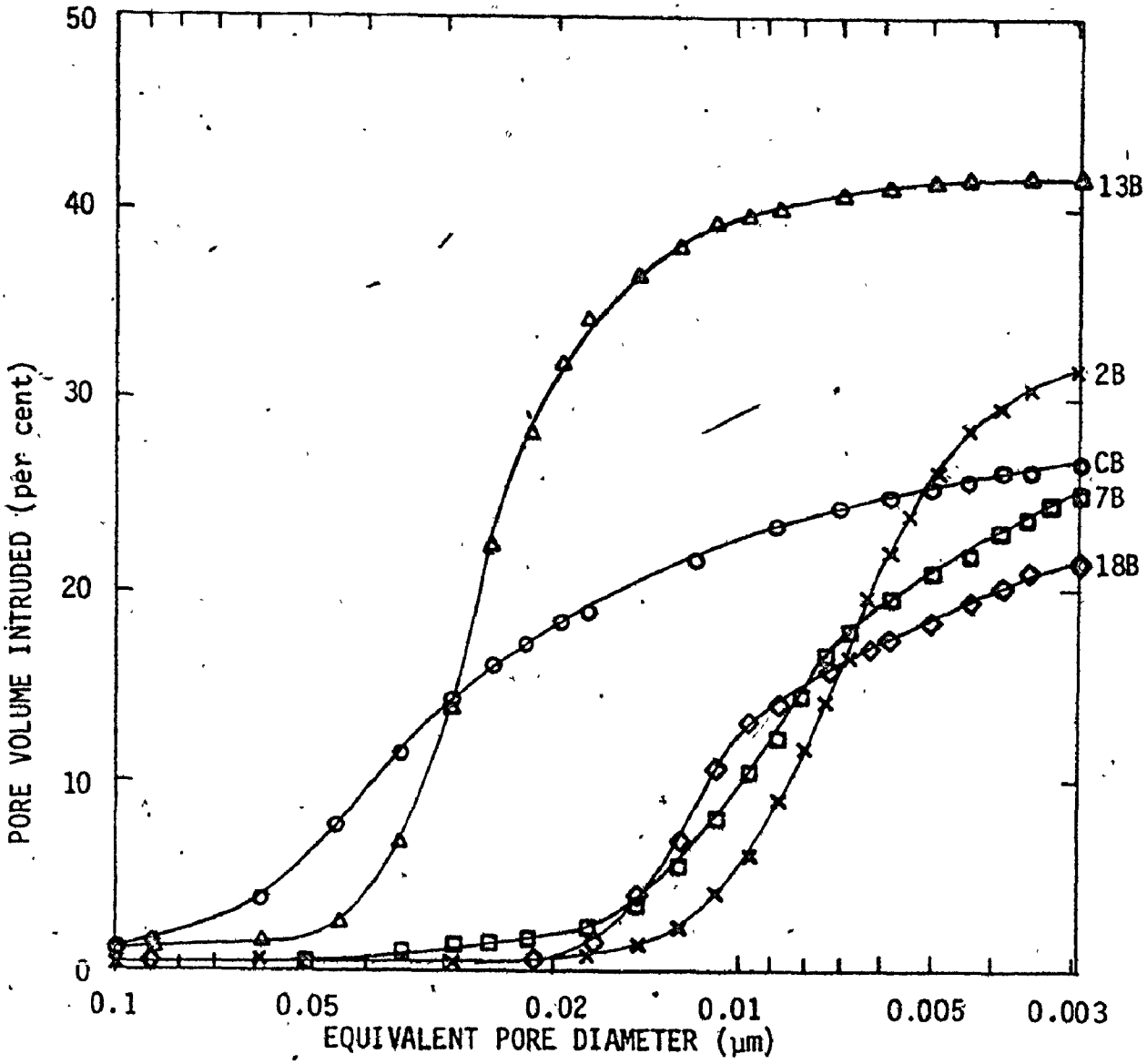

SYMBOL	PASTE	VOLUME INTRUDED AT 413MPa PRESSURE (per cent)
×	2B	31.72
□	7B	25.35
△	13B	41.73
◇	18B	21.80
○	CB	26.88

FIGURE 5.4: MERCURY INTRUSION PORE SIZE DISTRIBUTIONS OF SELECTED PASTES

likely responsible for its lower tensile strengths.

The low compressive strength of paste 13B is reflected in its coarse pore size distribution. Similarities can be seen with the distribution of the control paste CB. These curves are almost identical at pore diameters smaller than 0.01μm. The three pastes containing quenched slags have very similar distributions and much smaller pore size distributions than the control paste. Due to the similarity in distributions between pastes 2B, 7B, and 18B, it is considered likely that the other pastes of 60/20/20 composition with W/C equal to 0.32 would be the same.

5.4.4 Strength-Porosity Relationships

It is well known that porosity has a major influence on strength (Powers and Brownyard, 1948; Beaudoin and Feldman, 1975; Roy and Gouda, 1975), which was the reason for mixing each paste at three water/cement ratios and hence three different porosities. The porosity data in Table 5.5 indicates that the paste porosities at a single water/cement ratio vary over a fairly wide range. Therefore it was decided, in order to minimize porosity effects during subsequent analyses to determine whether strength development is dependent on slag properties, to interpolate the strengths for each set of pastes to a constant porosity value. This was accomplished by combining the porosity values with the logarithm of the corresponding strength values using least squares, linear regression analysis to obtain strength-porosity equations, as used by Beaudoin and Feldman (1975), of

$S = S_0 \exp(-m \cdot p)$ or re-written as,

$$\log S = \log S_0 + m \cdot p \qquad (5.4)$$

where, S = strength

S_0 = the potential strength at zero porosity (Y intercept)

p = porosity

m = slope of the line

The three point, line equation coefficients relating porosity to compressive strength (fc) for each paste series are given in Table 5.6. In a similar fashion, the modulus of rupture (MR) strength-porosity equation coefficients were calculated as given in Table 5.7.

The comparison of zero-porosity strengths (fc_0, MR_0) for each set of pastes was thought to be inappropriate since it has been shown elsewhere (Feldman and Beaudoin, 1974; Roy and Gouda, 1975), that the linear strength-porosity relationship, while valid over a wide range of porosities, does not hold true for porosities approaching zero. Also, inaccuracies in the data used to form the equations would be magnified by the extrapolation of strength values to zero porosity. Therefore a porosity more typical of the autoclaved pastes, 30 per cent, was chosen to provide strength comparisons at a constant porosity. These values were obtained using the equations described and are also shown in Tables 5.6 (fc_{30}) and 5.7 (MR_{30}).

TABLE 5.6

COMPRESSIVE STRENGTH - POROSITY EQUATION COEFFICIENTS AND INTERPOLATED STRENGTH AT 30 PER CENT POROSITY

PASTE SERIES	fc_o (MPa)	m*	R	fc_{30} (MPa)
1	195.2	-0.01488	-0.999	69.8
2	200.8	-0.01324	-0.992	80.5
3	111.2	-0.00806	-0.998	63.7
4	187.7	-0.01246	-0.994	79.4
5	165.6	-0.01060	-0.957	79.6
6	206.3	-0.01323	-0.985	82.7
7	132.0	-0.00888	-0.9999	71.5
8	109.3	-0.00924	-0.927	57.8
9	252.4	-0.01521	-0.999	88.3
10	236.7	-0.01565	-0.992	80.3
11	228.8	-0.01490	-0.951	81.7
12	310.1	-0.02049	-0.986	75.3
13	184.0	-0.02237	-0.9999	39.2
14	364.5	-0.01966	-0.997	93.7
15	225.1	-0.01434	-0.998	83.6
16	184.5	-0.01560	-0.999	62.8
17	238.9	-0.01628	-0.964	77.6
18	211.8	-0.01138	-0.994	96.5
19	263.1	-0.01710	-0.999	80.8
C	414.0	-0.02631	-0.989	67.2

* using logarithms to the base 10

TABLE 5.7

MODULUS OF RUPTURE - POROSITY EQUATION COEFFICIENTS AND INTERPOLATED STRENGTH AT 30 PER CENT POROSITY

PASTE SERIES	MR_o (MPa)	m*	R	MR_{30} (MPa)
1	24.9	-.01122	-0.949	11.5
2	34.9	-.01566	-0.994	11.8
3	17.6	-.00504	-0.951	12.4
4	43.4	-.01247	-0.935	18.3
5	25.0	-.01034	-0.997	12.2
6	23.5	-.00900	-0.984	12.6
7	24.7	-.01023	-0.992	12.2
8	21.5	-.00952	-0.879	11.2
9	37.2	-.01354	-0.991	14.6
10	39.1	-.01474	-0.973	14.1
11	55.3	-.01734	-0.947	16.7
12	56.2	-.02198	-0.960	12.3
13	38.0	-.00200	-0.996	9.5
14	35.0	-.01381	-0.982	13.5
15	62.0	-.01991	-0.959	15.7
16	55.1	-.01894	-0.996	14.9
17	29.6	-.01284	-0.872	12.2
18	-	-	-	-
19	10.1	-.00429	-0.949	13.6
C	7.5	-.01129	-0.998	3.4

* using logarithms to the base 10

5.4.5 Non-Evaporable Water Content

The non-evaporable water content determinations are given as per cents of the ignited pastes in Table 5.8. Several pastes were checked for CO_2 contents but the values obtained were found to be approximately the same as the CO_2 contents expected for the anhydrous binder materials. Corrections for the CO_2 contents of the binder materials were already included in the calculation of Wn using Equation 4.5.

Also given in Table 5.8 are the non-evaporable water contents of the pastes (expressed as fractions) divided by their water/cement ratios (Wn/Wo*). This ratio was used by Powers and Brownyard (1948) as a preliminary attempt to relate paste properties to strength as given by Equation 5.5.

$$fc = A(Wn/Wo) + B \qquad (5.5)$$

The rationale for using this relationship was that strength had been observed to increase with both Wn and the inverse of Wo. In the hydration of calcium silicates, Wn values are a reliable index of the C-S-H content. As shown in Section 5.5.4, Wo(W/C) is a determining factor governing the paste porosities. The Wn/Wo parameter is a convenient method of evaluating the physical properties of pastes but it lacks the rational basis of Powers' gel/space ratio (Powers and Brownyard, 1948) or Mills' (1966) adaptation of the C parameter. The ratio Wn/Wo has the merit of convenience when used as a basis for comparison of performance and even the gel/space ratio concept has limitations at low porosities (Roy and Gouda, 1975).

* Wo was the term adopted by Powers and Brownyard(1948) for the water/cement ratio corrected for the effects of bleeding. In this work, Wo was approximated by W/C.

TABLE 5.8

NON-EVAPORABLE WATER CONTENTS OF PASTES

PASTE SERIES	Wn (per cent of ignited weight) A	B	C	Wn/Wo ((Wn/C)/(W/C)) A	B	C
1	5.25	5.90	6.50	.188	.184	.163
2	7.31	6.81	9.48	.261	.213	.237
3	5.04	6.15	7.16	.180	.192	.179
4	6.19	6.59	8.15	.221	.206	.204
5	8.56	9.20	8.76	.306	.288	.219
6	5.63	6.13	7.14	.201	.192	.179
7	7.78	8.59	8.39	.278	.268	.210
8	4.88	5.44	6.27	.174	.170	.157
9	6.13	7.06	7.09	.219	.221	.177
10	6.15	7.07	7.85	.278	.221	.196
11	7.19	8.14	8.87	.257	.254	.222
12	3.21	3.78	3.78	.115	.118	.095
13	1.91	2.57	2.35	.068	.080	.059
14	6.69	6.81	8.61	.239	.213	.215
15	6.70	7.24	7.88	.239	.226	.197
16	7.25	8.11	9.35	.259	.253	.234
17	7.85	8.60	9.33	.280	.269	.233
18	7.55	7.96	8.94	.270	.249	.224
19	6.31	6.74	7.79	.225	.211	.195
C	10.23	11.41	11.82	.365	.357	.296
C*	9.53	10.83	11.12	.340	.338	.278

* corrected for CH contents as given in Section 5.4.7

Limitations to the use of this relationship are that a positive value of the coefficient B in Equation 5.5 implies either a finite strength for Wn/Wo equal to zero (i.e. no hydration) and a negative value for B implies negative strength below a certain value of Wn/Wo. For these reasons, Powers and Brownyard (1948), who had found a negative value for B, later abandoned this approach.

However, inspite of these limitations, it was thought that it would be of interest to evaluate the equation coefficients for the pastes in this work for comparison to those of Powers and Brownyard since they had concluded from tests of a single autoclaved portland cement-quartz paste that this relationship must change progressively as the curing temperature was raised. The Wn/Wo values obtained for the pastes in this study were plotted with compressive strength in Figure 5.5. With the exception of the control pastes C which were found to contain CH (Section 5.4.7), and the pastes containing slag 12 (which are labelled) there appeared to be a linear relationship. Therefore, with the exception of paste Series 19 and those previously mentioned, the remaining 51 values were used to develop the linear regression coefficients for Equation 5.5. The slope, A, was found to be 290.4 (significant to 0.001) while the value of the intercept, B, was not significantly different than zero (B=7.7). The correlation coefficient was 0.776 with the standard error of estimate equal to 12.3.

This compares with values of the coefficients A = 235.8 and B= -24.8 found by Powers and Brownyard (converted to MPa units for

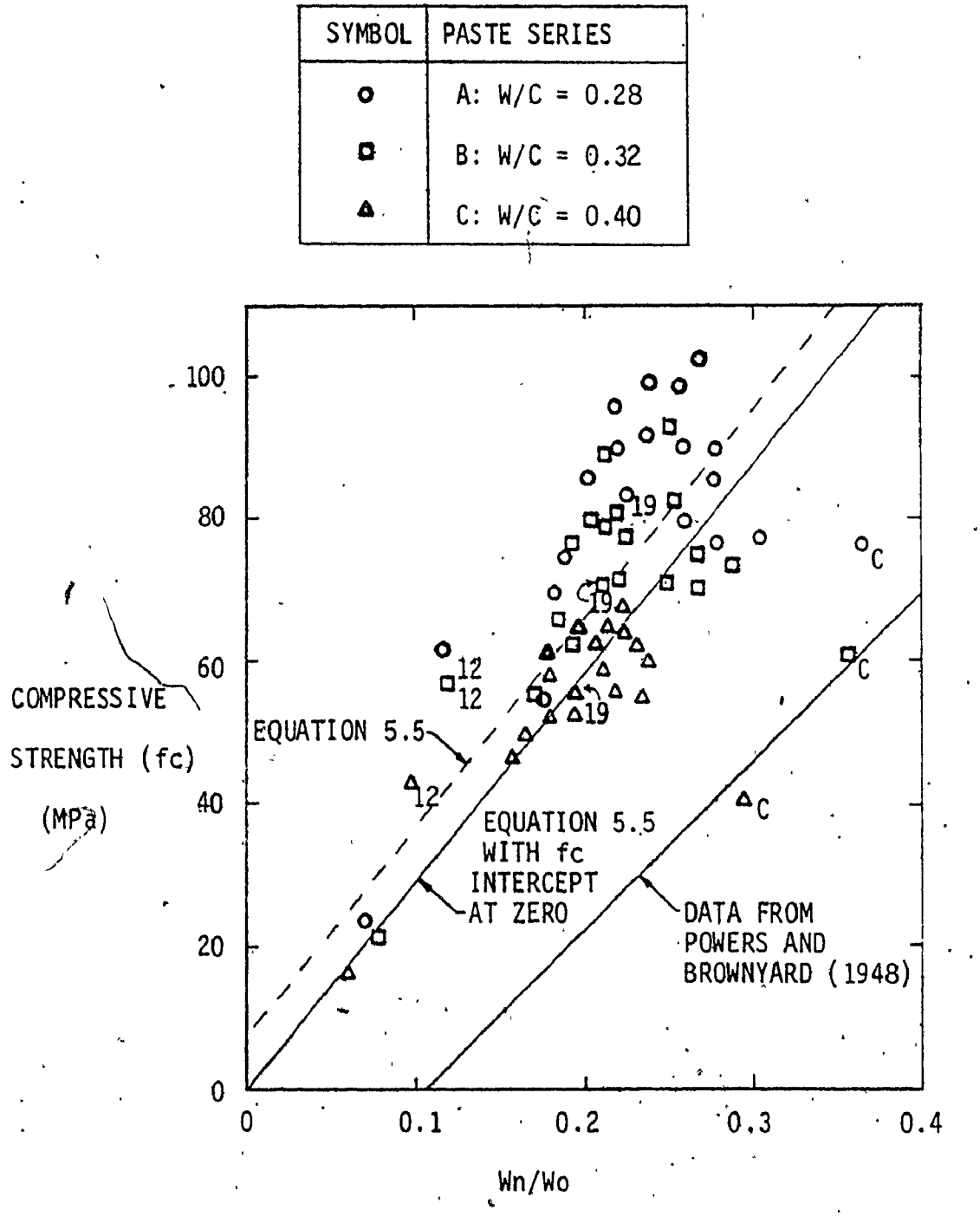

FIGURE 5.5: RELATIONSHIP BETWEEN COMPRESSIVE STRENGTH AND Wn/Wo (Paste series labelled 12, 19, C were not included in the regression)

pastes cured at about 22°C. The slope of Equation 5.5 found in this study was similar to that of Powers and Brownyard. The effect of autoclave curing, together with the effect of the binder composition, was the development of similar strengths at much lower Wn/Wo values than those of portland cement cured at ambient temperatures. This was not unexpected since the relatively well crystallized hydrates formed in autoclave curing, such as 11.3Å tobermorite, contain much less structural (non-evaporable) water than the C-S-H formed at ambient temperatures.

5.4.6 Unreacted Slag

The quantity of unreacted slag which could not be measured directly, as described in Section 5.3.1, was estimated by difference. The results are given in Table 5.14 and the discussion is included in Section 5.4.10.

The crystalline fractions of the slag which were considered non-reactive could be observed ty their peaks in XRD traces of the pastes. As further evidence of the inactivity of crystalline slag, the intensity of the 211 spacing of the crystalline melilite was measured on XRD traces of the series 13 pastes and compared to the intensities expected for the proportion of slag in the pastes. The results are given in Table 5.9.

TABLE 5.9
UNREACTED CRYSTALLINE MELILITE CONTENTS

PASTE	TOTAL SLAG IN PASTE* (per cent)	CRYSTALLINE MELILITE EXPECTED** (per cent)	CRYSTALLINE MELILITE DETECTED BY QXRD (per cent)
13A	58.9	50.3	49.0
13B	58.5	50.0	49.1
13C	58.6	50.0	50.6

The differences between the observed and calculated (assuming no reaction) quantities of crystalline melilite in the pastes were certainly within the error of the technique and it was concluded that crystalline melilite was inactive for the autoclave curing regime adopted and that hydration was only due to the portland cement and quartz fractions.

5.4.7 Unreacted Portland Cement and Calcium Hydroxide

Only very small quantities of unreacted alite could be observed in the XRD traces, making it difficult in many cases to distinguish the small peaks from the background. The results are given in Table 5.10 along with the fraction of portland cement reacted. This was calculated by taking the difference between the original portland cement content in the paste binder (corrected for the non-evaporable water content of the paste) and the unreacted quantity expressed as a fraction of the original portland cement content.

*Corrected for the non-evaporable water contents of the paste.
**From Table 3.4, Slag 13 contained 85.4 per cent crystalline melilite.

TABLE 5.10

UNREACTED PORTLAND CEMENT CONTENT OF PASTES

PASTE SERIES	UNREACTED PORTLAND CEMENT (PER CENT) A	B	C	FRACTION OF PORTLAND CEMENT REACTED A	B	C
1	4.7	1.4	0.9	.753	.926	.952
2	6.4	3.0	2.7	.657	.840	.852
3 *	5.0	3.1	6.3	.737	.835	.662
4	6.2	3.1	3.0	.671	.835	.838
5 *	4.3	3.7	4.5	.765	.795	.748
6	5.5	5.2	5.1	.710	.724	.727
7	4.3	5.2	4.4	.768	.718	.762
8 *	5.5	3.9	5.3	.712	.794	.718
9	3.4	2.8	3.4	.820	.850	.818
10 *	6.0	5.6	2.9	.677	.700	.844
11 *	5.0	2.9	4.1	.732	.843	.777
12 *	3.7	3.3	2.6	.809	.829	.865
13	4.7	8.2	4.8	.761	.580	.754
14 *	4.8	3.0	2.7	.744	.840	.853
15 *	5.8	7.4	3.7	.691	.603	.800
16	4.7	7.2	3.8	.748	.611	.792
17	3.5	3.3	5.0	.811	.821	.727
18 *	3.4	4.7	2.9	.817	.746	.842
19	4.0	4.1	4.2	.787	.781	.774
C	20.0	15.4	24.7	.685	.775	.605

* Indicates pastes where the unreacted portland cement was determined using the 2.602Å (34.45° 2θ) calibration Equation 5.1

It can be observed that in almost all cases at least 70 per cent of the portland cement had reacted. Comparison of values for pastes series 9 and 19 indicates a slightly lower degree of reaction for the Type 50 portland cement than for the normal portland cement. However, this may not be significant since the portland cement calibration equations were based on intensities of the normal portland cement. Calcium hydroxide (CH) was only detected in the control pastes and the quantities determined were 2.9, 2.4 and 2.9 per cent for pastes CA, CB and CC respectively.

5.4.8 Unreacted Silica Flour

The silica flour quantities determined using the methods described in Section 5.3.4 are given in Table 5.11. The fraction of reacted silica flour is also given and was determined by the same method as used to calculate the fraction of reacted portland cement in Section 5.4.7. It can be observed that in all the pastes containing slag the majority of the silica flour remained unreacted. This is contrasted with the control pastes, Series C, where approximately 60 per cent of the original 30 per cent content of silica flour did react to form hydration products.

The reacted fraction of silica flour in pastes containing the devitrified slag was much higher than with the vitreous slags. Therefore, it appears that the presence of vitreous slag retarded the reaction of quartz. This is probably due to the reactive amorphous slag competing with quartz for the calcium hydroxide liberated by the portland cement. This agrees with the findings of Kondo and co-workers (1975).

TABLE 5.11

UNREACTED SILICA FLOUR CONTENT OF PASTES

PASTE SERIES	UNREACTED SILICA FLOUR (PER CENT) A	B	C	FRACTION OF SILICA FLOUR REACTED A	B	C
1	14.9*	14.3*	13.9*	.216	.243	.259
2	14.8	15.2*	14.1	.206	.188	.228
3	14.8*	13.6*	14.1*	.222	.277	.243
4	13.6	14.2	13.7*	.278	.243	.259
5	15.3*	15.2*	15.2*	.161	.160	.150
6	14.6*	13.2	13.9*	.229	.300	.255
7	15.6*	15.0*	14.7	.158	.186	.203
8	15.5	13.9	14.2	.187	.267	.245
9	15.2*	14.6*	14.8	.192	.216	.208
10	13.1	14.5*	14.5*	.305	.224	.218
11	16.2*	14.3*	13.6*	.125	.221	.252
12	15.2*	13.8	14.6	.217	.284	.242
13	10.6*	10.5	11.3	.460	.462	.422
14	13.6*	13.5	14.0	.275	.279	.240
15	14.0	14.7*	12.7	.253	.211	.315
16	13.7	14.5*	13.2	.265	.216	.278
17	13.3	11.8	14.9*	.283	.359	.185
18	14.0*	14.4*	14.1*	.250	.255	.232
19	14.8	14.3*	14.5	.213	.235	.219
C	9.1	10.8	10.2	.666	.599	.620

* Indicates values obtained by extraction

5.4.9 C-S-H Contents

The quantities of C-S-H using the average values determined by the 3.07Å (Equation 4.9) and 2.97Å (Equation 4.10) calibration curves are given in Table 5.12. The average difference in C-S-H contents determined by each of the two calibration equations was 1.1 per cent for the 60 pastes. Also given is the degree of crystallinity (Yr) for the 0.32 water/cement ratio (series B) pastes as determined by the empirically derived expression developed by Hara and Midgley (1980) which was given in Equation 4.12. The quantities of C-S-H corrected for the influence of crystallinity, are given in Table 5.13. The assumption was made that the crystallinity of the C-S-H did not vary with the water cement ratio.

Corresponding to the trend found for non-evaporable water contents, the amount of C-S-H increased with increasing water/cement ratios in most cases. The amount of C-S-H determined for the set of control pastes was lower than all pastes containing slag. The discrepancy between this and their high non-evaporable contents is due to the presence of calcium hydroxide found in the control pastes. The surprisingly high C-S-H contents of the Number 13 set of pastes (made with the devitrified slag), are attributed to a higher degree of reaction between the portland cement and silica flour components alone, when the slag was not reactive. This was shown by the low, unreacted silica contents for these pastes, given previously in Table 5.11, and by the uniquely high crystallinity index (Yr = 45.2 per cent) for these hydrates. Paste Series 19, which contained the Type 50 portland cement, had lower C-S-H contents than Series 9. This may responsible for the lower strengths of Series 19.

TABLE 5.12

UNCORRECTED C-S-H CONTENTS AND CRYSTALLINITY INDEX

PASTE SERIES	AVERAGED C-S-H CONTENTS FROM EQUATIONS 4.9 AND 4.10 (per cent) A	B	C	CRYSTALLINITY INDEX-Yr (per cent B
1	6.2	6.4	10.8	8.9
2	8.6	9.3	12.5	15.7
3	5.3	8.5	13.8	27.5
4	8.7	11.4	14.1	11.0
5	6.2	8.8	10.0	20.2
6	11.0	13.8	17.8	12.8
7	7.1	9.3	9.6	18.4
8	9.7	9.3	13.1	15.5
9	10.1	10.0	14.7	16.6
10	12.3	19.9	22.6	13.1
11	8.7	10.4	15.3	11.8
12	12.5	12.7	14.7	23.5
13	11.5	12.9	14.5	45.2
14	9.2	12.6	14.3	7.7
15	7.6	10.0	12.2	19.7
16	12.3	10.6	14.1	10.9
17	12.5	8.3	8.2	10.1
18	6.6	8.4	8.9	17.4
19	7.2	8.4	10.6	26.5
C	4.7	5.4	8.1	11.1

TABLE 5.13

C-S-H CONTENTS OF PASTES, CORRECTED FOR CRYSTALLINITY

PASTE SERIES	CSHc (Weight per cent) A	B	C
1	16.1	16.6	28.1
2	22.4	24.2	32.5
3	13.0	20.8	33.8
4	22.6	29.6	36.7
5	16.1	22.8	26.0
6	28.6	35.9	46.3
7	18.5	24.2	25.0
8	25.2	24.2	34.1
9	26.3	26.0	38.2
10	32.0	51.7	58.8
11	22.6	27.0	39.8
12	31.6	32.1	37.2
13	24.1	27.0	30.4
14	23.9	32.8	37.2
15	19.8	26.0	31.7
16	32.0	27.6	36.7
17	32.5	21.6	21.3
18	17.2	21.8	23.1
19	17.8	20.7	26.2
C	12.2*	14.0*	21.1*

*Not including amorphous C-S-H

Feldman and Beaudoin (1976) concluded that at high porosities, the bonding, and consequently the strength, of well-crystallized material was poor in comparison to poorly-crystallized material of the same porosity. If Pastes 13A and 2C are compared, Paste 13A had the same porosity, 60 per cent less strength and its C-S-H was 2.9 times as crystalline as Paste 2A. The higher degree of crystallization of the C-S-H found in the Number 13 pastes could also be explained by the lower molar C/S ratio of the reactive components, portland cement and quartz. (Chan and Mitsuda, 1978). The C/S ratio would be about 0.57 compared with 0.86 for the total slag portland cement- silica content of the other pastes.

The crystallinity indices (Yr) for the other pastes, including the controls, are much lower, between 7.7 and 23.5 per cent. Partly due to the high crystallinity value for the pastes containing devitrified slag there is strong inverse realtionship between the glass content of the slag used (by QXRD) and Yr, as shown by Equation 5.6.

$$Yr = 45.5 - 0.3655\ (Glass - GLX) \qquad (5.6)$$

$(R = 0.872,\ S.E. = \pm 4.4)$

The amorphous C-S-H contents of the control pastes, estimated by difference, were 55.9, 57.4 and 41.1 per cent for pastes CA, CB and CC respectively.

5.4.10 Summation of Phase Quantities

The quantities determined for the C-S-H, unreacted portland cement and unreacted silica flour contents of each paste were summed, and the differences from one hundred per cent were calculated. These differences, given in Table 5.14, were mainly attributable to the unreacted slag contents of the pastes which could not be determined. However, from the maximum unreacted slag content values (assuming no reaction), which are also given in Table 5.14, it was observed that for 27 of the 57 pastes, unreacted slag could not account for the differences. While this may be due to cumulated errors from the determinations of the other phase quantities, it is more likely due to undetected amorphous C-S-H. The maximum difference unaccounted for was 11.0 per cent, which showed that even a relatively small quantity of amorphous C-S-H could be responsible for these differences.

Amorphous C-S-H was detected qualitatively in the control pastes by the amorphous hump in their XRD patterns and this was assumed to account for the large differences as discussed in Section 4.4.6.2. Amorphous humps were also noted in the XRD patterns of paste series 13, which must have been due to the presence of amorphous C-S-H since Slag 13 was devitrified.

In conclusion, the estimation of the quantity of unreacted slag by difference, after other phase quantities were calculated, was not satisfactory, likely due to the presence of amorphous C-S-H.

TABLE 5.14

UNDETERMINED PASTE CONTENTS AND MAXIMUM POSSIBLE UNREACTED SLAG CONTENT

PASTE SERIES	DIFFERENCE FROM QUANTIFIED PHASES (Weight per cent) A	B	C	SLAG CONTENT ASSUMING NONE REACTED* (Weight per cent) A	B	C
1	64.3	67.7	57.1	57.0	56.7	56.3
2	56.4	57.6	50.7	55.9	56.2	54.8
3	67.2	62.5	46.0	57.1	56.5	56.0
4	57.6	53.1	47.4	56.5	56.3	55.5
5	64.5	58.3	54.3	55.3	54.2	55.2
6	51.3	45.7	34.7	56.8	56.5	56.0
7	61.6	55.6	55.9	55.7	55.3	55.4
8	53.8	58.0	46.4	57.2	56.9	56.5
9	55.1	56.6	43.6	56.5	56.0	56.0
10	48.9	38.2	29.8	55.7	56.0	55.6
11	56.2	55.8	42.5	56.0	55.5	55.1
12	49.5	50.8	45.6	58.1	57.8	57.8
13	60.6	55.5	53.5	58.9	58.5	58.6
14	57.7	50.7	46.1	56.2	56.2	55.2
15	60.4	51.9	51.9	56.2	56.0	55.6
16	49.6	50.7	46.3	55.9	55.5	54.9
17	50.7	63.3	58.8	55.6	55.2	54.9
18	65.4	59.1	59.9	55.8	55.5	55.1
19	62.4	60.9	55.1	56.4	56.2	55.7
C	55.8	52.4	41.1	0	0	0

*Calculation = 60 per cent slag in binder / (1 + Wn/C)

5.4.11 Scanning Electron Microscopy

A limited SEM study of the autoclaved pastes was conducted.

Paste 1 B was examined and a massive, dense hydrate structure with no distinguishing features was generally observed as shown around the unreacted sericite particle in Figure 5.6. The sericite was identified using EDXRA which showed no calcium content but substantial aluminum, potassium and silica contents as indicated. Figure 5.7 of the same paste sample shows the same massive C-S-H background but with an acicular hydrate containing mainly calcium and aluminum. The appearance in similar to ettringite ($C_3A\ 3C\bar{S} \cdot H_{31}$) but any sulphur peak was obscured by the gold peak (from sample preparation) in the EDXRA analysis.

Paste 18B was also examined as shown in Figures 5.8 to 5.10. All three micrographs show unreacted grains of C_2MS_2 surrounded by hydrate shells containing CaO, MgO and SiO_2. The hydrates might be of the form C-M-S-H or separated into C-S-H and M-S-H as reported by Krüger (1976). The hydrates, as is typical in the high vacuum required for SEM operation, have been dessicated and have pulled away from the unreacted grains. In Figure 5.10, which is a magnified section of Figure 5.9, small white particles of possibly hydration products can be observed in surface pits on the unhydrated grain. The micrographs show that the C_2MS_2 glass has reacted and estimation by area measurement indicates that about 0.35 to 0.40 of the grains have reacted. While this measurement is very crude, it is at least an indication of the amount of slag reaction.

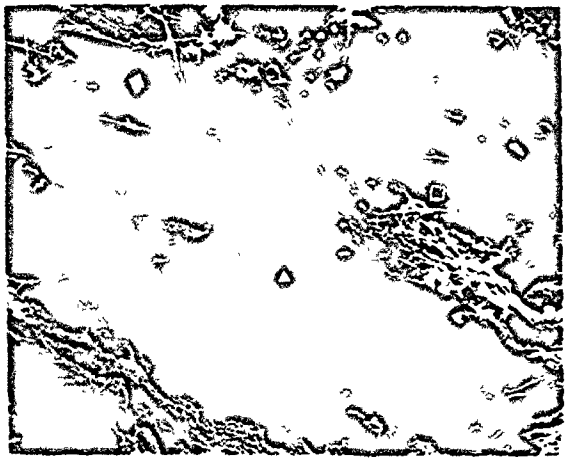

EDXRA ELEMENTAL COUNT RATIOS				
SYMBOL	ELEMENT			
	Ca	Si	Al	K
△	--	1.00	0.62	0.52
▲	--	1.00	0.57	0.45
□	1.68	1.00	--	--

FIGURE 5.6: UNREACTED SERICITE PARTICLE EMBEDDED IN A MASSIVE C-S-H STRUCTURE

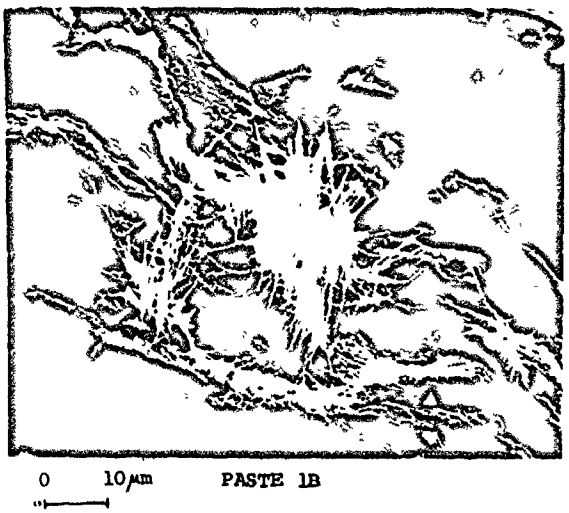

EDXRA ELEMENTAL COUNT RATIOS				
SYMBOL	ELEMENT			
	Ca	Si	Al	S
△	3.82	--	1.00	?
Ettringite	4.46	--	1.00	0.59
▲	1.09	1.00	--	?

FIGURE 5.7: ACICULAR HYDRATES ON TOP OF MASSIVE C-S-H STRUCTURE

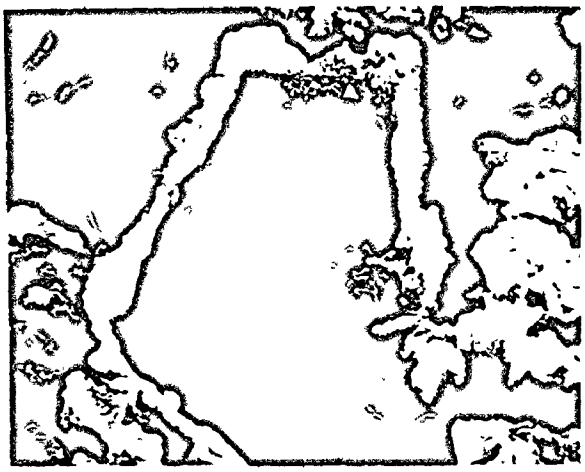

EDXRA ELEMENTAL COUNT RATIOS			
SYMBOL	ELEMENT Ca.	Si	Mg
△	1.11	1.00	0.09
▲	0.43	1.00	0.33
□	0.35	1.00	0.30

FIGURE 5.8: UNREACTED MELILITE PARTICLE SURROUNDED BY HYDRATE SHELL

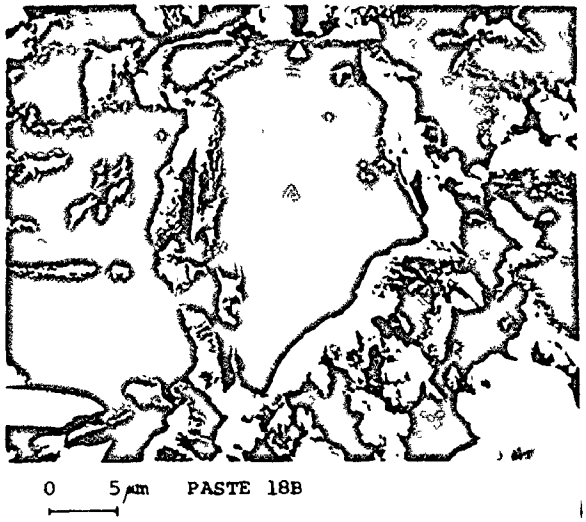

EDXRA ELEMENTAL COUNT RATIOS			
SYMBOL	ELEMENT Ca	Si	Mg
△	1.00	1.00	0.11
▲	0.32	1.00	0.28

FIGURE 5.9: UNREACTED MELILITE PARTICLE SURROUNDED BY HYDRATE SHELL

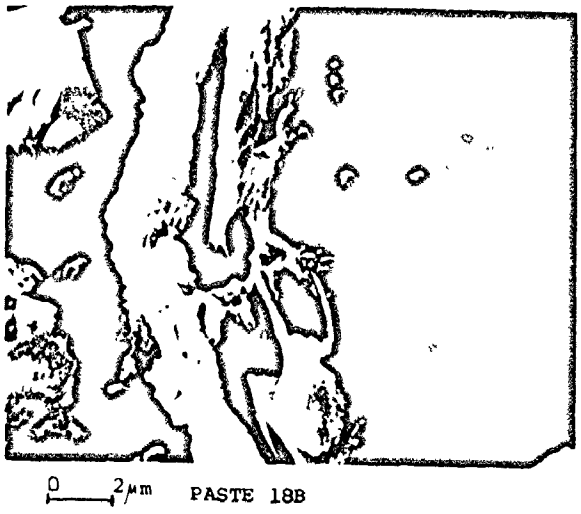

FIGURE 5.10: MAGNIFIED SECTION OF FIGURE 5.9

5.5 REGRESSION ANALYSIS OF SLAG VARIABLES WITH HYDRAULICITY

5.5.1 General

While hydraulic potential can be measured by several parameters, strength development is the parameter of most interest to engineers and is used in this work in most instances. Hydration parameters, such as the quantity of C-S-H found, the fraction of binder materials reacted, or the non-evaporable water contents could alternately be used to evaluate the hydraulic potential of slags.

The multiple linear regression analyses of slag parameters with hydraulic potential indices were performed on the CDC6400 computer using the Statistical Package for the Social Sciences (SPSS). As well as providing the regression coefficients and correlation coefficients for each regression, the level of significance of each coefficient (F significance test) and the standard error of estimate for the equation were calculated. The .05 or 5 per cent level of significance, a commonly used limit, was used to accept or reject variables in the regression analyses.

5.5.2 Slag Glass Content

Linear regression analyses showed slag glass content to be a significant factor contributing to strength development. The correlation coefficients obtained for several methods of glass content determination are given in Table 5.15. As can be observed, the glass contents determined by GLX, GAH, GMAC and GMAC + M all have approximately the same degree of correlation to strengths. The correlation

TABLE 5.15

CORRELATION COEFFICIENTS OF GLASS CONTENTS WITH STRENGTH

GLASS CONTENT METHOD	COMPRESSIVE STRENGTH LEVEL (18 SLAGS)			
	fcA	fcB	fcC	fc_{30}
GLX	0.681	0.723	0.760	0.533
GAH	0.677	0.715	0.765	0.506
GMAC	0.665	0.713	0.759	0.503
GMAC + M	0.625	0.668	0.742	0.438*
GLASS CONTENT METHOD	MODULUS OF RUPTURE (17 SLAGS -NO VALUE FOR PASTE 18)			
	MRA	MRB	MRC	MR_{30}
GLX	0.663	0.670	0.776	0.547
GAH	0.754	0.714	0.779	0.608
GMAC	0.662	0.728	0.779	0.570
GMAC + M	0.613	0.658	0.749	0.434
14 SLAGS - PASTES NUMBER 1, 12, 15 AND 18 REMOVED TO ELIMINATE EFFECTS OF EXTREME VALUES OF FINENESS OF GRINDING				
GLASS CONTENT METHOD	COMPRESSIVE STRENGTH			
	fcA	fcB	fcC	fc_{30}
GLX	0.702	0.750	0.805	0.549
GAH	0.661	0.702	0.757	0.510
GMAC	0.656	0.711	0.766	0.491
GMAC + M	0.632	0.685	0.775	0.452*

* Only significant at the 0.10 level.

coefficients for the GSA, GUV and GUV-N glass content values, determined in Chapter 3, are not given since there were no significant correlations with strength. Therefore, only the glass content methods which had significant correlations with the QXRD standard method (GLX) were related to strength development.

The best correlations were found for compressive strengths of pastes with W/C equal to 0.40 (fcC) while the poorest correlation was found for the strengths interpolated to a constant porosity of 30 per cent (fc_{30}).

The correlations between glass contents and modulus of rupture strengths were not as good, partially due to the larger coefficient of variations for these tests as mentioned in Section 5.4.1.

As also shown in Table 5.15, the removal of pastes containing slags having Blaine finenesses outside of the range 401 ± 9 m^2/kg (Slags Number 1, 12, 15 and 18), had no significant effect on the correlation of glass contents with strengths, except for a slight improvement using GLX values.

It should be noted that in all regression analyses of glass contents with strengths, the devitrified slag, Number 13, had a large effect on the correlation coefficients, owing to the relatively narrow range of glass contents for most of the other seventeen slags. However, had more slags with relatively low glass contents been available for study, the trends observed would almost certainly have been the same.

5.5.3 Glass Content and Chemical Composition

Many standard specifications for slags specify minimum values of chemical oxide moduli as methods of quality control and several other composition moduli have been developed as indices of slag reactivity. Several of these moduli were given in Section 2.3.3. For example, West Germany's DIN1164 :1967 standard and Canada's CSA-A363 M77 preliminary standard both contain the compositional requirement given previously by Equation 2.5.

$$M6 = (C + M + A) / S \geq 1.0 \qquad (2.6)$$

Therefore as a preliminary analysis, slags with similar (C + M + A) / S oxide ratios were evaluated to see if the strength-glass content relationships discussed in Section 5.5.2 would be improved. It was found as shown in Table 3.2 that nine slags, Numbers 1,2,9,10,11,13, 14,15 and 17, had oxide ratios of 1.605 ± 0.035. Using only these slags, the correlation coefficients of the compressive strength-glass content relationships were much better than those given in Table 5.15. In Table 5.16, the regression coefficients are given for equations of the form:

$$fc\ (MPa) = A(\text{Glass Content}) + B \qquad (5.7)$$

The best correlation coefficients were obtained using the McMaster individual particle analysis glass values, GMAC. The improved correlations between strength and glass content for slags with a constant value of this chemical oxide modulus indicated that chemical composition was also an influencing factor. As a second step in the analyses, the published composition moduli given previously

TABLE 5.16

REGRESSION COEFFICIENTS FOR EQUATION 5.7 FROM REGRESSION OF NINE SLAGS WITH CONSTANT (C+M+A)/S OXIDE RATIOS

PASTE STRENGTH EVALUATED	EQUATION COEFFICIENTS			
	A	B	R	SE
	(a) Glass Content by GLX:			
fcA	0.848	21.4*	0.912	10.4
fcB	0.727	18.4*	0.922	8.3
fcC	0.566	13.4*	0.918	6.7
fc_{30}	0.530	38.5	0.861	8.5
	(b) Glass Content by GMAC:			
fcA	0.891	22.9	0.970	6.2
fcB	0.762	19.9	0.978	4.5
fcC	0.582	15.3	0.955	5.0
fc_{30}	0.579	37.9	0.953	5.1
	(c) Glass Content by GAH:			
fcA	13.34	21.3	0.951	7.9
fcB	11.16	19.6	0.938	7.5
fcC	8.90	13.3	0.957	4.9
fc_{30}	8.11	39.4	0.874	8.2

* Only significant at the .10 level

in Equations 2.1 to 2.12 (m1 to M12) were evaluated with respect to relationships with compressive strength. Individually none of these moduli or groups of oxides showed any significant correlation with strength, even when the devitrified slag, Number 13, was removed from the regression analyses. Most of the moduli were developed assuming complete vitrification but in industrially quenched slags, complete vitrification is seldom achieved as exemplified by the results given in Table 3.3. Therefore, in agreement with Krüger (1976), it was concluded that the glass content must be taken into account when assessing the hydraulic potential of industrial slags using compositional moduli.

The moduli based solely on chemical composition, M1 to M12, were then evaluated together with slag glass contents in multiple regression analyses with compressive strengths. The McMaster individual particle analysis (GMAC) glass values were used since better correlation coefficients were obtained then with the other methods, as shown in Table 5.15. Of the twelve moduli, only M3 and M5 were found to contribute significantly to the correlation with strengths. The correlation coefficients are given in Table 5.17. The correlation coefficient for Modulus M13,which included glass content and M5, is also given as well as for GMAC alone.

TABLE 5.17
CORRELATION COEFFICIENTS FOR MODULI AND GLASS CONTENT

VARIABLES	STRENGTH LEVEL			
	fcA	fcB	fcC	fc_{30}
GMAC, M3	0.852	0.914	0.891	0.834
GMAC, M5	0.784	0.858	0.875	0.750
M13(GMAC included)	0.785	0.842	0.864	0.778
GMAC	0.665	0.713	0.759	0.503

It was interesting to note that the modulus M6 was not significant in this analysis even though the glass content-strength relation was shown previously to be improved by maintaining a constant value of this modulus.

Combining the product of GMAC and M5 values together with GMAC values yielded equations similar to the modulus M12 developed by Parker and Nurse and the coefficients are given in Table 5.18 for an equation of the form:

$$fc\ (MPa) = A(GMAC)\cdot(M5 - B) + C \qquad (5.8)$$

TABLE 5.18
COEFFICIENTS FOR EQUATION 5.8

STRENGTH LEVEL	A	B	C	R	SE
fcA	2.22	0.911	26.0	0.804	12.2
fcB	1.99	0.91	22.9	0.863	8.6
fcC	1.32	0.57	17.5	0.872	6.3
fc_{30}	2.06	1.02	42.4	0.778	9.2

While the regression coefficients in Table 5.18 were slightly better than the coefficients given Table 5.17 for M13 and GMAC with M5 in most cases, the best correlation coefficients were for GMAC combined with modulus M3 ((C + M) / (S + A)).

As the next step in the analysis, it was decided to leave the published compositional moduli and evaluate the effect of individual oxide contents of the slags (Table 3.2) in combination with glass contents on strength development. From these multiple regression analyses, the best correlations found for all strength levels, with coefficients which were significant to at least the 5 per cent (or 0.05) level, were for the glass, MgO and CaO contents as shown in Table 5.19 for equations of the form:

$$fc\ (MPa) = A(\text{Glass Content}) + B(MgO) + C(CaO) + D \qquad (5.9)$$

In individual cases for a particular glass content method or strength level, the inclusion of some minor components such as K_2O, Mn, Fe and S significantly improved the correlation coefficients. However, since these components were not significant in all cases, they are not included in the results.

Of the glass content determinations evaluated in Equation 5.9, the best correlations with compressive strengths at each water/cement ratio were for the McMaster-GMAC glass values and the calculated strengths using the GMAC values are plotted against actual strengths in Figures 5.11 and 5.14. The correlation with constant porosity strength values was not as good as with the strength values at each W/C. The correlations with the modulus of rupture values are not given

TABLE 5.19

REGRESSION EQUATION COEFFICIENTS FOR EQUATION 5.9
(FOR PASTE SERIES 1 TO 18)

GLASS CONTENT METHOD	EQUATION COEFFICIENTS					
	A	B	C	D	R	SE
	(a) Compressive Strengths at W/C = 0.28 (fcA)					
GLX	0.491	6.656	5.381	-239.6	0.885	9.9
GAH	7.067	6.173	4.787	-216.5	0.895	9.5
GMAC	0.504	6.811	6.655	-290.3	0.907	9.0
GMAC+M	0.648	6.521	7.240	-328.6	0.877	10.2
	(b) Compressive Strengths at W/C = 0.32 (fcB)					
GLX	0.447	5.226	4.885	-210.6	0.909	7.4
GAH	6.290	5.519	4.375	-190.4	0.912	7.2
GMAC	0.467	5.345	6.049	-257.3	0.940	6.0
GMAC+M	0.610	5.048	6.605	-293.9	0.911	7.3
	(c) Compressive Strengths at W/C = 0.40 (fcC)					
GLX	0.371	3.203	2.661	-112.4	0.878	6.3
GAH	5.348	3.422	2.211*	- 94.9*	0.893	6.0
GMAC	0.381	3.320	3.624	-150.7	0.909	5.5
GMAC+M	0.526	3.002	4.116	-183.8	0.898	5.8
	(d) Compressive Strengths at Constant Porosity (fc_{30})					
GLX	0.245	4.874	5.333	-212.4	0.837	8.2
GAH	3.186	5.083	5.312	-202.8	0.826	8.5
GMAC	0.266	4.910	6.178	-238.7	0.858	7.7
GMAC+M	0.320	4.814	6.456	-256.4	0.831	8.4

*Only significant to the 0.74 level

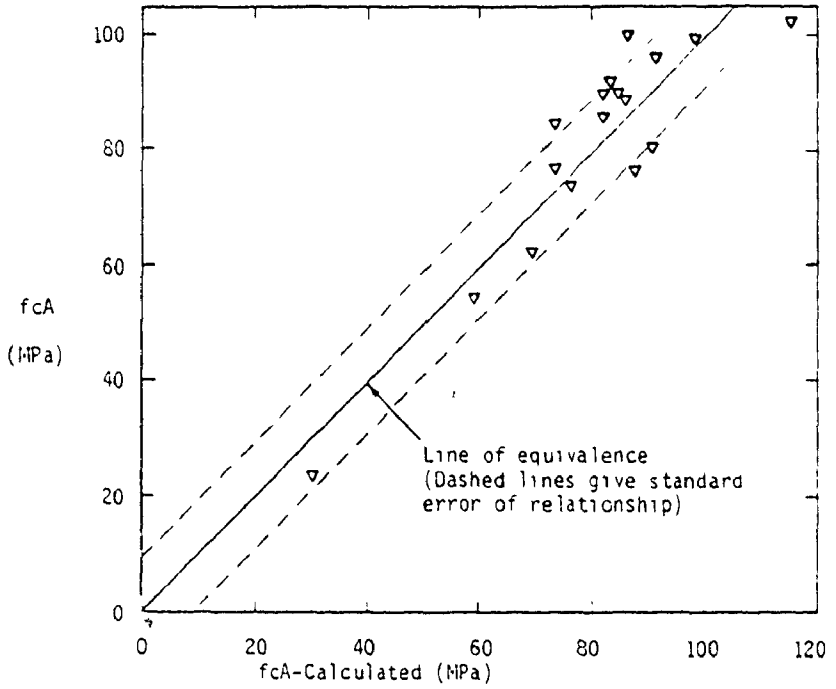

FIGURE 5.11: THE PRECISION OF CALCULATED STRENGTHS AT W/C = 0.28 USING EQUATION 5.9 AND GMAC GLASS VALUES

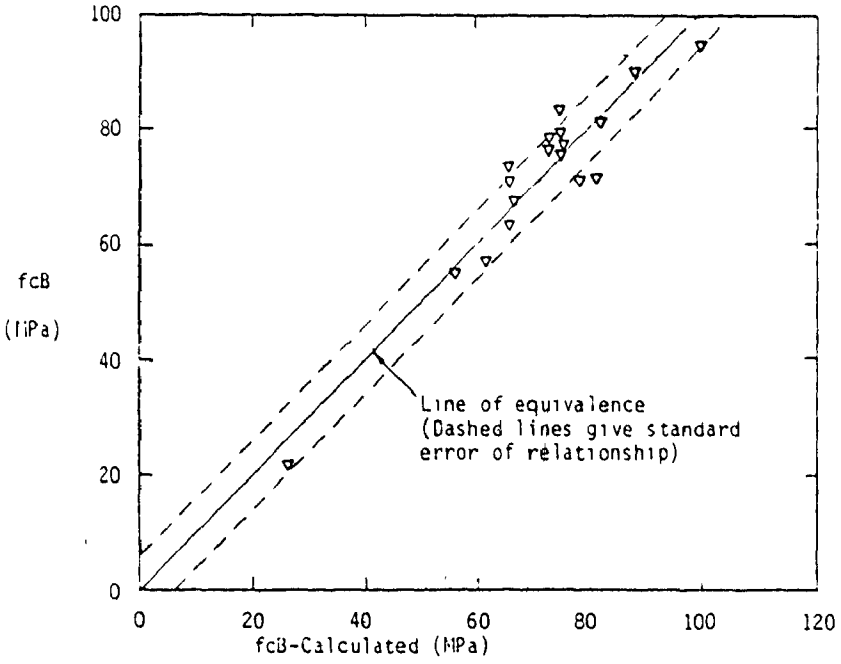

FIGURE 5.12: THE PRECISION OF CALCULATED STRENGTHS AT W/C = 0.32 USING EQUATION 5.9 AND GMAC GLASS VALUES

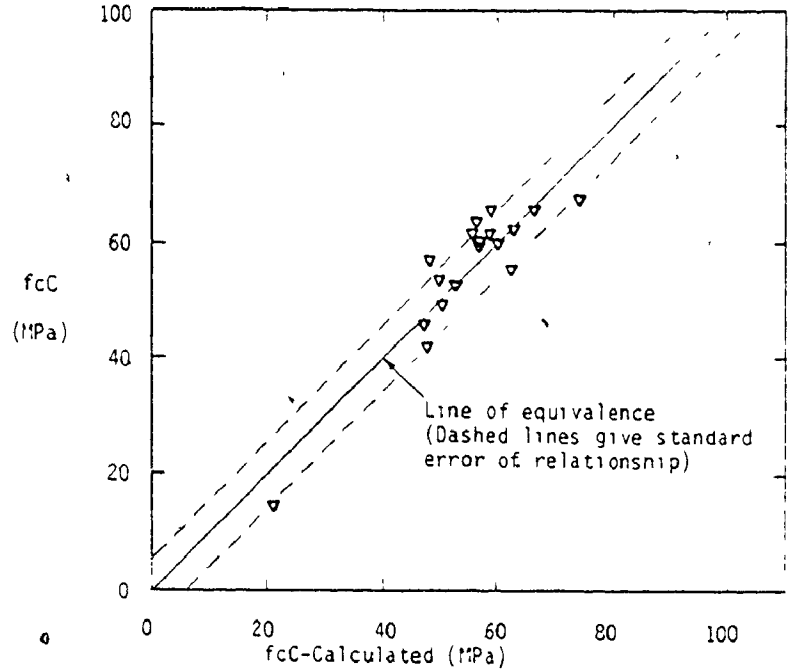

FIGURE 5.13. THE PRECISION OF CALCULATED STRENGTHS AT W/C = 0.40 USING EQUATION 5.9 AND GMAC GLASS VALUES

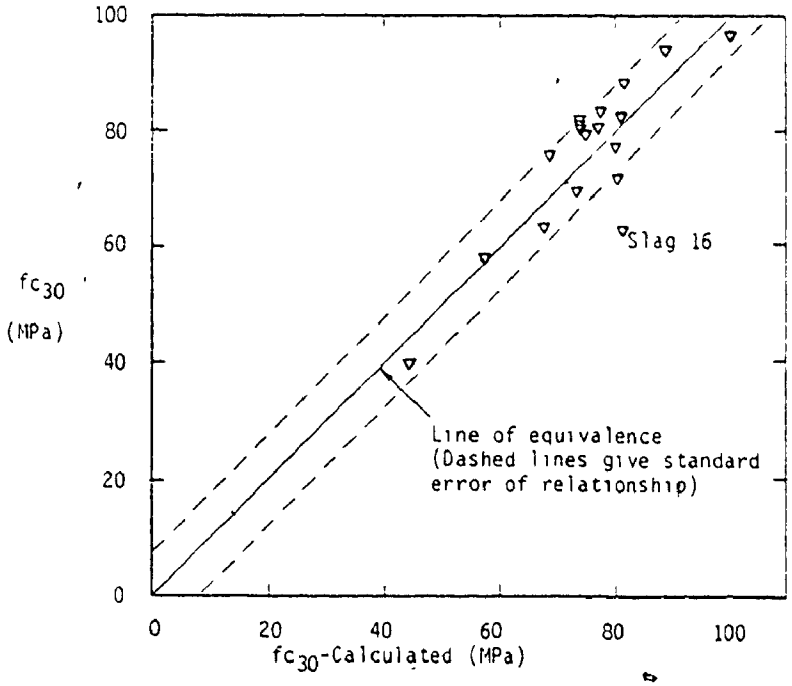

FIGURE 5.14: THE PRECISION OF CALCULATED STRENGTHS AT 30 PER CENT POROSITY USING EQUATION 5.9 AND GMAC GLASS VALUES

since the correlations were not as good and in many cases the equation coefficients were not significant. While the inclusion of most of the published slag composition moduli with glass contents in the regression analyses did not significantly improve the correlations with strength, and none of the remaining moduli provided as good as correlations given by the CaO and MgO oxide contents, it should be noted that none of these moduli were developed for evaluating autoclave hydraulicity. Since the high temperature used in autoclaving is a powerful activator in itself, enabling the reaction of quartz, it can not be automatically assumed that the effects of changes in slag composition would have similar effects on hydraulicity to those reported for ambient temperature curing.

However, from the fact that neither oxide contents nor compositional moduli were significantly related to strength development without glass content values being included, it was concluded that slag chemical composition was only of secondary influence in comparison to the degree of vitrification achieved.

5.5.4 Blaine Fineness

Regression analysis with all 18 slags did not show fineness to be significantly related to strength, with correlation coefficients only ranging from 0.21 to 0.36. In multiple regression analysis with glass and chemical contents, the Blaine fineness was not a significant parameter.

Therefore, the effect of variable slag fineness was checked indirectly by removing the pastes made with slags Number 1, 12,15 and 18 from the regression analyses used in developing Equation 5.9. The fourteen slags used in the preparation of the remaining pastes had relatively constant Blaine finenesses of 402 ± 9 m^2/kg. The regression coefficients are given in Table 5.20. From comparison of Tables 5.19 and 5.20, it can be observed that keeping the fineness of the slags constant slightly improved the correlation coefficients in each case, especially when GLX values were used as the measure of glass content.

Slags 9, 12 and 15, originally from the same sample and ground to different finenesses (401, 285 and 493 m^2/kg respectively) were analysed for strength-fineness relationships but due to the fact that there were only three slags in the regression, the equation coefficients were not significant at the 0.05 level even though strong correlation coefficients were obtained (R values ranged from 0.68 to 0.94 for the individual strength values).From comparison of compressive strength results for paste series 9 and 15 in Table 5.2, it can be observed that there is little benefit derived from grinding to Blaine finenesses greater than 400 m^2/kg. This was also found to be the case with commercially produced slag cement used in concrete cured at ambient

TABLE 5.20

REGRESSION EQUATION COEFFICIENTS FOR EQUATION 5.9 FOR SLAGS OF THE SAME BLAINE FINENESS (SLAGS 1,12,15 and 18, removed)

GLASS CONTENT METHOD	EQUATION COEFFICIENTS A	B	C	D	R	SE
(a) Compressive Strengths at W/C = 0.28 (fcA)						
GLX	0.491	8.010	6.027	-277.3	0.917	9.2
GAH	6.543	7.961	5.364	-245.9	0.895	10.3
GMAC	0.498	8.443	7.684	-346.0	0.929	8.5
GMAC+M	0.644	8.006	8.036	-373.3	0.901	10.0
(b) Compressive strengths at W/C = 0.32 (fcB)						
GLX	0.448	5.787	5.021	-220.7	0.920	7.4
GAH	6.083	5.713	4.387	-191.2	0.899	8.3
GMAC	0.462	6.162	6.544	-284.2	0.942	6.4
GMAC+M	0.616	5.712	6.897	-311.6	0.919	7.5
(c) Compressive Strengths at W/C = 0.40 (fcC)						
GLX	0.372	3.913	2.899	-128.0	0.930	5.2
GAH	4.979	3.870	2.390**	-104.1**	0.899	6.2
GMAC	0.373	4.251	4.149	-179.7	0.942	4.8
GMAC+M	0.523	3.818	4.476	-205.0	0.941	4.8
(d) Compressive Strengths at Constant Porosity (fc_{30})						
GLX	0.255	5.299	5.882	-231.3	0.834	8.9
GAH	3.260*	5.310	5.573	-216.1	0.813	9.4
GMAC	0.275	5.484	6.765	-268.7	0.855	8.3
GMAC+M	0.352	5.251	6.954	-283.2	0.835	8.9

* Only significant at .071 level
** Only significant at .107 level

temperatures (Warren, 1977). Hawthorn and co-workers (1980) also found that for pastes containing 80 per cent slag, increasing the slag fineness from 350 to 600 m^2/kg only improved strength development at early ages. On the other hand, the more coarsely ground slag, Number 12, did result in higher porosities and lower strengths at each water/cement ratio. The average reduction in strength compared to slag 9 was 32 per cent, which was approximately equivalent to the 29 per cent reduction in fineness.

Therefore, in the industrial application study using partially ground slag which was mentioned in Section 4.5, the reactivity of the minus 75μm particles (slag 12) would have resulted in a similar reduction in strength compared to the commercially available, 400 m^2/kg fineness slag cement. However the economic savings obtained using the partially ground slag process would have more than compensated for this.

5.5.5 Mineralogical Composition

The composition of slag glass, with respect to its position along the melilite solid solution series, was found by Akatsu and co-workers (1978) to have a pronounced effect on strength development at ambient curing temperatures. The melilite composition is obviously influenced by the chemical composition, but Regourd and co-workers (1980), while not finding chemical moduli of much value, concluded that the reactivity of slag was influenced by its glass content, the composition of the melilite solid solution (based on measurements of the melilite lattice parameters of the devitrified slags) and the amount of crystalline

merwinite.

In this work, simple observation of the low strengths developed using the low magnesia (hence low C_2MS_2) slag Number 8 and the high strengths of the high magnesia, high C_2MS_2 slag Number 18, indicated that the melilite composition of the glass might be an important parameter.

Therefore, it was decided to evaluate the slag glass, equalibrium melilite composition, and crystalline merwinite contents with respect to strength development. The crystalline merwinite content of each slag was expressed as a ratio to the crystalline melilite content. (Xmerw/Xmel). This ratio was also used by Budnikov and Gorskov (1964) to alter the reactivity of slags. The compositions of the melilites in the devitrified slags (all eighteen devitrified slags were composed of at least 90 per cent melilite) were calculated using the method of Ervin and Osborn (1949). This method consisted of measurement of the d-spacings for ten selected melilite peaks which were found to vary linearly with the composition of the melilite. An estimate of the percentage of akermanite was then determined for each spacing and the results averaged (designated Aker). The akermanite content of the melilites were found to range from 25 per cent for slag Number 8 to 75 per cent for slag Number 18. (The akermanite content of slag 18, estimated by its chemical composition, was 96 per cent. Therefore, the values obtained by the Ervin and Osborn method may be somewhat low.)

The regression coefficients for these variables are given in Table 5.21 for equations of the form,

$$fc\ (MPa) = A(glass) + B(Aker) + C(Xmerw/Xmel) + D \qquad (5.10)$$

TABLE 5.21

REGRESSION COEFFICIENTS FOR EQUATION 5.10

STRENGTH LEVEL LEVEL	EQUATION COEFFICIENTS					
	A	B	C	D	R	SE
	(a) For GLX glass contents:					
fcA	0.595	0.82	5.04	-13.5*	0.825	12.0
fcB	0.528	0.62	4.17	- 5.9*	0.845	9.5
fcC	0.419	0.33	2.82**	2.4*	0.836	7.3
fc_{30}	0.320	0.62	4.01	14.3*	0.738	10.1
	(b) For GMAC glass contents:					
fcA	0.610	0.80	7.05	-13.5*	0.857	10.9
fcB	0.547	0.60	5.97	- 6.4*	0.886	8.2
fcC	0.438	0.32	4.25	1.7*	0.889	6.1
fc_{30}	0.328	0.62	5.10	14.3*	0.758	9.8
	(c) For GMAC + M glass contents:					
fcA	0.783	0.78	7.17	-34.7*	0.825	12.0
fcB	0.700	0.58	6.07	-25.3*	0.850	9.3
fcC	0.588	0.30	4.37**	-15.7*	0.879	6.3
fc_{30}	0.391	0.61	5.11	- 54.*	0.715	10.5
	(d) For GAH glass contents:					
All	The coefficients were not significant at the 0.05 level					

*The D (fc-intercept) coefficients were not significantly different than zero.
**Significant at the 0.10 level

While the coefficients were significant, except for D, the correlation coefficients were not as good as those developed using Equation 5.9 (glass, MgO and CaO contents as variables). The positive values of the A, B and C coefficient values indicate that increasing glass contents, akermanite contents (in the melilite solid solution) and ratios of crystalline merwinite to melilite are beneficial to strength development. Increased akermanite contents are indicative of higher MgO contents, and the presence of merwinite is indicative of increased CaO contents (C_3MS_2 compared to C_2MS_2), so the results are in agreement with those given by the coefficients for Equation 5.9.

5.5.6 Discussion

Of all the analyses of slag properties with strength, the glass contents combined with CaO and MgO contents of the slags provided the best correlations (Equation 5.9). However, as can be seen by the scatter of predicted strengths with actual strengths in Figures 5.11 to 5.14, this relationship would not likely be accurate enough to use for predictive purposes, especially when comparing well vitrified slags.

It appears then that, while evaluation of the physical and chemical properties of slags can provide a guide to hydraulicity, the authority of physical strength testing remains unchallenged. Also the rejection of a well vitrified slag because of chemical composition would be unwise. The present work suggests that the use of chemical oxide ratios as indices of performance is unreliable and it appears that the only real purpose of the minimum values of chemical composition ratios incorporated into some standard specifications if to eliminate slags of unusual composition.

5.6 CONCLUSIONS

In this chapter, eighteen slags with variable glass content, chemical composition and fineness properties were autoclaved in pastes of 60/20/20 composition. The effects of these slag variables on strength development and hydration properties were studied.

Pastes containing each slag were mixed at three water/cement ratios to obtain a range of porosities in the autoclaved prisms. The strengths of pastes at a constant porosity of 30 per cent could then be calculated using linear log strength-porosity equations developed for each slag. While this was done in an attempt to eliminate porosity effects in subsequent analyses of slag parameters with strength, the correlations were found to be lower than for strengths of pastes mixed at a fixed water/cement ratio.

The compressive strengths developed using fifteen different vitrified slags were higher than those of the portland cement-quartz control pastes. The lower strengths in the other two vitrified slags were attributed to a much lower fineness of grinding (Slag 12), and to a different mineralogical and chemical composition (Slag 8). Therefore, it appears that, as long as Canadian slags are ground to cement finenesses and are at least partially vitrified, the strength of portland cement-quartz pastes can be equalled or exceeded.

The pastes composed largely of slag were less brittle, with flexural to compressive strength ratios approximately three times higher than those of the portland cement-quartz control pastes.

Since the solid densities of the pastes were found to decrease

with increasing slag glass contents and the hydrated compounds were less dense than the anhydrous slag, it was concluded that the paste densities were mainly influenced by the reactivity of the slag.

The pore size distributions of pastes containing vitrified slags were much finer than those of the portland cement-silica flour control pastes. This indicated a much finer structure of the calcium silicate hydrates contained in the slag pastes than those in the control pastes. This was thought to be largely responsible for the higher flexural and compressive strengths attained.

The pastes containing the devitrified slag exhibited very coarse pore size distributions with almost no pore volume intruded at fine pore diameters. The lack of reactivity of the devitrified slag was also indicated by high paste densities, low non-evaporable water contents and very low strengths.

The coefficients found for the strength- Wn/Wo relationship were compared to published values for portland cement cured at ambient temperatures. It was found that, for a fixed water/cement ratio, the autoclaved pastes in this study achieved equivalent strengths at much lower non-evaporable water contents. This is likely due to the lower water contents in the composition of autoclaved calcium silicate hydrates.

By XRD, the crystalline melilite in the devitrified slag was observed to be non-reactive for the autoclave curing regime adopted. Unfortunately, no satisfactory method was found to determine the content of reacted and/or unreacted vitreous slag. From the literature,

this is a major problem in studies of slag. Approximately three quarters of the portland cement in the pastes had reacted but in pastes containing vitrified slags, only about one quarter of the silica flour had reacted. The silica flour in the pastes containing the devitrified slag had reacted to a much higher degree, as it did in the portland cement-silica flour control pastes. It appears then that the presence of reactive vitreous slag retards the reaction of quartz through competition for the calcium hydroxide liberated by the portland cement component.

Poorly crystalline C-S-H of the tobermorite group was found to be the principal hydration product in all pastes containing vitrified slag. The crystallinity index of the C-S-H was found to be inversely proportional to the glass content of the slag. Also, amorphous C-S-H was detected qualitatively in the control pastes and in pastes containing the devitrified slag. In the other pastes, the presence of amorphous C-S-H was masked on XRD traces by the halo of unreacted amorphous slag.

Regression analyses showed that slag glass content had the largest effect on strength development. The QXRD methods of glass content determination, GLX and GAH, as well as the McMaster individual particle analysis, GMAC, were found to have approximately equivalent correlations with strength. The GMAC + M glass values were also related to strength development but the glass values determined using other methods (GSA, GUV and GUV-N) were not. The glass content of the slags

was also found to be related to the crystallinity of the C-S-H found in the pastes. While relative strengths of pastes could not be accurately predicted by glass content alone, extremely low glass contents were indicative of non-reactive slags.

The relationship between glass content and strength development was improved when the chemical composition of the slag remained relatively constant (more specifically at a constant value of the oxide modulus (C+M+A) /S). However, twelve commonly used hydraulic indices, based on chemical composition, were evaluated and only three showed any significant correlation with strength, and only when combined with a measure of the glass content. Except for the elimination of slags with unusual compositions, the incorporation of minimum values of oxide ratios in standard specifications appear to be of little value, and the rejection of a well vitrified slag on the basis of normal variations in chemical composition would be unwise.

The best improvements to the glass content-strength relationships resulted from the addition of the MgO and CaO contents of the slags, with correlation coefficients as high as 0.94. From regression analyses of strength with mineralogical parameters, the influence of the MgO parameter appeared to be related to the akermanite content of the melilite solid solution (based on examination of the slags when devitrified). Also for the range of slags studied, the CaO parameter appeared to be related to their crystalline merwinite fractions.

While hydraulic indices, such as the one developed in this work,

using the slag glass, MgO and CaO contents, can be of some use in the prediction of slag reactivity, they lack the conviction for engineering decision making. Since the correlations of the hydraulic indices with strength are primarily influenced by glass content, chemical composition appears to be of only secondary importance. Therefore, for the evaluation of well vitrified slags, the authority of physical strength testing remains unchallenged.

6. CONCLUSIONS

Detailed findings were presented in the conclusions of Chapters 3, 4, and 5. In this section the major findings are summarized and recommendations given.

While an amorphous structure is known to be fundamental to the reactivity of slag, there appeared to be no standard method used for the determination of the degree of vitrification. The most reliable method of estimating the degree of vitrification is the QXRD method, developed using synthetic mineral calibration standards, and it was adopted as the standard by which all other methods were judged. By comparison with five other techniques, it was found that one commercially used technique could not even distinguish between devitrified and amorphous slags and another was sensitive to minor oxide components of the slag. Therefore, it appears that the adoption of a suitable technique is critical to the evaluation of glass contents in slag.

Because of the disadvantage, that recourse must be made to expense and somewhat involved XRD analyses, an alternative optical technique was developed. This method, designated the McMaster Individual Particle Analysis (GMAC), proved to be comparable in accuracy to the QXRD standard and is thought to be simpler and more reliable than any previously used technique. This method has recently been adopted, with minor modifications by a Canadian cement producer.

The autoclave reactivity of mortars and pastes in the ternary binder system of slag-portland cement-silica flour (ground quartz) was

studied. It was found that up to 80 per cent slag could be included in mortar cube binders without suffering any degradation in compressive strengths in comparison to conventional portland cement-silica flour binders. Optimum strengths were found at 60 to 75 per cent slag contents. In pastes, high strengths were obtained with slag contents as high as 60 per cent. Silica flour, which enhances the performance of portland cement at autoclave temperatures, was found to have a similar beneficial effect on slag and slag-portland cement blends. The beneficial effect of silica flour was associated with the formation of tobermorite-like C-S-H instead of αC_2SH, for both portland cement and slag-portland cement blends. Pastes not containing silica flour in which both αC_2SH and poorly crystalline C-S-H were found also exhibited relatively high compressive strengths.

In pastes not containing portland cement, the slag was found to be activated by silica flour, with very high compressive strengths found at one combination where relatively well crystallized tobermorite was formed. As well, all of the non-portland cement binders exhibited high splitting tension to compressive strength ratios. The reactivity of slag-silica flour binders was considered to be unusual and further work in this area is warranted to elucidate the reaction mechanisms involved.

In a related industrial study, it was found that pelletized slag, even when only coarsely ground, could successfully replace up to 67 per cent of the conventional portland cement-silica flour binders in the production of autoclaved concrete block at considerable economic

benefit.

One of the reasons for the high mechanical strengths developed in pastes containing 60 per cent slag / 20 per cent portland cement/ 20 per cent silica flour, was found to be the very fine pore size distributions developed when reactive vitreous slags were used. Therefore the poorly crystalline C-S-H found must have much finer structure than the mainly amorphous C-S-H found in portland cement-silica flour pastes.

The physical and chemical properties of slag, which have been generally found to influence its reactivity for curing at ambient temperatures, were also found to affect its reactivity for autoclave curing at 185°C. It was found that the degree of vitrification has the most significant influence on the autoclave reactivity of slag. However, for well vitrified slags, the relationship between glass content and strength is not as clear, with glass contents approaching 100 per cent not necessarily indicating higher strength development.

Of the glass content determination methods evaluated, only the ones which gave values relating to the QXRD standard values showed any correlation with strength. The suitability of the previously mentioned McMaster optical procedure, for assessing slag quality, was confirmed by these results.

In autoclaved pastes made from 60 per cent slag/20 per cent portland cement/20 per cent silica flour, it was found that pelletized slags with glass contents as low as 54 per cent (QXRD method) could

develop compressive strengths equivalent to those of the portland cement-silica flour control pastes. Therefore it appears that such low slag glass contents do not preclude their use for cementitious purposes.

Slag chemical composition was found to have less influence on its reactivity. Most of the published chemical oxide moduli were not significantly related to strength development even when combined with a measure of the glass content. Therefore the common use of such moduli to evaluate slag hydraulicity appears to be of questionable value, at least in terms of autoclave reactivity. The most significant chemical parameters affecting strength development were the CaO and MgO contents. For the range of Canadian slag compositions, it appears that all are suitable for use in autoclave applications.

There appeared to be little benefit derived from grinding slag finer than 400 m^2/kg (Blaine) but grinding to a coarser value (285 m^2/kg) had a detrimental effect on strength.

In summary, while requiring some activation, slag contents as high as 80 per cent can be used in autoclaved binders, with strengths and hydrated phases similar to conventional portland cement-quartz binders. The main parameter influencing slag reactivity is its degree of vitrification, but partially vitrified slags can be used successfully. A new method for determining the degree of vitrification has been found to give reliable results and is thought to be convenient for commercial use. However, for evaluating slag hydraulicity, it is suggested that only physical strength testing has the authority for engineering decision making.

The following topics could be usefully studied in connection with expanding the use of slag cements in Canada:

a) Cement Manufacture

1. The pre-reduction of pelletized slag, in hammer mills or high speed intensive mixers (similar to the machine described in Section 4.5) before introduction to ball mills, may well require less total energy than the existing ball mill methods. This aspect requires further investigation in order to optimize grinding procedures.

2. The introduction of a certain percentage of undried pelletized slag directly to the ball mills would reduce drying energy costs as well as reducing mill temperatures. Investigation would be required to determine the amounts which could be added under different operating conditions without leaving harmful residual moisture contents in the ground product.

b) Product Manufacturing

1. Further work is required to optimize concrete mix designs and curing regimes for autoclave products incorporating pelletized slag cement.

2. The influence of using other energy efficient by-products, such as cement kiln dust, in conjunction with slag cement in autoclaved products should be further investigated. The durability of products made with such materials would have to be studied with regard to possible corrosion

resulting from high chloride contents.

3. The beneficial effects of carbon dioxide curing should be studied, principally to increase the initial rate of hardening.

4. The investigation of non-corrosive admixtures and gypsum addition levels should be studied to improve initial strength development at high slag contents without sacrificing durability.

5. The corrosion protection offered by concrete mixes with high slag content, while apparently adequate for reinforced concrete, should be studied with regard to its use in prestressed concrete.

The following areas of research are also suggested in the study of autoclaved slags:

1. The autoclaved slag-silica flour binders require further study both to elucidate the mechanism of activation involved and to further study the mechanical properties developed.

2. A technique needs to be developed to accurately estimate the unreacted slag contents remaining in autoclaved pastes.

REFERENCES

Abo-El-Enein, S.A., Gabr, N.A. and Mikhail, R.Sh., 1977. Morphology and microstructure of autoclaved clinker and slag-lime pastes in presence and in absence of silica sand, Cement and Concrete Research, 7, 231-238.

Abo-El-Enein, S.A., Mikhail, R.Sh., Daimon, M. and Kondo, R., 1978. Surface area and pore structure of hydrothermal reaction products of granulated blast furnace slag, Cement and Concrete Research, 8, 151-160.

ACI committee 516, 1965. High pressure steam curing: modern practice, and properties of autoclaved products, Journal of the American Concrete Institute, 62, 869-907.

Aitken, A. and Taylor, H.F.W., 1960. Hydrothermal reactions in lime-quartz pastes, Journal of Applied Chemistry, 10 (1), 7-15.

Aitken, A. and Taylor, H.F.W., 1962. Steam curing of cement and cement-quartz pastes, Proceedings of the Fourth International Symposium on the Chemistry of Cement, Washington D.C.1960, 3, 285-290.

Akaiwa, S. and Sudoh, G., 1966. Strength and microstructures of hardened cement pastes cured by autoclaving, Proceedings of a Symposium on Structure of Portland Cement Paste and Concrete, Washington D.C.1965, HRB, SR-90, 36-47.

Akatsu, K., Ikeda, I. and Sadatsune, K., 1978. Practical properties of slag cement prepared with a series of glasses of the gehlenite-akermanite system (English Abstract), Review of the 32nd. Meeting of the Cement Association of Japan, 57-58.

Alexanderson, J., 1979-1. Relations between structure and mechanical properties of autoclaved aerated concrete, Cement and Concrete Research, 9, 507-514.

Alexanderson, J., 1979-2. Swedish Cement and Concrete Research Institute, Personal communication, October 10.

Alunno-Rossetti, V., Chiocchio, G. and Collepardi, M., 1973. Influence of precuring on high pressure steam hydration of tricalcium silicate, Cement and Concrete Research, 3, 665-676.

Anon, 1909. The manufacture of portland cement from blast-furnace slag at the Coltness Iron Company's works, The Iron and Coal Trades Review, October 29, 694-695.

ASTM C114-80, 1980. Standard methods for chemical analysis of hydraulic cement, Annual Book of ASTM standards, Part 13, 86-126.

Beaudoin, J.J. and Feldman, R.F., 1975. A Study of mechanical properties of autoclaved calcium silicate systems, Cement and Concrete Research, 5, 103-118.

Beaudoin, J.J. and Feldman, R.F., 1978. The significance of helium diffusion measurements in studying the removal of structural water in inorganic hydrated systems, Cement and Concrete Research, 8, 223-232.

Berardi, M.C., Chiocchio, G., Collepardi, M., 1975. The influence of precuring on the autoclave hydration of quartz-tricalcium silicate mixtures, Cement and Concrete Research, 5, 481-488.

Blondiau, L., 1951. Influence d'allure de la granulation sur la qualité des laitiers utilisés en cimentérie (in French), Silicates Industriels, 16, 105-109.

Budnikov, P.P. and Gorskov, V.S., 1964. Steigerung der wasseraktivität von hochofenschlacken durch gerichtete kristallisation (in Russian), Stroiteljnye Materialy, 9, 22-23.

Chan, C.F. and Mitsuda, T., 1978. Formation of 11Å tobermorite from mixtures of lime and colloidal silica with quartz, Cement and Concrete Research, 8, 135-138.

Chan, C.F., Sakiyama, M. and Mitsuda, T., 1978. Kinetics of the CaO-quartz-H_2O reaction at 120° to 180°C in suspensions, Cement and Concrete Research, 8, 1-6.

Chen, H., 1979. Canada Cement Lafarge Limited, Personal Communication, August 9.

Cheron, M. and Lardinois, C., 1969. The role of magnesia and alumina in the hydraulic properties of granulated blastfurnace slags, Proceedings of the Fifth International Symposium on the Chemistry of Cement, Tokyo 1968, 4, 277-285.

Coale, R.D., Wolhuter, C.W., Jochens, P.R. and Howat, D.D., 1973. Cementitious properties of metallurgical slags, Cement and Concrete Research, 3, 81-92.

Copeland, L.E. and Hayes, J.C., 1953. The determination of non-evaporable water in hardened portland cement paste, ASTM Bulletin, 194, December, 70-74.

Cotsworth, R.P., 1979. National Slag Limited, Personal communication, September 13.

Crennan, J.M., Dyczek, J.R.L. and Taylor, H.F.W., 1972. Quantitative phase compositions of autoclaved cement-quartz cubes, Cement and Concrete Research, 2, 277-289.

Crennan, J.M., El-Hemaly, S.A.S. and Taylor, H.F.W., 1977. Autoclaved lime-quartz materials: I, Cement and Concrete Research, 7, 493-502.

D'Ans, J., Eick, H., 1954. Investigations on the setting process of hydraulic blast furnace slag (in German), Zement-Kalk-Gips, 7, 449-459.

Davey, D., 1979. Cooke Concrete Limited, Personal communication, February 22.

De Langavant, J.C., 1949. Considérations théoretiques sur la nature du laitier de cimenterie (in French), Revue des Matériaux de Construction et de Travaux Publics, 401, 381 to 411, 425.

Demoulian, E., Gourdin, P., Hawthorn, F. and Vernet, C., 1980. Influence of slags chemical composition and texture on their hydraulicity (in French), Proceedings of the Seventh International Congress on the Chemistry of Cement, Paris 1980, 2(III), 89-94.

Diamond, S., White, J.L. and Dolch, W.L., 1966. Effects of isomorphous substitution in hydrothermally-synthesized tobermorite, The American Mineralogist, 51, 388-401.

Dron, R. and Petit, Ph., 1975. A physico-mechanical model of the cohesion of a granulated slag paste, Cement and Concrete Research, 5, 455-460.

Dyczek, J. and Petri, M., 1974. The mechanical properties of calcium silicate hydrates existing in autoclaved cement-quartz materials, Pre-print of the Sixth International Congress on the Chemistry of Cement, Moscow, II, 8pp.

Dyczek, J.R.L., Taylor, H.F.W., 1971. X-ray determination of tobermorite, quartz and α-dicalcium silicate hydrate in autoclaved calcium silicate materials, Cement and Concrete Research, 1, 589-605.

Eitel, W., 1966. Silicate science, Volume 5:ceramics and hydraulic binders, Academic Press, New York, 618pp.

El-Hemaly, S.A.S., Mitsuda, T. and Taylor, H.F.W., 1977. Synthesis of normal and anomalous tobermorites, Cement and Concrete Research, 7, 429-438.

Emery, J.J., 1978. Slags as industrial minerals, Proceedings of the Third Industrial Minerals International Conference, Paris 1978, 127-142.

Emery, J.J., Cotsworth, R.P. and Hooton, R.D., 1976. Pelletized blast furnace slag, Proceedings of a Seminar on Energy Resource Conservation in the Cement and Concrete Industry, Ottawa, Paper 4.1, 1-23.

Emery, J.J. and Hooton, R.D., 1978. Ground pelletized slag autoclaved blocks, Proceedings of the International Conference on the Use of By-Products and Wastes in Civil Engineering, Paris 1978, 2, 303-307.

Emery, J.J., Kim, C.S. and Cotsworth, R.P., 1976. Base stabilization using pelletized blast furnace slag, Journal of Testing and Evaluation, 4(1), 94-100.

Ervin, G. and Osborn, E.F., 1949. X-ray data on synthetic mellilites, American Mineralogist, 34, 717-722.

Feldman, R.F., 1971. The flow of helium into the interlayer spaces of hydrated portland cement paste, Cement and Concrete Research, 1, 285-300.

Feldman, R.F., 1972. Helium flow and density measurement of the hydrated tricalcium silicate-water system, Cement and Concrete Research 2, 123-136.

Feldman, R.F. and Beaudoin, J.J., 1974. Microstructure and strength of hydrated cement, Presented at the Sixth International Congress on the Chemistry of Cement, Moscow 1974.

Feldman, R.F. and Beaudoin, J.J., 1976. Microstructure and strength of hydrated cement, Cement and Concrete Research, 6, 389-400.

Feldman, R.F. and Sereda, P.J., 1970. A new model for hydrated portland cement and its practical implications, Engineering Journal, 53(819), 53-59.

Fierens, P., 1979. Université de l'État à Mons, Personal communication, July 4.

Fierens, P. and Poswick, P., 1977. Etude cinetique de l'hydratation de laitiers synthétiques (in French), Silicates Industriels, 42(4-5), 235-245.

Foster, J.R., 1978. Dravo Lime Company, Private communication, June 30.

Foster, J.R., 1979. Dravo Lime Company, Private communication, April 30.

Foster, J.R., 1980. Dravo Lime Company, Private communication, March 18.

Frodingham Cement Co. Ltd., 1979. Method of establishing the amount of non-crystalline material in granulated slag, Scunthorpe, Great Britain, March 15, 1pp.

Govorov, A.A., 1974. Hydrothermal hardening of slag glasses dispersions, Preprint, The Sixth International Congress on the Chemistry of Cement, Moscow 1974, Paper III-2, 14pp.

Grattan-Bellow, P.E., Quinn, E.G. and Sereda, P.J., 1978. Reliability of scanning electron microscopy information, Cement and Concrete Research, 8, 333-342.

Gupta, R.P., 1976. Utilization of pelletized slags, M.Eng. thesis, McMaster University, 173pp.

Gutt, W., 1971. Manufacture of cement from industrial by-products, Cement and Industry, 7, 189-197.

Hara, N. and Midgley, H.G., 1980. The determination of crystallinity of tobermorite in autoclaved products, Cement and Concrete Research, 10, 213-221.

Hawthorn, F., Demoulian, E., Gourdin, P. and Vernet, C., 1980. Blast-furnace slags and clinkers-mutual influences (in French), Proceedings of the Seventh International Congress on the Chemistry of Cement, 2(III), 145-150.

Heller, L. and Taylor, H.F.W., 1956. Crystallographic data for the calcium silicates, HMSO, London, 79pp.

Hooton, R.D. and Emery, J.J., 1980. Pelletized slag cement: autoclave reactivity, Proceedings of the Seventh International Congress on the Chemistry of Cement, Paris 1980, 2(III), 43-47.

Jenvay, L. and Pugh, R., 1980. St.Marys Cement Company, Personal communication, September 25.

Kalousek, G.L., 1954-1. The reactions of cement hydration at elevated-temperatures, Proceedings of the Third International Symposium on the Chemistry of Cement, London 1952, 334-355.

Kalousek, G.L., 1954-2. Studies on the cementitious phases of autoclaved concrete products made of different raw materials, Journal of the American Concrete Institute, 50, 365-378.

Kalousek, G.L., 1957. Crystal chemistry of hydrous calcium silicates: I, Journal of the American Ceramic Society, 40(3), 74-80.

Kalousek, G.L., 1969. High-temperature curing of concrete under high pressure, Proceedings of the Fifth International Symposium on the Chemistry of Cement, Tokyo 1968, 3, 523-540.

Kamel, A.J., 1973-1. High pressure steam curing of slag cement I: Composition of the hydrated cement, Journal of Applied Chemistry and Biotechnology, 23(7), 483-488.

Kamel, A.H., 1973-2. High pressure steam curing of slag cement. II: Strength of Cement Sand Mixes, Journal of Applied Chemistry and Biotechnology, 23(7), 489-492.

Kamel, A.H., 1975. Strength of autoclaved portland blast furnace cement, Journal of Applied Chemistry and Biotechnology, 25, 57-61.

Kayyali, O.A., Page, C.L. and Ritchee, A.G.B., 1980. Frost action on immature cement paste-microstructural features, Journal of the American Concrete Institute, 77(4), 264-268.

Keil, F., 1954. Slag cements, Proceedings of the Third International Symposium on the Chemistry of Cement, London 1952, 530-571.

Keil, F. and Gille, F., 1949. Hydraulische eigenschaften basischer gläser mit der chemischen zusammentsetzung der gehlinit und akermanits (in German), Zement-Kalk-Gips, 2, 229-232.

Kholin, I.I. and Royak, S.M., 1962. Blastfurnace cement in the USSR, Proceedings of the Fourth International Symposium on the Chemistry of Cement, Washington D.C. 1960, 2, 1057-1065.

Kim, C.S., 1975. Waste and secondary product utilization in highway construction, M.Eng.thesis, McMaster University, 256pp.

Klug, H.P. and Alexander, L.E., 1974. X-ray diffraction procedures for polycrystalline and amorphous materials, John Wiley and Sons, Toronto, 2nd edition, 966pp.

Komar, A., 1974. Building Materials and Components (English translation), Mir Publishers, Moscow, 480pp.

Kondo, R., 1962. Discussion of : Blast-furnace slags and slag cements (by W.Kramer), Proceedings of the Fourth International Symposium on the Chemistry of Cement, Washington D.C. 1960, 2, 973-975.

Kondo, R., Abo-El-Enein, S.A. and Daimon, M., 1975. Kinetics and mechanisms of hydrothermal reaction of granulated blast furnace slag, Bulletin of the Chemical Society of Japan, 48(1), 222-226.

Kondo, R., Daimon, M., Chong-Tak, S. and Jinawath, S., 1980. Effect of lime on the hydration of supersulfated slag cement, American Ceramic Society Bulletin, 59, 848-851.

Kondo, R. and Ohsawa, S., 1969. Studies on a method to determine the amount of granulated blastfurnace slag and the rate of hydration of slag in cements, Proceedings of the Fifth International Symposium on the Chemistry of Cement, Tokyo 1968, 4, 255-262.

Kondo, R. and Ueda, S., 1969. Kinetics and mechanisms of the hydration of cements, Proceedings of the Fifth International Symposium on the Chemistry of Cement, Tokyo 1968, 2, 203-248.

Kramer, W., 1962. Blast-furnace slags and slag cements, Proceedings of the Fourth International Symposium on the Chemistry of Cement, Washington D.C. 1960, 2, 957-973.

Krüger, J.E., 1962. The use of DTA for estimating the slag content of mixtures of unhydrated portland cement and ground granulated blastfurnace slag, Cement and Lime Manufacture, 35(6), 104-108.

Krüger, J.E., 1976. Contributions to the knowledge of the characteristics of vitreous blast-furnace slag with a high magnesia content, D.S.thesis, University of Pretoria, R.S.A., 175pp.

Krüger, J.E., 1980. National Building Research Institute, Pretoria, South Africa, Personal communication, September 30.

Krüger, J.E. and Visser, S., 1971. Study of the hydration of vitreous blastfurnace slag with a high magnesia content and of related materials, Proceedings of the Third International Conference on Thermal Analysis, Davos, Switzerland 1971, 523-531.

Lea, F.M., 1971. The chemistry of cement and concrete, Chemical Publishing Co. Inc., New York, third edition, 687pp.

Locher, F.W., 1962. Hydraulic properties and hydration of glasses of the system $CaO-Al_2O_3-SiO_2$, Proceedings of the Fourth International Symposium on the Chemistry of Cement, Washington D.C. 1960, 1, 267-275.

Ludwig, U., 1964. The influence of various sulphates on the setting and hardening of cements (in German), Zement-Kalk-Gips 16 (2), 81-90, (3), 109-119, (4), 175-180. English Translation 61-143, Cement and Concrete Association, London 1970.

Maiko, V.P., Gusev, B.V. and Ratinov, V.B., 1976. Role of additives in the hardening of portland-slag cement and slag minerals (in Russian), Zhurnal Prikladnoi Khimii, 49(3), 507-512.

Margesson, R.D.and England, W.G., 1971. Processes for the pelletization of metallurgical slag, United States Patent No. 3594142, July, National Slag Ltd., Hamilton, Ontario, 4pp.

Mascolo, G., Nastro, A. and Sabatelli, V., 1977. Study of the hydration behaviour of vitreous blastfurnace slags in realtion to the MgO content, IL Cemento, 74(2), 45-52.

Massidda, L. and Sanna, U., 1979. Structure and characteristic of compacts of blastfurnace slag activated by $CaSO_4$ $2H_2O$, Cement and Concrete Research, 9, 127-134.

Mather, K., 1974-1. Member of ASTM Committee C.1, Personal communication, June 12, 2pp.

Mather, K., 1974-2. Member of ASTM Committee C.1, Personal communication, August 23, 5pp.

Mathews, J.S. and Baker, R.S., 1976. Building Research Station, Great Britain, Private communication, September.

McCrone, W.C. and Delly, J.G., 1973. The Particle Atlas, Ann Arbor Science Publishers, Inc., 2nd edition, Volume 1.

Menzel, C.A., 1934. Strength and volume change of steam-cured portland cement mortar and concrete, Journal of the American Concrete Institute, 31, 125-149.

Midgley, H.G., 1976. Quantitative determination of phases in high alumina cement clinkers by x-ray diffraction, Cement and Concrete Research, 6, 217-224.

Midgley, H.G. and Chopra, S.K., 1960. Hydrothermal reactions between lime and aggregate fines, Magazine of Concrete Research, 12(35), 73-82.

Millet, J., Hammey, R.and Brivot, F., 1977. Dosage de la phase vitreuse dans les matériaux pouzzolaniques (in French), Bulletin de Liaison des Laboratoires des Ponts et Chaussées, 92 (November -December),101-104.

Mills, R.H., 1960. Strength-maturity relationship for concrete which is allowed to dry, RILEM Symposium on Concrete and Reinforced Concrete in Hot Countries, Haifa.

Mills, R.H., 1966. Factors influencing cessation of hydration in water cured cement pastes, Proceedings of a Symposium on Structure of Portland Cement Paste and Concrete, Washington D.C. 1965, HRB, SR-90, 406-424.

Mills, R.H., 1976. The case for separate grinding and batching of blast furnace slag and portland cement, Proceedings of a Seminar on Energy and Resource Conservation in the Cement and Concrete Industry, Ottawa, Paper 3.3, 1-3.

Mindess, S., 1970. Relation between the compressive strength and porosity of autoclaved calcium silicate hydrates, Journal of the American Ceramic Society, 53, 621-624.

Mollard, P., 1976. Canadian experience with the use of blended cements, Proceedings of a Seminar on Energy and Resource Conservation in the Cement and Concrete Industry, Ottawa 1976, Paper 3.5, 1-4.

Nassau, K., Wang, C.A. and Grasso, M., 1979. Glassy and crystalline phases in the system lithium-sodium-potassium -metaniobate-tantalate, Journal of the American Ceramic Society, 62, 503-510.

Negro, A., 1969. Discussion of: Slags and slag cements (by F.J.Schröder), Proceedings of the Fifth International Symposium on the Chemistry of Cement, Tokyo 1968, 4, 199-200.

Neville, A.M., 1972. Properties of Concrete, The Copp Clark Publishing Company, Toronto, 686pp.

Noorlander, A., 1967. Reducing the shrinkage of calcium silicate bricks, Proceedings of the Symposium on Autoclaved Calcium Silicate Building Products, London 1965, 152-153.

Nurse, R.W., 1949. Steam curing of concrete, Magazine of Concrete Research, 1(2), 79-88.

Nurse, R.W., 1964. Slag cements, in The Chemistry of Cements (H.F.W. Taylor, editor), Academic Press London, 2, 37-67.

Osborn, E.F., Devries, R.C., Gee, K.H. and Kraner, H.M., 1954. Optimum composition of blast furnace slag as deduced from liquidus data for the quaternary system CaO-MgO-Al_2O_3-SiO_2, Journal of Metals, 6(1), 33-45.

Osbourne, G.J., 1977. Grinding characteristics of vitreous blastfurnace slags, Building Research Note No. N125/77, 11pp.

Pai, V.N. and Hattiangadi, R.R., 1969. Reactive slag-like glasses of the S-A-F-C-M system, Proceedings of the Fifth International Symposium on the Chemistry of Cements, Tokyo 1968, 4, 248-254.

Parker, T.W., 1954. Discussion of: Slag Cements (by F.Keil), Proceedings of the Third International Symposium on the Chemistry of Cement, London 1952, 577-579.

Parker, T.W. and Nurse, R.W., 1949. Investigations on granulated blastfurnace slags for the manufacture of portland blastfurnace cement, National Building Studies, Technical Paper 3, D.S.I.R., HSMO, London.

Pirotte, P., 1954. Discussion of: Slag cements (by F.Keil), Proceedings of the Third International Symposium on the Chemistry of Cement, London 1952, 575-576.

Powers, T.C. and Brownyard, T.L., 1948. Studies of the physical properties of hardened portland cement paste, Portland Cement Association, Chicago, Bulletin 22, 382pp. (reprinted from the Journal of the American Concrete Institute October 1946-April 1947).

Regourd, M., Mortureux, B., Gautier, E., Hornain, H. and Volant, J., 1980. Characterization and thermal activation of slag cements (in French), Proceedings of the Seventh International Congress on the Chemistry of Cement, Paris, 2(III), 105-111.

Roper, H., 1980. Composition, morphology, hydration and bond characteristics of some granulated slags, Proceedings of the Seventh International Congress on the Chemistry of Cement, Paris 1980, 2(III), 13-18.

Roy, D.M. and Gouda, G.R., 1975. Optimization of strength in cement pastes, Cement and Concrete Research, 5, 153-162.

Sanders, L.D., and Smothers, W.J., 1957. Effect of tobermorite on the mechanical strength of autoclaved portland cement-silica mixtures, Journal of the American Concrete Institute, 54, 127-139.

Satarin, V., 1974. Slag portland cement, Preprint, The Sixth International Congress on the Chemistry of Cement, Moscow 1974, 51pp.

Schrämli, W., 1963. The characterization of blastfurnace slags by means of differential thermal analysis, Zement-Kalk-Gips, 15(4), 140-147.

Schröder, F., 1969. Slags and slag cements, Proceedings of the Fifth International Symposium on the Chemistry of Cement, Tokyo 1968, 4, 149-199.

Schwiete, H.E., Ludwig, U., Würth, K.E.and Grieshammer, G., 1969. New compounds formed in the hydration of blastfurnace slags (in German), Zement-Kalk-Gips, 22(4), 154-160.

Schwiete, H.E. and Dölbor, F., 1963. The effect of the cooling conditions and the chemical composition on the hydraulic properties of haematitic slags (in German), Forschungsbericht des Landes Nordrhein-Westfalen, No. 1186.

Smith, R.A., 1979. The effect of autoclaving time on the physical and chemical properties of calcium silicate bricks, Transactions of the Journal of the British Ceramic Society, 78, 40-43.

Smolczyk, H.G., 1978. The effect of the chemistry of the slag on the strengths of blastfurnace cements (in German), Zement-Kalk-Gips, 31(6), 294-296.

Smolczyk, H.G., 1980. Slag structure and identification of slags, Proceedings of the Seventh International Congress on the Chemistry of Cement , Paris 1980, 1(III), 3-17.

Smolczyk, H.G. and Romberg, H., 1976. Der einflub der nachehandlung der langerung auf die nacherärtung und porverteilung von beton (in German), Tonindustrie Zeitung, 100, 349-357, 381-390.

Solacolu, S., 1958. Die bedentung der thermischen gleichgewichte des systems MgO-CaO-SiO_2-Al_2O_3 für das schmelzen und granulieren der hochofenschlacken (in German), Zement-Kalk-Gips, 11, 125-137.

Sopora, H., 1959. Bewertung von hochofenschlacken für das schmelzen und granulieren der hochofenschlacken (in German), Zement-Kalk-Gips, 11(4), 125-137.

Speakman, K., 1970. Reactions in the system CaO-MgO-SiO_2-H_2O), Mineralogical Magazine, 37(289), 578-587.

Steyn, J.G.D., 1965. The identification, mode of occurence, and quantitative determination of crystalline phases in granulated blastfurnace slag, Mineralogical Magazine, 35, 108-117.

Stokes, K.R., 1971. Investigations into hydrothermal reactions between lime and silicates, PhD. thesis, University of London.

Stutterheim, N., 1960. Properties and uses of high magnesia portland slag cement concretes, Journal of the American Concrete Institute, 56, 1027-1045.

Stutterheim, N., 1969. Portland blast-furnace cements- a case for separate grinding of slag, Proceedings of the Fifth International Symposium on the Chemistry of Cement, Tokyo 1968, 4, 270-276.

Taylor, H.F.W., 1962. Hydrothermal reactions in the system $CaO-SiO_2-H_2O$ and the steam curing of cement and cement-silica products, Proceedings of the Fourth International Symposium on the Chemistry of Cement, Washington D.C. 1960, 3, 167-190.

Taylor, H.F.W., 1964. (editor and author) The Chemistry of Cements (2 volumes), Academic Press Inc., London, 460 pp and 442 pp.

Taylor, H.F.W., 1967. A review of autoclaved calcium silicates, Proceedings of the Symposium on Autoclaved Calcium Silicate Building Products, London 1965, 195-205.

Taylor, H.F.W., 1977. Discussion of: Microstructure and strength of hydrated cements, (by R.F.Feldman and J.J.Beaudoin), Cement and Concrete Research, 7, 465-468.

Taylor, H.F.W. and Roy, D.M., 1980. Structure and composition of hydrates, Proceedings of the Seventh International Congress on the Chemistry of Cement, Paris 1980, 1(II), 1-13.

Teoreanu, I. and Georgescu, M., 1974. The behaviour of synthetic and industrial blast-furnace slags in the presence of activators (in German), Zement-Kalk-Gips, 27(6), 308-312.

Terrier, P., 1973. Research into the hydraulicity of granulated blast-furnace slags (in French), CILAMS Informations, 8(1), 1-6.

Verbeck, G. and Copeland, L.E.,1972. Some physical and chemical aspects of high pressure steam curing, Proceedings of the Menzel Symposium on High Pressure Steam Curing, Chicago 1969, 1-13.

Visser, S., Krüger, J.E., Van Aardt, H.H.P. and Brandt, 1975. XRD, DTA and EM data for autoclaved glasses, minerals and mechanical mixtures corresponding in composition to some of the minerals encountered in portland cement and granulated blastfurnace slag, CSIR Special Report Bou 33, Pretoria, R.S.A., 74pp.

Warren, R., 1977. Standard Slag Cement Company, Personal communication, October 10.

Weaver, W.S., 1974. Manager of Research and Quality Control, Canada Cement Lafarge Limited, Personal communication,September 17.

Yang, J.C., 1969. Chemistry of slag-rich cements, Proceedings of the Fifth International Symposium on the Chemistry of Cement, Tokyo 1969, 4, 296-309.

APPENDIX A

MANUFACTURE OF SYNTHETIC AKERMANITE GLASS

Reagent grade $CaCO_3$, $MgCO_3$ and silica gel were used to prepare this mineral of composition C_2MS_2 (Melting point = 1454°C). Correcting for ignition losses, the powders were weighed according to their molar proportions in akermanite and dry mixed in a small alumina ball mill. The materials were calcined at 1050°C before being melted for 2h at 1475°C in an electric furnace. After slow cooling, the akermanite crystals were ground in a tungsten carbide puck mill and their composition verified by XRD.

The crystalline powder was then placed in a non-wetting (5 per cent gold) platinum crucible and re-melted in an electric, RF coil induction furnace. Using an optical pyrometer to monitor the temperature, the crucible and contents were removed at 1500°C and immediately quenched into cold water. This process was repeated until 150g of material was obtained. The final product was ground to a powder in a tungsten carbide puck mill. Using QXRD, the akermainite was found to contain 10.8 per cent crystalline material along with the glass. Chemical analysis by XRF showed 1.22 per cent alumina content. Since akermanite is an end member of the melilite solid solution series akermanite (C_2MS_2) - gehlinite (C_2AS), the alumina simply shifted the composition of the glass (and crystal) along the solid solution series. From the chemical analysis, the composition was determined to contain 96 per cent akermanite and 4 per cent gehlinite in the solid solution.

APPENDIX B

INDIRECT GLASS CONTENT DETERMINATION BY QUANTITATIVE X-RAY DIFFRACTION

Background

Each crystalline element and compound can be characterized by its unique set of x-ray diffracted crystal d-spacing reflections. Knowing the radiation wavelength and the diffraction angle, these crystal d-spacings can be calculated using the Bragg equation. Amorphous (glassy) materials, on the other hand, lack long range structural order and as a result, do not exhibit distinct reflections. On an X-ray diffraction chart a broad halo or hump, spaced around the nearest neighbour atomic distance, indicates the presence of an amorphous structure.

Intensities of peaks for a single mineral in a multi-component mixture on a diffractometer trace are related directly to its concentration in the mixture. The technique of adding a known amount of an internal standard mineral in order to calibrate intensities of unknown minerals has been widely used since the theory was detailed by Klug and Alexander (1954).

Slag Minerals

The major mineral present in air cooled and devitrified blast furnace slags is the melilite solid solution series between akermanite (C_2MS_2) and gehlenite (C_2AS). In vitrified slags, therefore, the glassy structure has a composition of mostly melilite. In this study, merwinite (C_3MS_2), diopside (CMS_2) and monticellite (CMS) were also detected, although merwinite was never present in the devitrified slags.

Typical traces of pelletized slags showed the broad amorphous hump between about 25 and $36^{o}/2\theta$(Cukαradiation) with perhaps the most intense peak of one or two of the crystalline minerals present.

Intensity Calibration

Estimation of the amount of glass present was made indirectly. The intensities of the crystalline components were measured, the amounts estimated from calibration curves, and then the amount of glass was obtained by difference.

One hundred parts by weight of each slag sample (the minus 45μm fraction) was interground with 10 parts calcium fluoride (CaF_2) internal standard with acetone in an agate mortar. As mentioned previously, the presence of an internal standard not only allows calibration of the d-spacings of the peaks but also their intensities by expressing them as intensity ratios relative to the characteristic peak of the internal standard.

While a mineral's concentration is in theory proportional to the integrated intensity of its reflections, peak heights were used in calculations, since they were much more easily obtained, and it was found that the method was not improved using integrated intensities. The peak height of the strongest peak for each mineral was measured and expressed as a ratio relative to the peak height of the 3.15Å reflection of CaF_2 (I_1/I_{CaF_2}).

Initially the large range of 6^{o} to $70^{o}/2\theta$ (Cukα) was scanned at $1^{o}/2\theta$/minute to identify the minerals present. Then the 24^{o} to $37^{o}/2\theta$ range, containing the hump, CaF_2 peak, and most intense slag mineral peaks, was scanned 3 to 5 times to average the intensity

ratios obtained.

To calibrate the intensity ratios, 100 per cent akermanite and 50 per cent akermanite/50 per cent gehlenite solid solution series minerals were synthesized from reagent grade chemicals by melting at 1600°C, cooling, then igniting at 1050°C. Synthetic standards for merwinite, diopside and monticellite were obtained from the Building Research Station, England. The intensity calibration ratios developed for the standard peaks are given in Table B.1.

The synthetic melilite mixture containing 50 per cent akermanite was chosen as the intensity standard for the slags since it was found, by the XRD method of Ervin and Osborn (1949) that the slags, with the exception of Number 18, contained between 30 and 60 per cent akermanite in their melilite solid solutions.

TABLE B.1

CALIBRATION STANDARDS FOR SLAG MINERALS

Mineral	Miller Indices hkl	d Spacing Å	Diffraction Angle $^{o}/2\theta$ (CuKα)	$\frac{I_{standard}}{I_{CaF_2}}$
CaF_2	111	3.153	28.30	1.00
C_2MS_2	211	2.87	31.17	9.17 (50:50 Solid Solution)
C_2AS	211	2.85	31.39	
C_3MS_2	$\bar{4}11$	2.672	33.54	5.46
CMS	131	2.676	33.50	3.14*
CMS_2	$\bar{2}21$	2.992	29.88	5.41
$C\bar{C}$	10·4	3.035	29.43	15.613

*This intensity ratio was calculated indirectly using an αAl_2O_3 internal standard due to overlap of the 3.19Å (002) peak of CMS with the 3.15Å peak of CaF_2. The intensity ratio relative to αAl_2O_3 was converted to CaF_2 as shown, since the proportions of CMS found in the slags was low and the low intensity 3.19Å CMS peak did not interfere.

APPENDIX C

GLASS CONTENT DETERMINATION BY MEASUREMENT OF THE XRD AMORPHOUS HUMP AREA (GAH)

As detailed in Appendix A, the presence of glass can only be detected directly by XRD by a hump in the base line. For slags this hump occurs between approximately 25^{o} and $36^{o}/2\theta$ (CuKα) as shown in Figure C.1. Drawing a line through the background intensity on either side of the hump and lines around the hump outline, the area of the hump has been approximated by,

$$AH = h_1w_1/2 + (h_1 + h_2/2)\ w_2 + h_2w_3/2 \qquad (C.1)$$

The CaF_2 internal standard peak is superimposed on the shoulder of the hump. Using the peak width at half height, the area of the standard is

$$As = h_sw_s \qquad (C.2)$$

The hump area ratio is then calculated by

$$GAH = AH/As \qquad (C.3)$$

It was found by repetitions that the GAH values can be quite variable due to small changes in hs. Therefore at least three repetitions should be made.

Note: In Figure C.1, the 201 and 211 peaks of crystalline melilite can be seen superimposed on the amorphous hump.

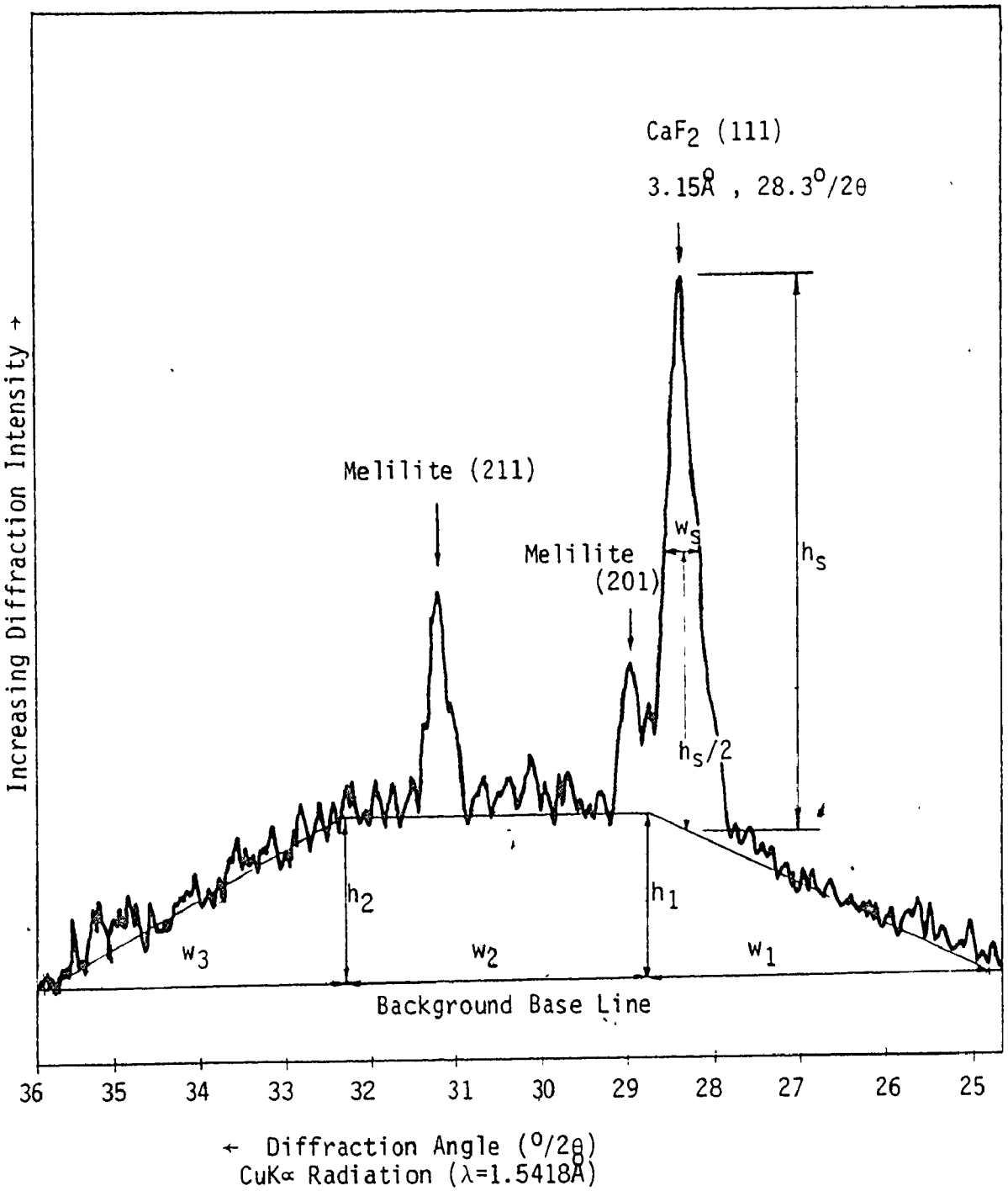

FIGURE C.1: SAMPLE XRD TRACE OF A MAINLY AMORPHOUS SLAG SHOWING DIMENSIONS FOR CALCULATION OF GAH.

APPENDIX D

DETERMINATION OF GLASS CONTENT BY

"THE McMASTER METHOD"*

Microscope

While an Olympus Trinocular Model ECE TR-1 microscope has been used, any microscope with the general polarizing features indicated below will be suitable. This microscope is equipped with a Model LSE high power interchangeable illuminator with transformer, eyepiece of POlOX (polarizing), and objectives of 4X, 10X, 40X and 100X. This allows magnifications of 40X, 100X, 400X and 1000X which is more than adequate for glass content determinations (400X is the magnification used in this technique). the lower polarizing element is carefully adjusted to insure that cross-polarization can be achieved, and the eyepiece can be adjusted quickly from plane to cross-polarized light.

Preparation of Slag Samples:

1. For Unground Slag Samples:

Representative samples are mixed and quartered down to about 15 to 20 grams, and the whole of this amount is then ground to pass a 63μm sieve with as much as possible retained on a 45μm sieve.

---

*Originally developed in the Construction Materials Laboratory, Department of Civil Engineering, McMaster University by Dr. J.J. Emery and Mr. R.P. Cotsworth (National Slag Limited, Hamilton) in consultation with Dr. P.S. Nicholson (Ceramic Engineering) in 1972. This general method of amorphous glass content determination followed that used by McCrone and Delly (1973) and was described by Emery, Kim and Cotsworth (1976). A modified method was circulated by R.D. Hooton (Dated Dec. 1977) and this final method, was further modified by R.D. Hooton using the method of Parker and Nurse (1949) to distinguish milky, opaque particles.

A ceramic mortar and pestle is used to pulverize the slag sample. Care must be taken not overgrind the slag which causes much of the material to pass through the 45μm sieve. This is most easily accomplished by grinding for a short time, sieving, then regrinding the plus 63μm sieve material and sieving again. This process can be repeated until all of the sample passes through the 63μm sieve. If desired, the material retained on the 45μm sieve can be washed and dried to remove any surface dust.

2. For Ground Cementitious Hydraulic Slag Samples:

a) To obtain a sample of cementitious hydraulic slag, suitable for this procedure, a representative sample of approximately 100g is dry sieved through the 63μm and 45μm sieves. Only a small portion of the slag will be retained on the 45μm sieve since slag cement is normally ground to 400 m^2/kg Blaine fineness, with less than 20 per cent retained plus 45μm. Unfortunately, using optical methods, particles less than 45μm diameter are not easily observed, so the assumption must be made that the glass content of the plus 45μm material is similar to that of the minus 45μm material. It was found by QXRD that this is a reasonable assumption. The plus 63μm material is discarded since it contains tramp iron and agglomerated slag particles from grinding.

b) The material retained on the 45μm sieve is then wet sieved to remove small adhering particles . The sieve and the remaining minus 63μm, plus 45μm material is then dried at 110°C.Very little slag would be dissolved or hydrated during the short time of washing, and wet sieving leaves uniform, dust-free particles making optical examination much easier.

c) Tramp iron in cementitious hydraulic slag (less than 1 per cent) has been found to be contained almost exclusively in the +63μm and +45μm fractions and therefore is not representative of the whole sample, and should be removed. When dry, the +45μm particles are placed on a piece of wax paper and a magnet is used below the paper to separate the iron particles.

Preparation of Slide Specimens

A very small amount of the sieved slag is then sprinkled on a microscope slide. A drop of Ethylene Glycol ($HOCH_2CH_2OH$) (or camphorated oil) is applied to the centre portion of the sprinkled sample. A cover plate is then placed on top of the sample. The Ethylene Glycol then spreads below the cover plate by capillary attraction. After this occurs, the cover plate is sheared gently to form a uniform, single layer of particles, and care must be taken to avoid air bubbles forming. Prepared slides should be labelled and handled carefully. The prepared slides should be examined within a few hours to avoid evaporation of the fluid. Slides have also been successfully mounted using clear fibreglass type resins.

Examination of Specimens

The prepared specimen slide is mounted on the stage of the microscope, which has fine vernier horizontal movement controls. This mounted specimen is then examined under plane and cross-polarized light a 400X magnification. The determination of glass content of the sample is based on the average of 2 or 3 counts of 50 individual particles each (depending on variability of material).

Only the particles which "touch" the cross-hair are counted as the sample in traversed. The horizonal vernier is used until the edge of the slide is reached, then the vertical vernier is moved slightly, and the slide is horizontally traversed in the reverse direction (see Figure D.1). This is continued until 100 or 150 particles have been evaluated.

Evaluation of Individual Particles

In general, amorphous (glass) particles do not transmit cross-polarized light, while most crystalline materials do, and tend to glow due to birefringence. However, the identification of glassy and crystalline materials is not that simple, and the types of particles likely to be encountered are listed.

1. Clear (in plane light), no birefringence, may or may not contain bubbles, often can see evidence of concoidal fractures along edges - count as glass. (Note: Minor oxides can stain the glass particle but they are generally transparent.)
2. Opaque (in plane light), glows slightly white or milky but no definite birefringent colours, these "milky" particles may be due to micro-crystalline material or due to hydrated surfaces - count as milky.
3. Bright, coloured birefringence - count as crystal (Note: Strain birefringence can occur in glass. These particles appear clear and "glassy" under plane light but show definite birefringence, often along one side. This may be due to differential cooling

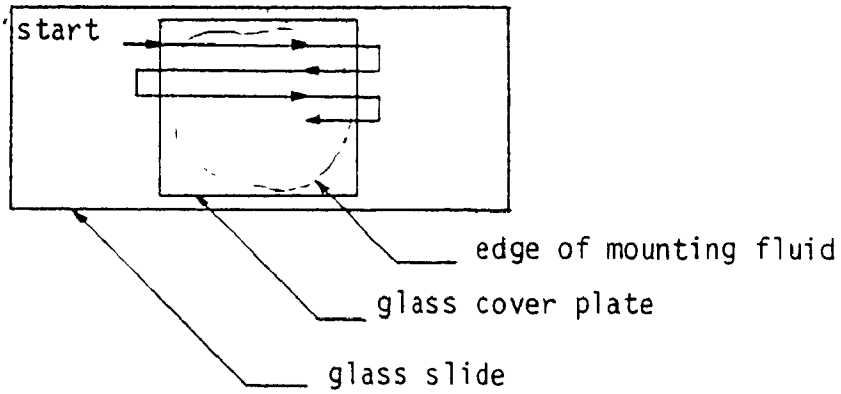

FIGURE D.1: PATH OF TYPICAL TRAVERSE ACROSS SLIDE

TABLE D.1

SAMPLE TALLY SHEET SHOWING EXAMPLE DESIGNATIONS

N	A		B		C		D		E		
	Glass (G)	MIlky (M)	G	M	G	M	G	M	G	M	
1	100	-	← 100 per cent glass particle								
2	50	50	← 50 per cent glass, 50 per cent milky particle								
3	70	-	← 70 per cent glass, 30 per cent crystal particle								
4	-	50	← 50 per cent milky, 50 per cent crystal particle								
5	100	-									
6	100	-									
7	100	-									
8	100	-									
9	100	-									
10	20	40									
Sum	740	140									
Average	74	14									

from the melt or due to impact stresses during grinding - count as crystal since identification is difficult and only a small fraction is involved.)

4. Iron particles do not show normal birefringence but, appear black and opaque in plane light and may glow dull red in cross-polarized light - do not count these particles at all. (As mentioned previously, about 1 per cent tramp iron seems to predominate in the coarser sieve sizes and is not representative of the total slag sample.)

Examples of these particle types can be seen in Figure D.2. Each particle is estimated to the nearest 10 per cent for each of glass, milky or crystalline material. A sample tally sheet is shown for a 50 particle count in Table D.1. For convenience, the crystal portions are not listed since they can be calculated (100 per cent - per cent glass - per cent milky). Therefore, for the 10 particles listed in Table D.1, there is 74 per cent glass, 14 per cent milky material and 100 - 74 - 14 = 12 per cent crystal.

Usually the percentage of glass is tallied after each 50 particle interval, so the variability between 50 particle groups can be checked. More 50 particle groups are evaluated if the variation in glass is large, and these values are averaged.

Recent Developments

The St.Marys Cement Company, Bowmanville has recently adopted this procedure, but with some modifications (Jenvay and Pugh, 1980).

1. Dry sieving is eliminated and a small amount (10g) of the

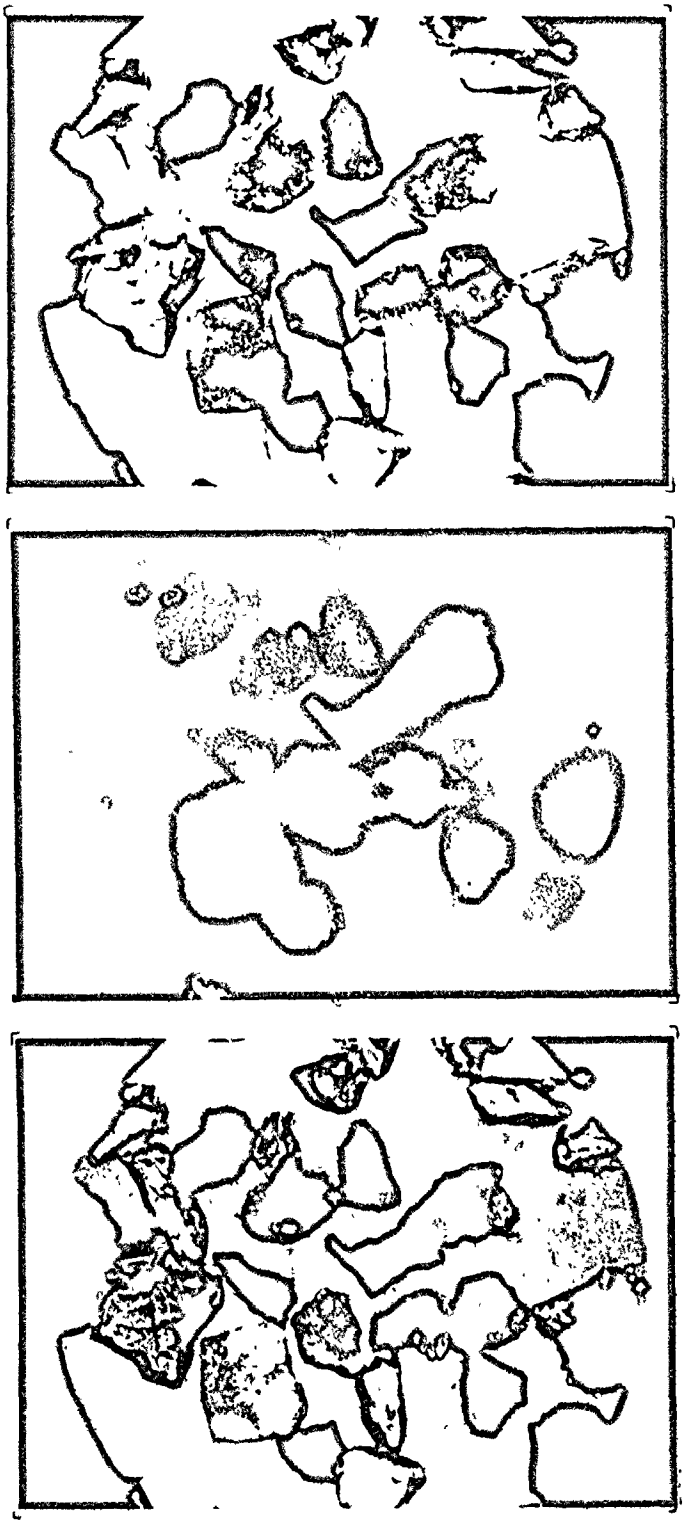

FIGURE D.2: PHOTOMICROGRAPHS OF SLAG GRAINS UNDER TRANSMITTED (a) PLANE LIGHT, (b) CROSS POLARIZED LIGHT, AND (c) PLANE LIGHT WITH A GYPSUM FILTER INSERTED (See text for explanation of particle types)

sample is wet sieved in small 75μm stainless steel sieves with methanol, which saves time.

2. A Nikon polarizing microscope with a sliding gypsum plate was used at 500 times magnification. The gypsum plate is used in addition to the plane and cross - polarized light. With the gypsum plate inserted, the background and glass particles are bright pink, while the crystalline material appears blue or yellow as shown in Figure D.2(c)(If the sample is rotated, the blue and yellow areas eventually extinguish, then alternate colours on further rotation). The milky particles also appear blue and yellow but can be divided into two groups, depending on whether the colours extinguish upon rotation. Most of the milky particles do show extinction and are counted as crystalline. A small number do not extinguish and it is thought by the writer that these may represent hydrated surfaces, and might be counted as glass. However, due to the small amount of this material, the impact on the total glass count is not great.

The advantages of these modifications appear to be less operator eye strain, due to the pink coloured field, and easier identification of previously questionable particles.

APPENDIX E

GLASS COUNT DETERMINATION BY "THE SOUTH AFRICAN PROCEDURE"*

Sample Preparation

A representative sample of the granulated slag clinker is dried and ground, with material passing the 63μm and retained on the 45μm sieve, kept for the test.

Slide Preparation

Place one or two drops of oil of camphor (camphorated oil) on a clean slide, and introduce to this sufficient graded ground slag so that when dispersed in the oil and viewed under the microscope approximately 70 individual particles can be counted per quadrant of the cross hairs.

Microscope

The microscope shall have the following minimum requirements:

Magnification : 100-120
Coarse and fine focusing
Adjustable cross hairs in the eyepiece
Transmitted light
Orange filter (OG2)
Crossed Nicols polarization

Method of Count

The prepared slide is viewed under the microscope through the transmitted light modified by the orange filter. The crossed Nicols is not in use at this time. A quadrant total particle count is taken, assumed to be representative of the total viewing area and multiplied by four.

The crossed Nicols is inserted and a total view count is taken

---

* For glass content methods developed elsewhere, the style but not the technical content was modified by the writer.

of all orange translucent particles, care being taken to count individual separate orange translucent particles and allowances made for particles that are partially translucent and opaque. The orange translucent particles are assumed to be crystalline, the opaque particles glass.

Determination of Percentage

$$\text{Glass count (per cent)} = \frac{100\ (\text{total particles} - \text{crystalline orange translucent particles})}{\text{Total Particles}} \qquad \text{(E.1)}$$

The counting procedure should be repeated, on four or five other areas of the slide, to obtain a more representative count.

APPENDIX F

GLASS CONTENT DETERMINATION BY THE AUTOMATED U.V. REFLECTANCE METHOD

This method of assessing slag glass is currently used by Dravo Lime Company at its Pittsburgh Laboratory (Foster,1978, 1979, 1980).

An Aminco-Bowman Spectrophotofluormeter was adapted to examine solid, powder samples by reflectance (solutions are normally used when measuring U.V. transmission). The U.V. values represent the percentage of emission at 590 namo meters compared to a standard sample arbitrarily assigned a value of 100 per cent glass (some samples, therefore, can have values greater than 100 per cent). The largest number ever assigned to a slag was 165 per cent (Foster, 1980).

APPENDIX G

GLASS CONTENT DETERMINATION BY THE PARKER AND NURSE OPTICAL METHOD

A representative 5 gram slag sample is ground until it all passes a 150μm sieve. Of this material, the amount passing a 90μm sieve and retained on a 53μm sieve is used for the test. A small amount is placed on a microscope slide in bromoform and examined by transmitted light at 200 times magnification, using an eye-piece with a graticule. The total number of grains in the field is counted and also the number of these which are substantially opaque. The percentage of opaque particles is calculated and subtracted from 100 to obtain the percentage glass (Parker and Nurse, 1949).

APPENDIX H

GLASS CONTENT DETERMINATION USED BY THE FRODINGHAM CEMENT CO.LTD.(1979)

A representative sample of the granulate to be tested is obtained, or if possible, a number of random samples are checked and an average figure for these samples is produced.

The sample is mixed and quartered down to about 10 to 15g. The whole of this amount is ground through a 300μm sieve. Then the sample is sieved through a 90μm and 53μm sieve.

Using the material retained on the 53μm sieve, a small amount is sprinkled on a microscope slide (the operator will become acquainted with the amount required through experience), but it should be sufficient to produce a layer one particle thick on the slide covering about $100mm^2$. A microscope slide cover is placed on top and a drop of Bromoform is placed at the edge of the slide cover and normally spreads throughout the layer by capillary attraction.

The slide is viewed under a microscope at 200 times magnification, the eye-piece having a squared graticule. The number of black pieces (i.e. allowing no light through) are counted and the area covered by the black pieces is estimated. Since the graticule is composed of 100 squares, then the estimated area covered by the black particles, subtracted from 100, is the per cent of glass or "Glass Count". This counting is repeated using 3 separate positions on the slide. An average of these three counts is taken as the "Glass Count" expressed to the nearest 0.5 per cent. When the "Glass Count" of ground blast furnace slag samples is measured, preparation begins by passing the sample through the 90μm and 53μm sieves.

APPENDIX I

GLASS CONTENT DETERMINATION BY "THE RHEINHAUSEN OPTICAL METHOD"

In the Research Institute for Blast Furnace Slags, Rheinhausen, the glass content and the content of crystalline portions in granulated slags are determined as follows: the specimen reduced to a particle size of 40µm to 60µm is bedded into a plastic material and a polished section is made. The latter is etched with 1 per cent alcoholic HNO_3 and HG-vapour, and subsequently the amount of vitreous and crystalline components (the latter possibly separated according to minerals) are counted by means of an integration ocular. When the vitreous content of granulated slags in blast furnace slag cements is checked, a cement dispersion specimen (grain size 30µm to 40µm) is bedded into Canada balsam. With the aid of the polarizers the proportion of purely vitreous grains, of grains differing in respect of their crystal content and of entirely crystalline grains are then determined. (Schröder,1969)

APPENDIX J

MODIFIED METHOD* FOR DETERMINING FREE SILICA IN AUTOCLAVED CEMENT PASTES

1. The paste samples, previously ground to minus 150μm, are dried at 110°C and weighed (to 0.0001g).
2. The samples are then transferred into, pre-weighed pyrex centrifuge tubes (about 25mm diameter by 130mm long, 50ml capacity). About 30ml of 2N HCl is added to each tube and the tubes are placed in a distilled water bath (distilled to prevent salts from evaporating on outside of tubes and affecting weights) and heated to 60°C plus for 15 minutes. The solutions are stirred occasionally with a glass rod and a drop of solution placed on indicator paper to ensure its acidity.
3. The tubes are removed from the bath, weight balanced with distilled water and centrifuged for 2 or 3 minutes or until the solutions have cleared.
4. The acid is decanted as much as possible without disturbing the solid residue in the bottom.
5. The tubes are then filled (∿30ml) with distilled water, centrifuged again and decanted (to remove any dissolved $Ca(OH)_2$, preventing the precipitation of $CaCO_3$ after the Na_2CO_3 is added).
6. The tubes are then filled with a 5 per cent Na_2CO_3 solution (to neutralize the acid), stirred (pH checked to be sure basic), placed in the water bath and boiled for 20 minutes.
7. The tubes are then balanced and balanced and centrifuged until clear (about 10 minutes).

*Based on the method of Kondo et al (1975).

8. The liquid is decanted and the residue "washed" with distilled water and centrifuged. This washing is repeated until the liquid has a pH=7.0 (3 washings are usually sufficient).
9. The tubes are (with residue and remainder of the decanted, neutralized liquid) stood up in a beaker and dried at 110°C. The beaker is removed from the oven and cooled in a dessicator. The tubes are then weighed.

Calculations

$$\text{Wt. of residue } (SiO_2) = \text{wt(tube + residue)} - \text{tube wt.}$$

$$\text{Free } SiO_2 \text{ (per cent)} = \frac{\text{wt of residue}}{\text{original sample at}} \times 100 \qquad \text{(J.1)}$$

Note

The residues from several autoclaved slag-portland cement-silica flour pastes were analysed by XRD and found to only contain quartz and the minor amount of sericite mica which was contained in the silica flour material.

APPENDIX K

TOBERMORITE SYNTHESIS

A relatively crystalline 11.3Å tobermorite with C/S molar=0.80 was synthesized using commercial silica flour (quartz) (ground finer to 1000 m^2/kg Blaine) and fresh reagent grade calcium hydroxide. A slurry of the pre-mixed powders was made in a 1 litre stainless steel beaker using freshly boiled, distilled water. The water/solids ratio was about 2. The beaker was loosely covered and autoclaved 72h at 185°C. The contents were dried at 110°C and stored in a dessicator to avoid carbonation.

XRD analysis showed well crystallized 11.3Å tobermorite but also xonotlite with a small amount of unreacted quartz and sericite mica (an impurity in the silica flour). The amount of sericite plus quartz was found to be 2.9 per cent by the extraction method described in Appendix J. By XRD of the extraction residue, it was estimated that it contained 2.4 per cent quartz and 0.5 per cent sericite. Assuming a constant chemical composition of $C_5S_6H_5$ for tobermorite and C_6S_6H for xonotlite, and measuring the loss on ignition, the tobermorite content of the synthetic mixture was estimated to be 69.0 per cent.